Desalination 621 (2026) 119718

Contents lists available at ScienceDirect

Desalination

journal homepage: www.elsevier.com/locate/desal

A global outlook of the desalination industry and state-of-the-art technologies for brine valorisation

C. Morgante [a], M. Herrero-Gonzalez [b,*], J. Lopez [c,d,*], J. Imholze [e], V. Boffa [a], R. Ibañez [b], J.L. Cortina [c,d]

[a] Department of Chemistry and Bioscience, Aalborg University, Fredrik Bajers Vej 7H, 9220, Aalborg, Denmark
[b] Departamento de Ingenierías Química y Biomolecular, Universidad de Cantabria, Avenida de los Castros 46, 39005, Santander, Cantabria, Spain
[c] Chemical Engineering Department, Escola d'Enginyeria de Barcelona Est (EEBE), Universitat Politécnica de Catalunya (UPC)-BarcelonaTECH, Av. Eduard Maristany 16, Campus Diagonal-Besòs, 08019, Barcelona, Spain
[d] Barcelona Research Centre in Multiscale Science and Engineering (CCEM), Universitat Politècnica de Catalunya - BarcelonaTech (UPC), Av. Eduard Maristany, 16, 08019 Barcelona, Spain
[e] Department of Engineering Thermodynamics, University of Bremen, 28359, Bremen, Germany

HIGHLIGHTS

- Global assessment of desalination capacity and brine production.
- Brine valorisation as an opportunity for the recovery of minerals, water and energy.
- Quantification of mineral recovery potential from seawater desalination brine.
- Evaluation of 30+ technologies across salinity and TRL used in MLD/ZLD scenarios.
- Identification of key obstacles in energy use, scalability and material performance.

GRAPHICAL ABSTRACT

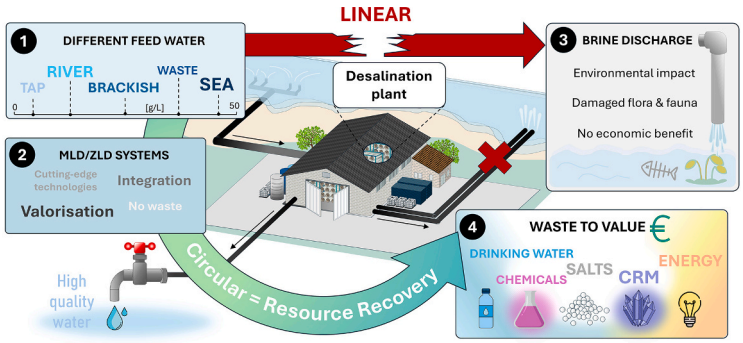

ARTICLE INFO

Keywords:
Resource recovery
Critical raw materials
Circular economy
Minimum liquid discharge
Zero liquid discharge
Desalination
Brine valorisation

ABSTRACT

Desalination is increasingly recognized not only as a solution to water scarcity but also as a potential source of valuable resources through brine valorisation. This review presents a comprehensive assessment of the global desalination landscape, focusing on the feasibility of resource recovery within circular economy frameworks. Using the DesalData database, the study maps the distribution and capacity of desalination plants, revealing the dominance of seawater reverse osmosis (SWRO) and the substantial volume of brine produced globally. A quantitative analysis shows that SWRO brine could meet or exceed current production levels for several commodities. Over 30 technologies are evaluated across membrane-based, thermal, and electrochemical categories, with varying maturity and salinity tolerance. While some, such as thermal brine concentrators and crystallisers, are commercially deployed, others like bipolar membrane electrodialysis (BMED), membrane distillation crystallisation (MDC), and forward osmosis (FO) remain at pilot or lab-scale. The review highlights the potential to recover freshwater, salts, critical raw materials, chemicals, and energy, in brine valorisation and identifies more

* Corresponding authors.
E-mail addresses: herrerogma@unican.es (M. Herrero-Gonzalez), julio.lopez.rodriguez@upc.edu (J. Lopez).

https://doi.org/10.1016/j.desal.2025.119718
Received 4 October 2025; Received in revised form 27 November 2025; Accepted 1 December 2025
Available online 3 December 2025

specifically the key challenges to recover such resources of the analysed technologies including energy consumption, material durability, and economic viability. Industrial case studies demonstrate that large-scale brine mining currently focuses on water and NaCl recovery, while multi-resource recovery remains limited to pilot-scale implementations. Overall, brine valorisation emerges as a promising strategy to transform desalination from a waste-generating process into a circular and resource-efficient solution, though further technological development and scale-up are essential to realize its full potential.

1. Introduction

Over the past few decades, climate change and rapid global population growth have driven the scientific community to embrace circular economy approaches across various fields, including the recovery of valuable resources essential to daily life. Specifically, the lack of primary mineral resources and freshwater sources has led to the exploration of alternative strategies for extracting key resources, such as minerals, water and energy, from non-traditional sources.

When it comes to minerals, among such sources, seawater (SW) garners significant attention due to its "limitless" supply of nearly all elements in the periodic table. A few of the elements exist in appreciable concentrations (g/L levels), including sodium (Na^+), magnesium (Mg^{2+}), calcium (Ca^{2+}), and potassium (K^+), along with chloride (Cl^-), sulphate (SO_4^{2-}), and bromide (Br^-) as major anions [1]. These "major" elements are commonly recovered as hydroxide and carbonate salts [2]. In contrast, trace elements such as lithium (Li^+) and uranium (U) exist at much lower concentrations, typically at parts per million (mg/L) and parts per billion (μg/L) levels, respectively [3]. While element concentrations can vary by geographical region, the relative ratios of these elements in SW remain largely consistent. Today, commercially viable extraction focuses on major elements such as Na^+, Mg^{2+}, Ca^{2+} and K^+, while the recovery of several trace elements remains economically and technically challenging due to their low concentrations [4,5].

An interesting opportunity arises from desalination brine, which comes from desalination processes of SW or other feedwater sources (i.e., brackish water (BW), river water etc.). Desalination is a widely used method for supplying drinking water in regions with limited freshwater resources. It is mainly performed using membrane-based technologies like Reverse Osmosis (RO), which is now the most common due to its compact design, flexibility, and energy efficiency, or thermal-based methods such as Multi-Effect Distillation (MED) [6,7]. These processes inevitably produce a by-product called brine, a concentrated saline solution (see Table S1, Section S1 in Supplementary Material), which may differ in density and temperature from the original feedwater and may contain residual chemicals from the desalination process (e.g. anti-scalants and biocides). As most desalination plants are located near coastlines (three-quarters of desalination operations are within 10 km from the coastline [8]), surface water discharge (direct discharge of brine into oceans and rivers) is the most common (and least expensive) disposal method [9], though it can negatively affect marine ecosystems by increasing salinity and reducing dissolved oxygen levels. For inland desalination facilities, other methods, such as deep-well injection [10], sewer disposal [11], land application and evaporation ponds (EPs) [12], are applied, but each face challenges in terms of cost, environmental impact, or technical feasibility.

In the case of SW desalination, previous studies have reported that brine outflow from desalination plants can increase salinity by an additional 2.24, 0.81, and 1.16 g/L in the Gulf, Mediterranean Sea, and Red Sea, respectively [13]. This phenomenon is accompanied by a corresponding reduction in dissolved oxygen levels, although these effects are generally more pronounced in the vicinity of the discharge area. Other environmental impacts of brine discharge include eutrophication due to phosphate supplementation, changes in pH, discoloration from iron concentration, elevated suspended solids, and the accumulation of toxic transition metals [14,15]. It is reported that currently, more than 51.7 billion cubic meters of brine (from all different feedwater sources) are discharged annually into the environment worldwide [8,16].

An appealing aspect of one specific brine, SW reverse osmosis (SWRO) brine, is that it has roughly double the concentration of SW (due to RO water recovery values spanning between 40 and 45 %), making it an attractive target for mineral recovery [17]. Elements in SW and desalination brine can generally be categorized into three groups based on their economic feasibility: (i) major elements that are commercially recoverable, (ii) trace elements with potential for economic recovery (e.g., lithium, boron, strontium and rubidium, with concentrations in mg/L), and (iii) trace elements whose extraction remains highly challenging (e.g., uranium, caesium, cobalt and scandium among others, with concentrations in μg/L). As can be observed from Fig. 1, the highest market values coincidentally correspond to the elements that are present in the lowest concentrations. However, it is to be noted that the market value is related to the scarce distribution of the elements in the lithosphere [18].

Among the elements presented in Fig. 1, magnesium stands out as having an optimal balance between high concentration in SW and significant market value. Notably, it is worth mentioning that as early as 1914, Dow Chemical Company began producing magnesium from brine in USA [6]. By 2022, SW and brines accounted for nearly 70 % of magnesium compounds production in USA [21]. More in general, as proof that SW/brine mining is already in practice, it is reported that USA recovers about 45 million tons of salt from which, over which 70 % of the recovered salt are used subsequently, reducing the cost of desalination while providing an additional value to it [22]. Therefore, brine mining is already in practice for certain elements and is increasingly recognized as a more sustainable alternative to traditional ore mining. It is less energy-intensive, eliminates the need for large-scale land excavation and has minimal impact on biodiversity [23]. Furthermore, the high cost of traditional brine disposal (accounting for 5-33 % of a

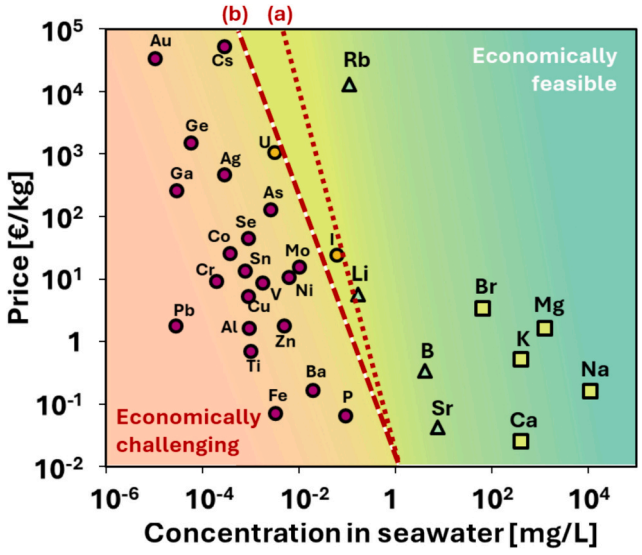

Fig. 1. Economic feasibility of SW mining based on specific price [€/kg] vs concentration [mg/L] of elements in SW where (a) and (b) represent the economic feasibility threshold of mineral recovery from SW reported by Shahmansouri et al. (2015) [19] and Loganathan et al. (2017) [20], respectively. Adapted from Morgante et al. [18].

desalination plant's overall cost [24]) has driven further research into using desalination brine as a resource rather than a waste product.

Over the past decade, several projects have been initiated both within Europe and globally, attempting to demonstrate the technical feasibility of multiple resource recovery from SW and desalination brine at the pilot scale, using Minimum Liquid Discharge (MLD) or Zero Liquid Discharge (ZLD) approaches. MLD and ZLD systems integrate various technologies (either membrane-based or thermal-based) designed to significantly reduce (or eliminate in the case of ZLD) the volume of brine disposed of. Initially, the focus was on recovering as much water as possible, leaving behind only a small volume of waste to be disposed of. However, over time, the idea of recovering valuable minerals concurrently has driven the evolution of the MLD concept. Today, MLD is defined as the reduction of disposed brine by producing valuable salts, minerals and water, with typical water recovery rates around 80 %. In contrast, ZLD systems aim for much higher water recovery, generally achieving between 95 % and 99 % [25,26]. MLD/ZLD systems are believed to offer both environmental and economic benefits, including: (i) mitigation of the environmental impact of brine disposal due to the reduced volume of waste produced, (ii) lower costs associated with brine disposal and desalination, (iii) the production of resources at a lower cost than their current market price, and (iv) the ability for companies to internally utilise the recovered resources (valuable salts, water, chemicals and energy).

MLD and ZLD systems typically consist of three main stages: (i) the pretreatment stage, which separates undesirable components from the brine, (ii) the concentration stage, where additional freshwater is recovered, sometimes split into two consecutive steps, and (iii) the crystallisation/conversion stage, in which valuable resources (minerals, additional water or energy) are recovered [27]. These final two stages are estimated to account for 60-70 % of the capital and operational expenditures (CAPEX and OPEX) of MLD/ZLD systems [6].

Given the growing importance of desalination in recent decades and the increasing interest in resource recovery within this sector, numerous review articles have emerged (see Fig. 2), particularly between 2019 and 2024. These works attempt to provide updated overviews of the potential for recovering resources from desalination brine. For instance, Mavukkandy et al. (2019) explored the transformation of brine from a waste product into a valuable resource, emphasizing the recovery of minerals, energy, and water [28]. Similarly, Ihsanullah et al. (2022) advanced the discussion by reviewing updated technologies, although their focus was limited to mineral recovery [29]. However, both reviews cover only a limited range of technologies (around ten), relying mostly on lab-scale data, whereas no information is provided on the potential mineral recovery, which is essential to evaluate the economic feasibility. Other recent reviews, such as those by Sajna et al. and Kumari et al., also address brine valorisation but are geographically or contextually limited, focusing on specific plants or regions like the Middle East [30,31]. Similarly, reviews by Bello et al. (2021), Cipolletta et al. (2021), and Lee et al. (2024) analysed only a narrow selection of technologies, without offering a comprehensive overview [15,32,33]. Sharkh et al. (2022) took a different approach by emphasizing the types of minerals that can be recovered, but provided limited detail on the technologies themselves [34].

Overall, no review article offers a comprehensive and comparative analysis of all technologies developed for brine valorisation, including the recovery of minerals, water, energy, and chemicals. Specifically, in the context of mineral recovery, there is a lack of information on the current implementation scale of each technology and their respective limitations. Moreover, no existing review quantifies global brine production or its geographic distribution, which is essential to assess whether specific regions could meet global demand for certain minerals. Finally, it is not possible to evaluate the current implementation scale of MLD/ZLD integrated schemes in previous review articles as no specific information about these processes at pilot plant or full scale is present.

This review aims to address these substantial gaps by providing a global, in-depth overview of desalination and brine valorisation technologies. Such a perspective is essential to understand where, and under what conditions, resource recovery from desalination brine is technically and economically feasible. Given the potential of resource recovery from brine and the growing interest in MLD/ZLD approaches within the desalination sector, this review article first examines the global state of desalination and brine production, detailing the primary water sources, leading contributors to brine production by region, key industrial sectors utilizing desalination, and the most widely used desalination technologies. The analysis of the global state of desalination brine identifies the potential production of minerals that can be produced through ZLD/MLD processes. The results revealed that SWRO represents the highest percentage of desalination processes; therefore, the following sections were dedicated to exploring the different technologies employed in the

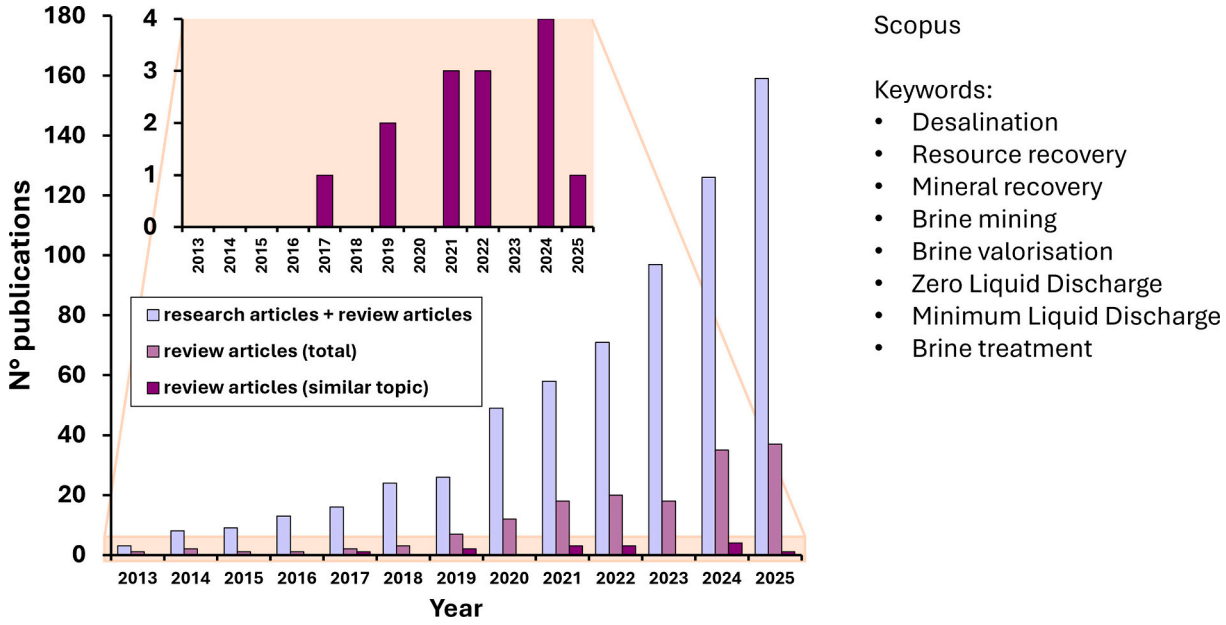

Fig. 2. Number of publications and review articles related to desalination, brine mining and ZLD/MLD processes. Review articles (total) refer to those with the specific keywords used by the authors and review articles (similar) relate to those specifically covering multiple technologies aimed at resource recovery from brine.

last 15 years to treat SW desalination brines, aiming at recovering water, minerals, or energy. For each technology, a brief explanation of its fundamentals is provided, followed by different case studies and technical limitations. Subsequently, industrial examples of close to full-scale ZLD and MLD approaches to valorise brines are provided. Finally, the review outlines future perspectives on achieving the technical feasibility of MLD/ZLD schemes, offering insights into the advancements needed for successful implementation.

2. Global outlook of desalination and brine production

The primary objective of this review is to assess the potential for recovering valuable resources from desalination brine produced worldwide. To this end, the current state of desalination worldwide was initially evaluated through the use of the DesalData database (version 2024), developed by Global Water Intelligence (GWI) [35]. This comprehensive database provides up-to-date, high-value business intelligence on over 20000 plants operating within the global water sector. More precisely, for each desalination plant, the database includes detailed information such as geographical location (region, country, coordinates) and site type (land-based, online or offshore), desalination technology, feedwater type, production capacity [m^3/d of freshwater], operational status (under construction, operational or decommissioned), commissioning year, customer type and, where available, specific technical and economic details (e.g. type of pretreatment, water production costs, commissioning authority, equipment suppliers etc.).

It is important to emphasize that the insights presented in this study, derived from the DesalData database, are both robust and reflective of current global trends in desalination. To ensure the reliability of the dataset, the authors undertook a robust data-filtering process. This involved identifying and removing potential duplicate entries based on matching plant names, geographic coordinates, and commissioning dates; excluding entries with incomplete or unverifiable information that could compromise the integrity of the analysis; and standardizing technology classifications and customer categories to maintain consistency across records.

To balance granularity and manageability in the analysis, the original regional classifications in the database were refined into 13 subregions: (1) Latin America, (2) Central America/Caribbean, (3) North America, (4) Oceania, (5) East Asia, (6) South East Asia, (7) Central Asia, (8) Sub Sahara Africa, (9) North Africa, (10) South Europe, (11) North Europe, (12) East Europe and (13) the Middle East.

Feedwater sources for each desalination plant were categorised into 6 types based on the concentration of the total dissolved solids (TDS): (1) tap water (TDS < 500 mg/L), (2) river water (500–3000 mg/L TDS), (3) BW (3000–20000 mg/L TDS), (4) wastewater, (5) SW (20000–50000 mg/L TDS) and (6) brine (> 50000 mg/L TDS).

Customer types for each desalination plant were grouped into 7 categories: (1) demonstration (Research & development purposes), (2) discharge, (3) industry, (4) irrigation, (5) military purposes, (6) drinking water and (7) power station. It is to be noted that in the case of industrial applications, 10 sub-sectors were considered: (1) electronics, (2) food & beverage, (3) metals, (4) mining, (5) oil & gas, (6) power, (7) pulp & paper, (8) refining/chemicals, (9) textiles, and (10) general (the specific field is not indicated for the specific desalination plant).

The desalination technologies were separated into 11 categories: (1) RO, (2) Nanofiltration (NF), (3) Ultrafiltration (UF), (4) Electrodialysis (ED), (5) Electrodialysis Reversal (EDR), (6) Electrodeionization (EDI), (7) Membrane Distillation (MD), (8) Multi Stage Flash (MSF), (9) MED, (10) Mechanical Vapour Compression (MVC) and (11) Other (unspecified technologies).

The analysis focused on land-based desalination plants with a minimum production capacity of 2000 m^3/d. This threshold was selected based on both economic and practical considerations relevant to resource recovery from desalination brine. Firstly, this threshold aligns with the upper limit of small-scale desalination plants typically serving remote communities. For example, the Lampedusa desalination plant in the Mediterranean with a production capacity of 750000 m^3/y supplies potable water to a population of 6000 inhabitants [36]. This capacity is representative of the scale at which desalination becomes critical for community-level water supply, yet still small enough to be considered non-industrial. Although the DesalData database lists approximately 14221 plants worldwide with capacities below 2000 m^3/day, collectively producing around 8 million m^3/day, these small-scale facilities contribute only about 6 % of the total global desalinated water output. More specifically, 391 plants (with capacity <100 m^3/d) produce a total of 0.02 Mm^3/d, 7545 plants (with capacity 101-500 m^3/d) produce 1.82 Mm^3/d, 3386 plants (with capacity 501-1000 m^3/d) produce 2.28 Mm^3/d and 2899 plants (with capacity 1001-1999 m^3/d) produce 3.89 Mm^3/d. More importantly, their brine volumes are generally too low to support economically viable resource recovery. Recent studies confirm that resource recovery from brine, such as salt, acid, base, or mineral extraction, is only feasible at larger scales due to the energy and infrastructure requirements involved [37]. Therefore, they were excluded from the scope of this study and the 2000 m^3/day threshold was selected to focus the analysis on plants with sufficient brine volumes to make resource recovery technically and economically viable, while excluding facilities where such processes are unlikely to be feasible.

Fig. 3 presents the distribution of land-based desalination plants with a production capacity of at least 2000 m^3/day, categorized by feedwater source and desalination technology. The data indicate that SW is the most commonly treated feedwater, with 2508 plants, followed by BW, which is processed by 1911 plants. In contrast, significantly fewer plants treat river water (715 plants) and wastewater (600 plants), while only 31 facilities are dedicated to brine desalination.

Regardless of the feedwater source, RO is the predominant desalination technology. However, the choice of technology also reflects the salinity of the feedwater. For instance, ED is more prevalent in BW treatment (151 plants), followed by river water treatment (42 plants). As feedwater salinity increases, technologies capable of handling higher salinity levels become more common. This is evident in the use of MSF and MED for SW desalination, with 420 and 332 plants, respectively.

Among the less common technologies, NF is primarily used for low-salinity feedwaters. There are 20 NF plants each for river and BW treatment, 8 for wastewater, and none for SW or higher-salinity sources. Although ED is mainly applied to BW, 22 ED plants are currently used for SW desalination. For brine treatment, where salinity can exceed 50 g/L, MED is the most widely adopted technology, with 5 operational plants. Other technologies such as MD, EDR, EDI, and MVC are represented by only a few large-scale installations.

It is also noteworthy that if desalination capacity (rather than the number of plants) was considered, the overall trends would remain largely consistent. The main exception is that SW desalination plants collectively exhibit a total production capacity more than twice that of BW plants, as illustrated in Fig. S1 of the Supplementary Material (see Section S2).

Among all feedwater sources, wastewater is the most compositionally diverse and challenging to treat. This complexity arises primarily from the varied origins of industrial wastewater. As illustrated in Fig. 4a, wastewater is generated and treated via desalination in nine specific industrial sectors. Industries not explicitly categorized are grouped under the label “general.” Fig. 4a also shows the global distribution of wastewater desalination plants. Notably, the power industry leads with 80 plants, followed by the refining/chemicals and oil & gas sectors, with 49 and 30 plants, respectively. In contrast, wastewater desalination is less prevalent in the textile and food & beverage industries, each with a maximum of 9 plants.

RO is the most widely adopted technology across all industrial sectors. MED ranks second, particularly prominent in the power industry, where 24 MED plants are operational. An exception is observed in the pulp & paper industry, where MED (12 plants) slightly surpasses RO (10 plants). ED is the third most common technology, though its adoption is

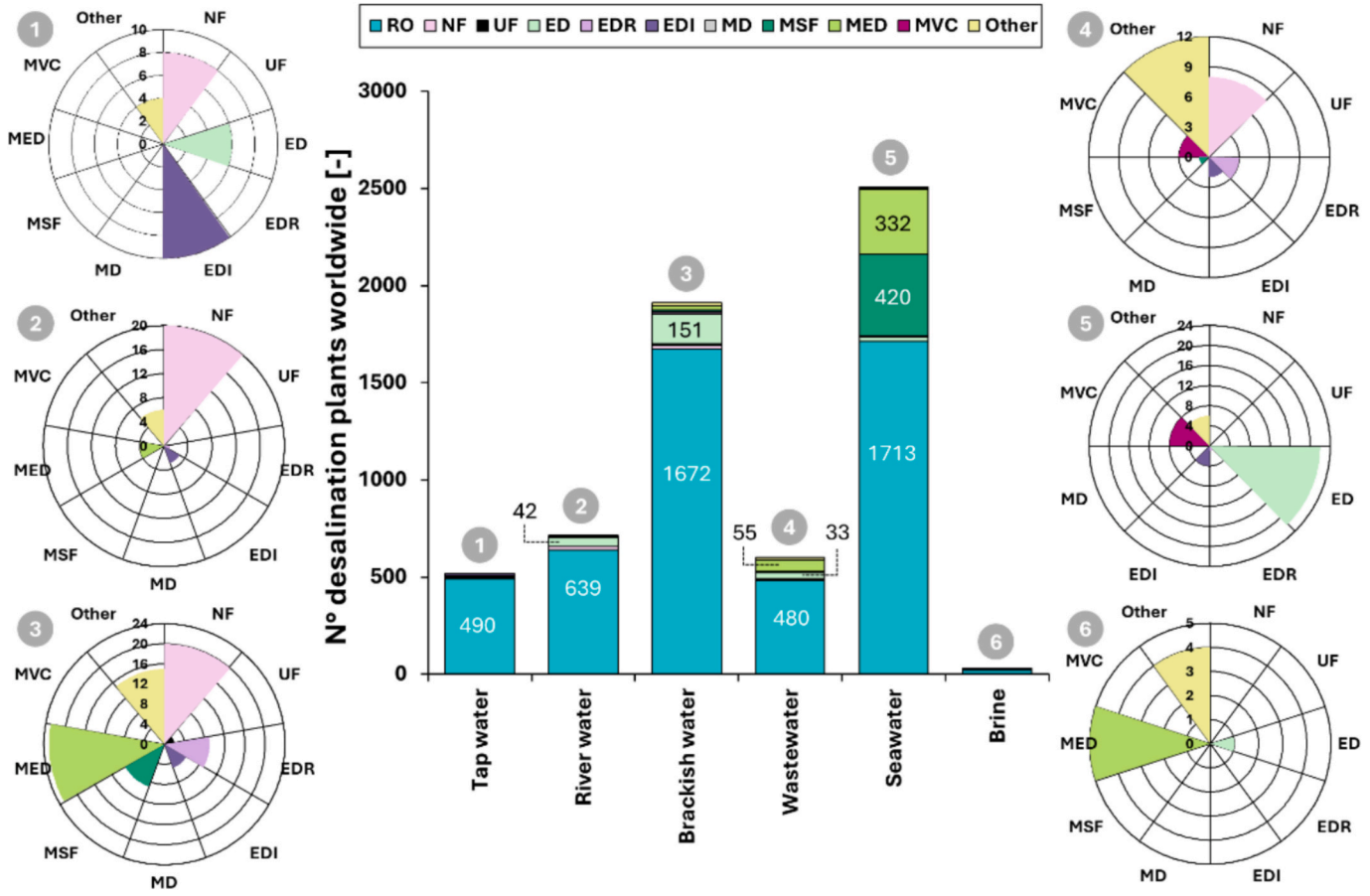

Fig. 3. Number of desalination plants installed worldwide categorised based on the feedwater source and technology. Rose diagrams 1–6 illustrate, for each feed source, the global distribution of desalination plants employing less common technologies.

significantly lower than RO and MED. Interestingly, MSF, a thermal-based counterpart to MED, is not employed for wastewater desalination. Fig. 4b–d depict the geographical distribution of desalination plants by technology across 13 sub-regions for the three main industrial sectors: power, refining/chemicals, and oil and gas. In the power industry (Fig. 4b), 51 % of wastewater desalination plants are located in North America, evenly split between RO and MED technologies. Other notable regions include Central Asia and East Asia. No plants with a capacity $\geq$2000 m^3/d are found in Latin America or Southern Europe. RO remains the dominant technology across all sub-regions, with the sole exception of Northern Europe, where only one MED plant is present.

In the refining/chemicals sector (Fig. 4c), the majority of plants (27 plants) are situated in East Asia, all employing RO except for one MED plant. No facilities are reported in Central America, Southeast Asia, or Southern Europe. RO is again the predominant technology, except in Latin America, where the only plant uses MED technology. The oil & gas industry (Fig. 4d) exhibits greater diversity in both technology and geographic distribution. Seven plants are located in North America, with the remainder spread relatively evenly across other regions, excluding Southeast Asia, Sub-Saharan Africa, North Africa, and Northern Europe, which have no installations. RO remains the most common technology. However, ED is the secondary technology in Latin America and Southern Europe, while MED holds that position in North America and the Middle East. Fig. S2 a-d in Supplementary Material (see Section S3) report the geographical distribution of the capacity of the wastewater desalination plants by technology across 13 sub-regions for the three main industrial sectors: power, refining/chemicals, and oil and gas.

In addition to the comprehensive analysis of industrial wastewater desalination plants, both in terms of technological classification and global geographical distribution, it is essential to examine in greater detail the status of BW and SW desalination plants. As BW desalination represents the second most widely employed method globally—both in terms of the number of operational plants and overall production capacity—a detailed analysis is provided in the Supplementary Material for conciseness. Specifically, the geographical distribution of BW desalination plants by technology across four primary end-user categories—industrial, agricultural (irrigation), military, and municipal (drinking water)—is illustrated in Section S4, Fig. S3a–d. Additionally, a global overview of BW desalination plants, classified by technology and customer type, is presented in Section S4, Fig. S3e–f. For completeness, the corresponding desalination capacity is also included in the Supplementary Material (Section S4, Fig. S4a–f). It is to be stated that the two feedwater sources, BW and SW, constitute the majority of desalination operations worldwide.

As with BW desalination, RO is the predominant technology for SW desalination (see Fig. 5), accounting for 68 % of plants (1655 facilities). However, this share is lower than that of BWRO plants globally (89 %), due to the broader application of thermal-based technologies in SW desalination—specifically, MSF and MED, which represent 17 % and 14 % of SW plants, respectively. ED plays a minimal role in SW desalination, comprising only 1 % (22 plants), primarily because ED is less technically efficient than RO when treating high-salinity feedwater.

In terms of customer distribution, SW desalination differs notably from BW. The majority of SW desalination plants serve municipal drinking water needs (56 %, or 1369 plants), followed by industrial applications (41 %). In contrast, the number of SW desalination plants for irrigation and military purposes is approximately half that of their BW counterparts.

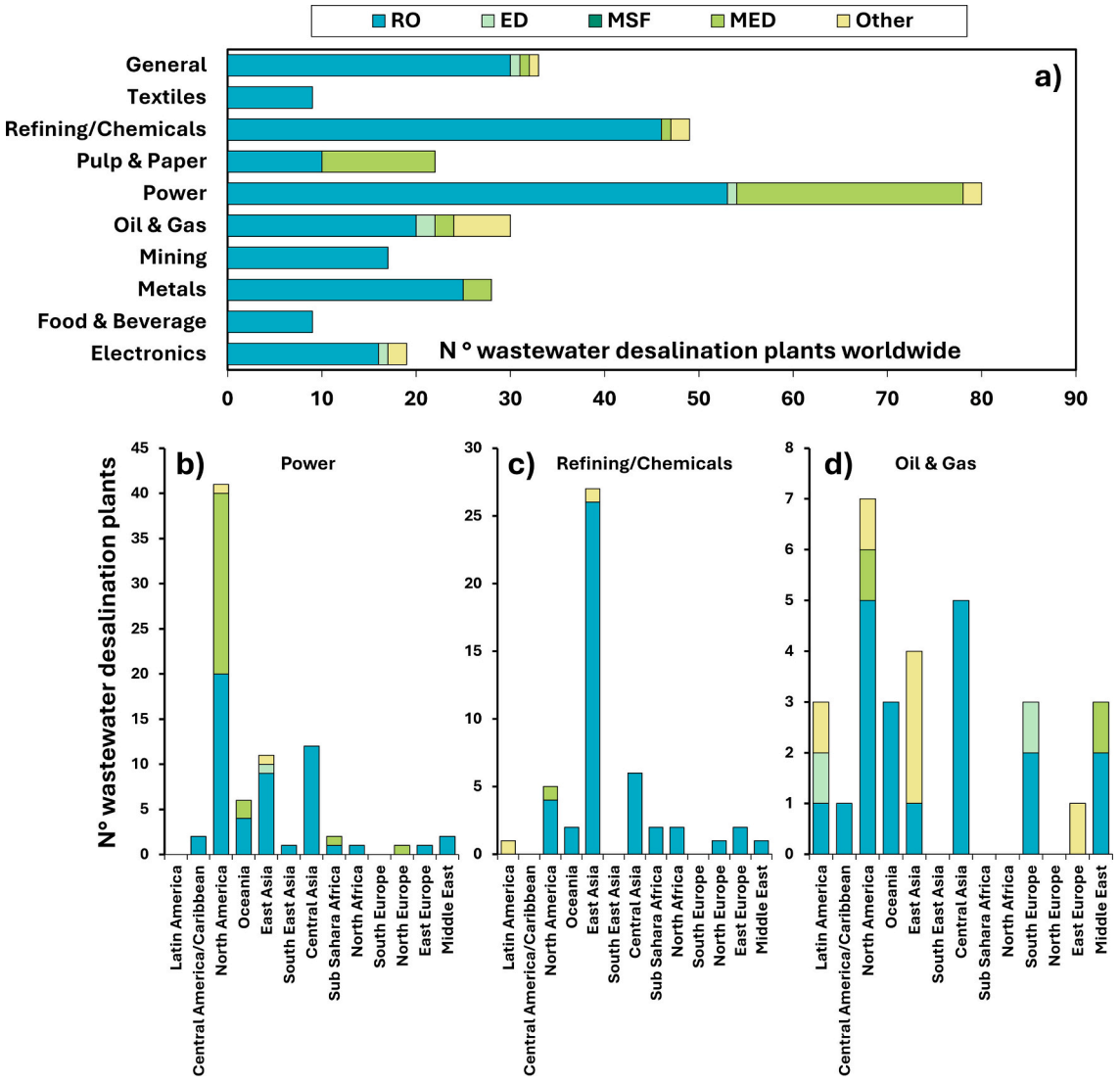

Fig. 4. a) Classification of wastewater desalination plants by technology installed worldwide across 10 industrial sectors; b) Geographical distribution of wastewater plants classified by technology within the industrial sector of Power (b), Refining/chemicals (c) and Oil and gas (d).

Geographically, within the industrial sector, RO remains the most widely used technology (58 % with 588 plants), but MSF and MED are also significantly employed (18.4 % and 20.4 %, respectively). Both membrane- and thermal-based technologies are distributed across all global sub-regions. Unlike BW desalination, where industrial plants are concentrated in East Asia and North America, SW industrial desalination is predominantly located in the Middle East (275 plants), with more than twice as many plants as in East Asia (130 plants), Central Asia (123 plants), and Southeast Asia (106 plants).

For irrigation, SW desalination plants are primarily located in Southern Europe, followed by the Middle East. In the military sector, SW desalination plants are mainly found in the Middle East (50 %). However, SW desalination for military use is also prominent in North Africa (27 %) and Central America (15 %) —regions where BW desalination is less common. While only MSF and RO are used for military purposes in the Middle East, Central America also employs MED.

Finally, for municipal drinking water production, most SW desalination plants are located in the Middle East (512 plants), followed by Southern Europe (237 plants), North Africa (219 plants), and Central America (141 plants). Fig. 5a-f, presented in terms of desalination capacity, are reported in Supplementary Material (Section S5, Fig. S5a-f).

In summary, notable differences exist between BW and SW desalination in terms of technology deployment, customer application, and geographical distribution. These distinctions highlight the influence of feedwater characteristics and regional needs on desalination strategies worldwide.

Given that the majority of global desalination capacity is dedicated to SW desalination, regardless of the end-user type, the authors subsequently focused on the potential for mineral recovery from brine generated during SW desalination. Specifically, the study aims to assess whether the volume of brine produced globally is sufficient to recover quantities of minerals that could meet or exceed current global production levels. Furthermore, it investigates whether any single subregion could independently satisfy global demand for all elements present in SW brine, or for specific elements.

This analysis provides, for the first time, a quantitative assessment of the feasibility of brine valorisation in terms of mineral recovery. It is important to note that for each mineral, the global demand does not solemnly depend on the factor of recovery volume. Purity is a critical factor, as many applications require minerals of specific quality standards. The achievable purity depends on both the concentration of target ions in SW/brine and the selectivity of the recovery technologies employed.

However, evaluating the potential purity of recovered minerals is

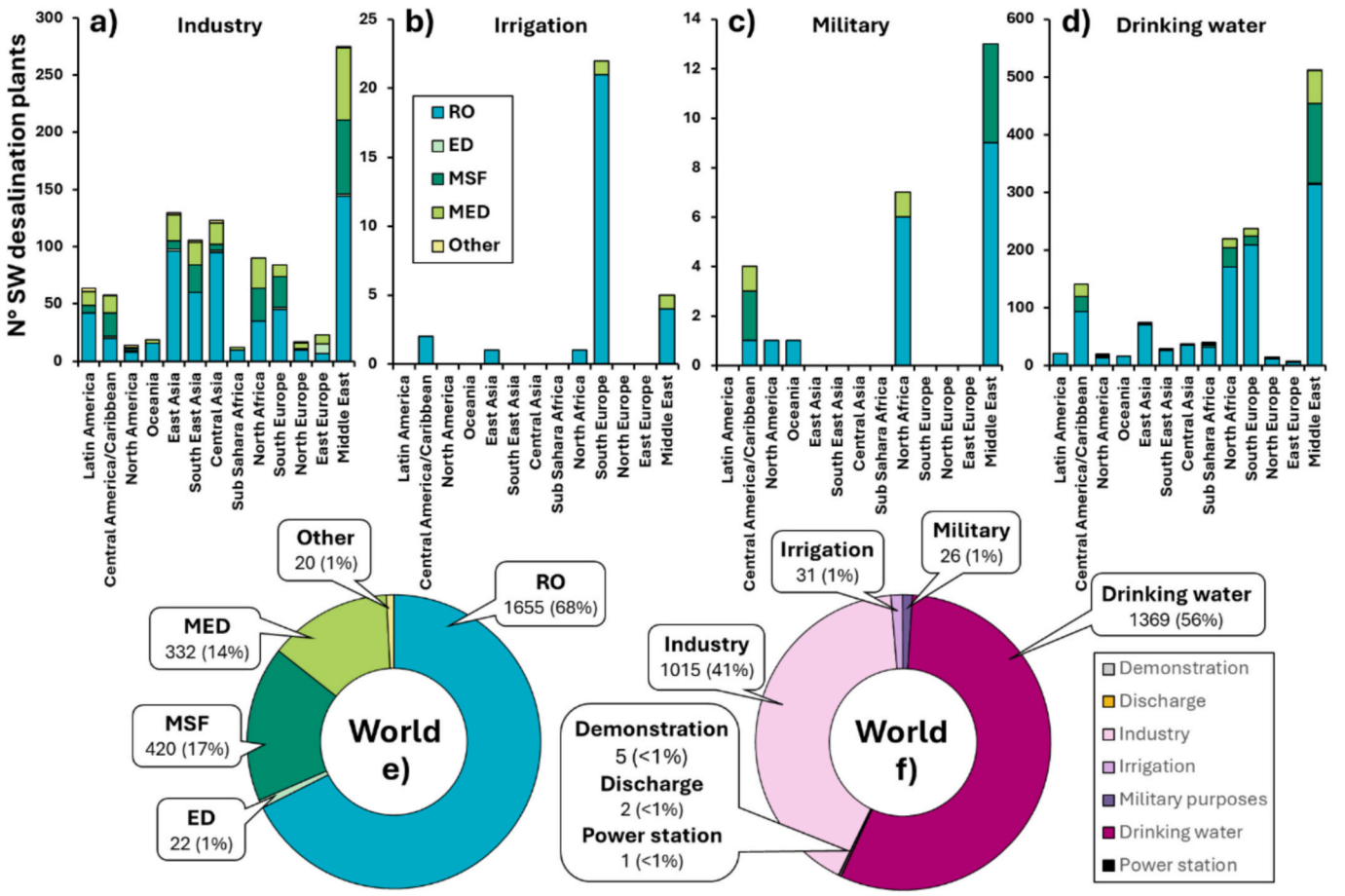

Fig. 5. Geographical distribution of SW desalination plants, classified by technology for industry (a), irrigation (b), military purposes (c) and drinking water (d). Global overview of SW desalination plants, classified by technology (e) and customer type (f).

particularly challenging, as current literature does not comprehensively report recovery technologies for all minerals, most studies focus on a limited subset. Consequently, a reliable comparison of technologies based on purity is not feasible at this stage. Therefore, this study concentrates on the global potential for mineral recovery from SW brine, an aspect not previously assessed in the literature.

The analysis incorporates data on both the number of SW desalination plants and their cumulative global capacity, as illustrated in Fig. 6a and b. Currently, there are 2449 SW desalination plants worldwide with a minimum capacity of 2000 m^3/day. As shown in Fig. 6a, 33 % of these plants are located in the Middle East, followed by Southern Europe (14 %) and North Africa (12 %). Regions with the fewest plants include Eastern Europe (1.3 %), Northern Europe (1.3 %), North America (1.4 %), and Oceania (1.5 %).

Interestingly, the distribution of SW desalination capacity (Fig. 6b) differs from the distribution of plant numbers. Over 60 % of global SW desalination capacity is concentrated in the Middle East, more than double its share of plant numbers, indicating that Middle Eastern facilities are not only numerous but also significantly larger in scale. A similar trend is observed in Oceania, where 1.5 % of the plants installed worldwide account for 2.3 % of the global capacity.

In contrast, regions such as North Africa, Central Asia, and East Asia show a modest decline in capacity share relative to plant numbers, suggesting the presence of large-scale facilities. Conversely, Northern and Eastern Europe exhibit capacity shares less than half their respective plant shares, indicating that desalination facilities in these regions are predominantly small to medium in size.

Once the global SW desalination capacity had been assessed, the potential volume of SW brine generated by these facilities was estimated based on two key assumptions regarding water recovery rates. These assumptions varied depending on the type of desalination technology employed. Specifically, for membrane-based technologies, a typical permeate recovery rate of 42.5 % was assumed, whereas a lower average recovery rate of 32.5 % was applied to thermal-based technologies. For SW desalination plants categorized as "other," where the specific technology was not identified, a conservative average recovery rate of 40 % was used.

Additionally, an average plant availability of 95 %, corresponding to 8322 operating hours per year, was considered. Fig. 7 presents the global geographical distribution of SW desalination brine production, detailing the volume generated by each desalination technology across various sub-regions. As anticipated from Fig. 6b, the Middle East emerges as the predominant source of SW desalination brine.

Notably, Fig. 7 highlights the technological diversity of SW desalination plants across different regions. The Middle East, East Asia, North America, and Central America exhibit a wide range of desalination technologies, encompassing both membrane-based processes (RO, ED and EDR) and thermal-based processes (MSF, MED, and MVC). In contrast, Oceania relies primarily on RO and MSF technologies for large-scale desalination.

Given its widespread adoption, RO accounts for the largest share of global SW brine production, generating approximately 69 million m^3/day, with 34.6 million m^3/day originating from the Middle East alone. RO is followed by MSF and MED, which produce 38.8 million m^3/day and 13.3 million m^3/day, respectively, both predominantly in the Middle East, where thermal desalination remains more prevalent than in other regions.

In comparison, ED, EDR, and MVC contribute with significantly

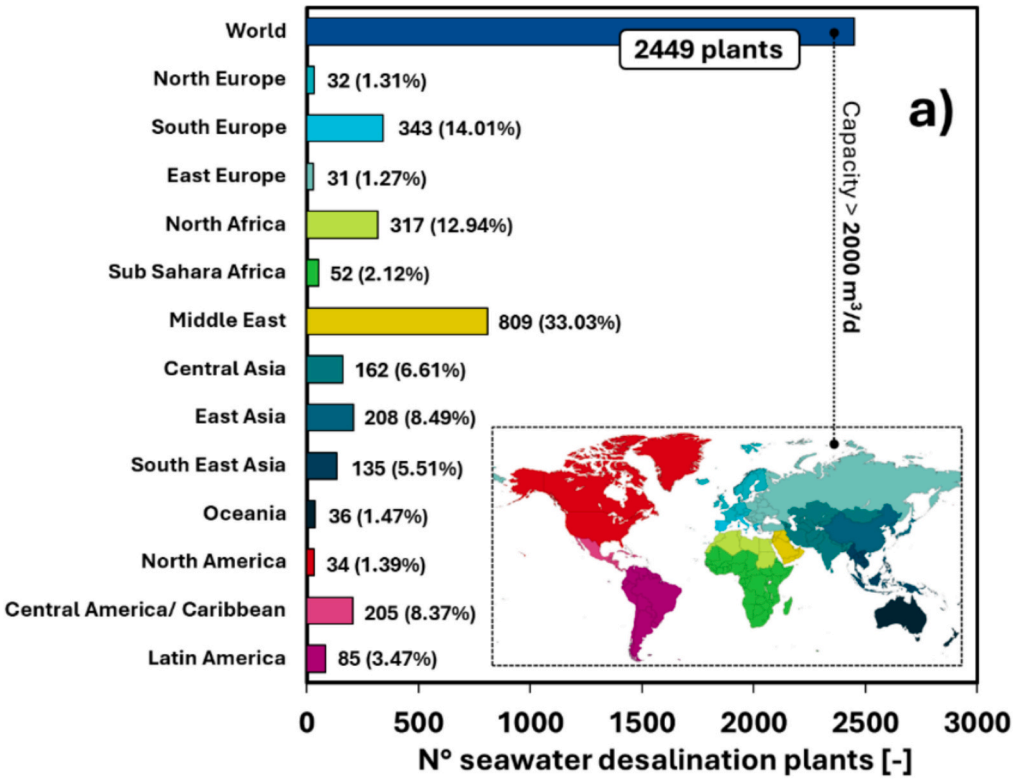

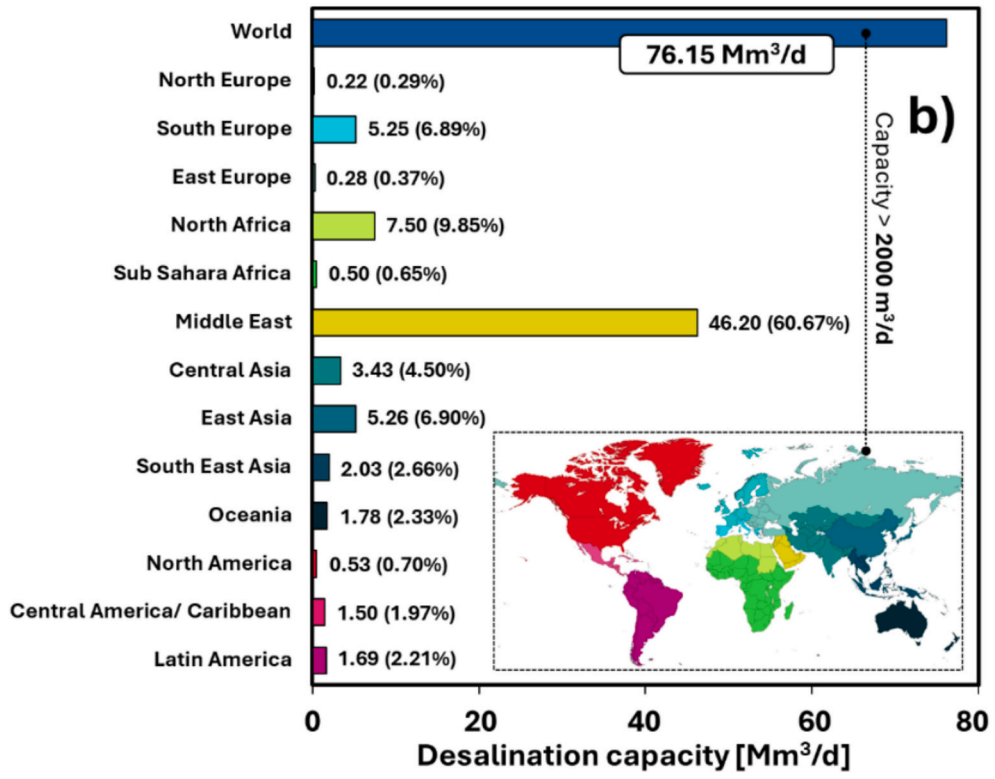

Fig. 6. a) Geographical distribution of the number of SW desalination plants worldwide with a minimum production capacity of 2000 m^3/d; b) Geographical distribution of the SW desalination capacity worldwide.

smaller volumes of SW brine, producing 104000 m^3/day, 2700 m^3/day, and 65500 m^3/day, respectively. Overall, global SW desalination activities result in a total brine output of approximately 121.2 million m^3/day.

Given the amount of SW brine produced in each region, the final step of the assessment involved estimating the quantity of minerals recoverable from brine and comparing these values with current production levels from conventional extraction methods. To ensure accuracy, it was

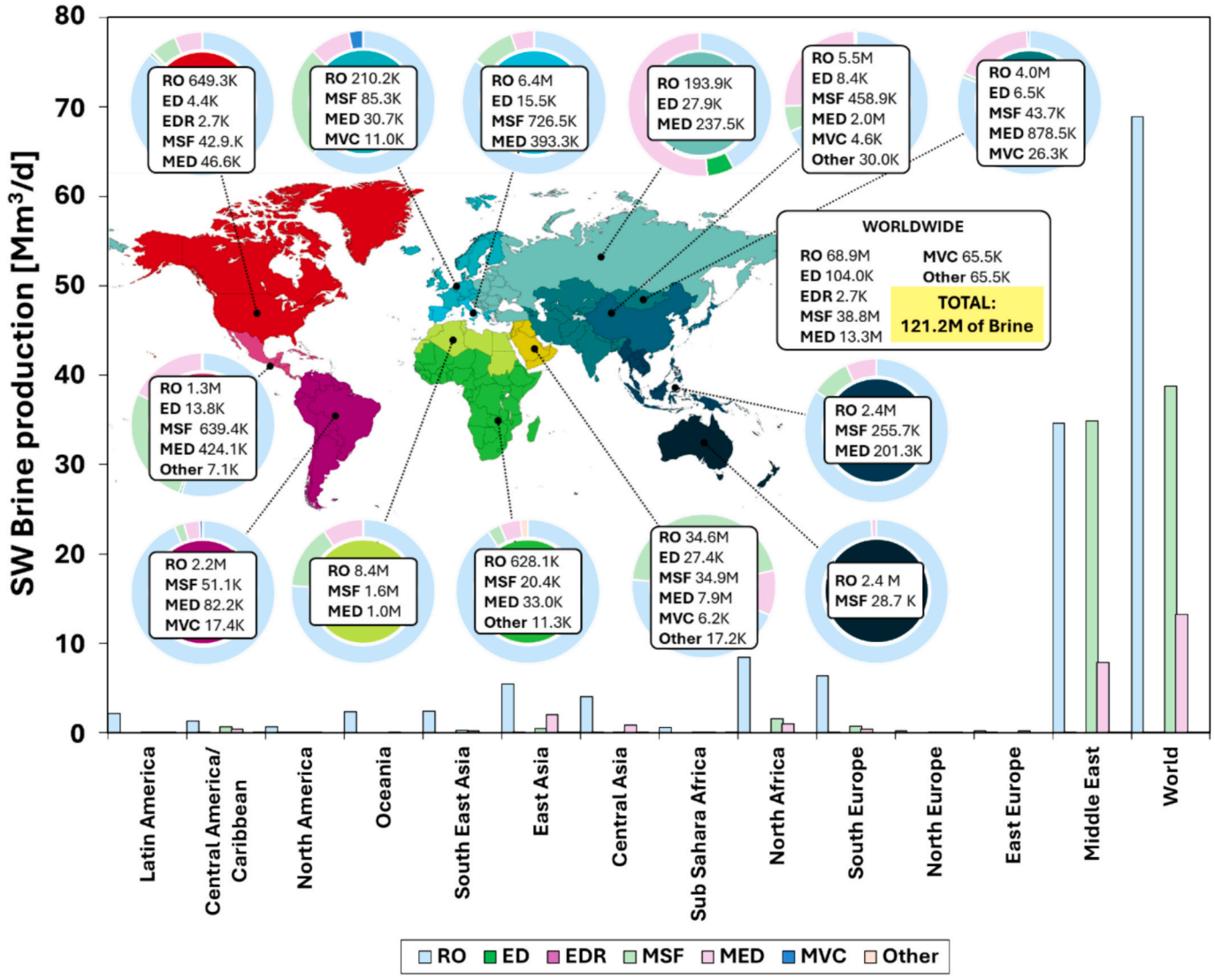

Fig. 7. Total SW brine production worldwide classified by region and applied desalination technology.

first necessary to determine the concentration of each target mineral in SW specific to each geographical region, as SW—and consequently its composition, varies across regions. For instance, the Baltic Sea exhibits the lowest salinity, while the Red Sea has the highest.

To obtain region-specific SW composition data, the open-source Sea4Value database was utilized [38]. The database provides detailed elemental compositions of SW across a wide range of global regions. Calculations to subsequently determine the specific quantities of each mineral that can be potentially recovered from SW desalination brine globally can be directly consulted in the Supplementary Material (see Section S6).

Fig. 8a, b, and c compare global production levels of various minerals with their corresponding potential yields from SW brine sources. The specific quantities are provided in Table S2 of the Supplementary Material (see Section S6). Notably, only a limited number of elements exhibit a potential recovery from brine that surpasses current production via conventional methods. These include Na, Ca, and Mg, elements typically abundant in SW, as well as several trace elements such as strontium (Sr), rubidium (Rb), beryllium (Be), palladium (Pd), scandium (Sc), and rhodium (Rh) among others.

In particular, the recovery of magnesium from SW desalination brine appears highly promising. The volume of brine generated is sufficient to potentially exceed the annual global production of Mg from conventional sources. Furthermore, in several sub-regions, the quantity of Mg recoverable from SW desalination brine alone is comparable to, or significantly greater than, that obtained through traditional extraction methods.

3. Technologies for desalination and resource recovery

Based on the preceding analysis, it is evident that the global production of SW desalination brine is comparable to the current worldwide output of only a limited number of minerals present in such brine, where these minerals are more accessible than in the case of SW due to higher concentrations and pre-treated conditions. However, it is equally important to identify the technologies capable of treating desalination brine and to determine which specific resources they can recover, whether individual minerals, salts, chemicals, or energy.

To this end, this section presents a comprehensive review of the technologies reported in the literature and employed to date, either individually or as part of integrated systems for SW and brine mining. For clarity and ease of comparison, the technologies are categorized into two main groups: (i) membrane-based and (ii) membrane-less technologies, and sub-categorised according to their primary driving force, as illustrated in Fig. 9.

Each technology presented in Fig. 9 can have a specific role in a ZLD/

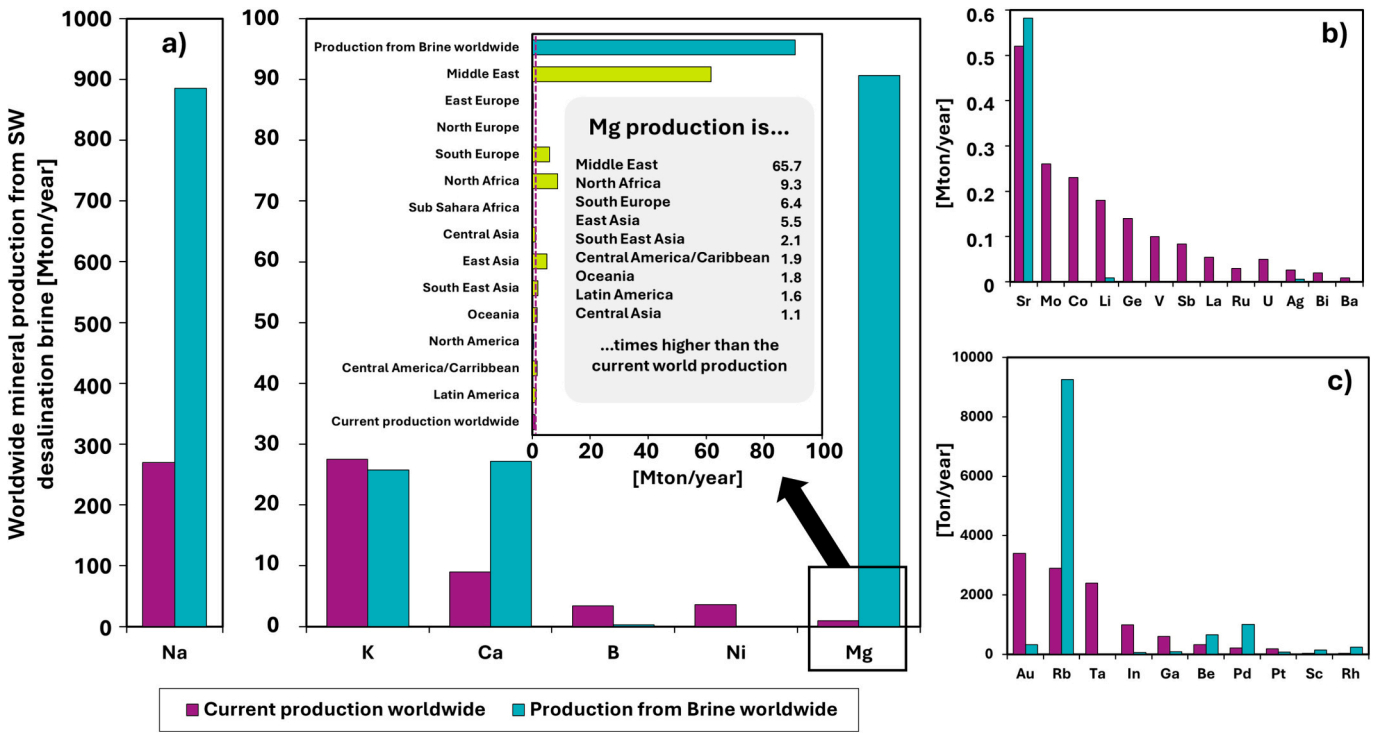

Fig. 8. Comparison between the current production worldwide and the potential production from SW brine worldwide for elements: a) Na, K, Ca, B, Ni, and Mg; b) Sr, Mo, Co, Li, Ge, V, Sb, La, Ru, U, Ag, Bi, Ba, and Au; and, c) Rb, Ta, In, Ga, Be, Pd, Pt, Sc, and Rh.

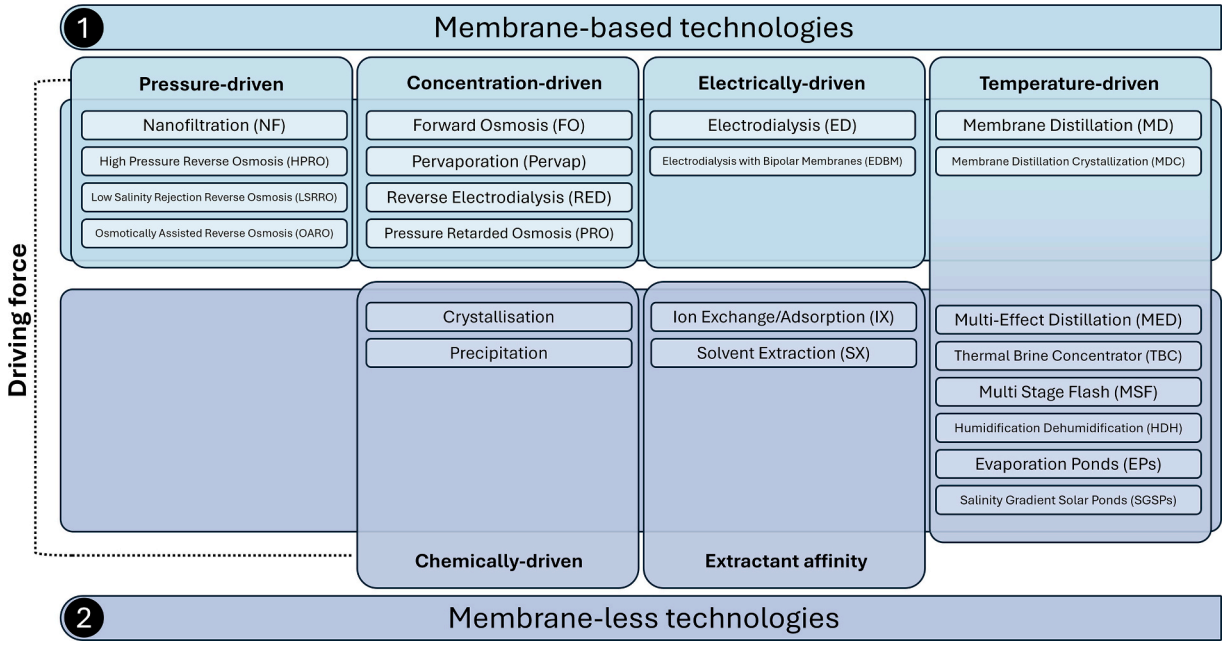

Fig. 9. Classification of the technologies assessed for desalination and resource recovery from brine within this work.

MLD scheme. For the case of membrane-based technologies, the selectivity of the NF membrane to separate ions allows for obtaining a NaCl-rich permeate stream, whereas multi-charged ions (i.e., Mg^{2+}, SO_4^{2-}) are concentrated in the retentate side. Other pressure-driven technologies, such as High-Pressure RO (HPRO), Low-Salinity Rejection RO (LSRRO), and Osmotically-Assisted RO (OARO), allow for brine concentration, whereas HPRO is also able to produce freshwater as permeate. Other technologies, such as Forward Osmosis (FO) are commonly integrated to treat wastewater, allowing the dilution of brine (or SW) prior to its discharge (or intake) to minimise brine discharge (or increase water recovery in a SWRO facility). Apart from that, if FO is used to treat the brine, it is possible to concentrate the ions in solution. MD and Pervaporation, both of which rely on the transport of vapour, allow for a secure source of freshwater while concentrating further the brine. Membrane Crystallisation (MDC) combines the features of MD reaching the saturation of a mineral phase, allowing its recovery as a solid. Moreover, energy can be targeted through membrane technologies, such as Reverse ED (RED) or Pressure Retarded Osmosis (PRO), that also

allow a partial dilution of the brine before its discharge. Electromembrane processes, such as ED, have a double feature, allowing both brine concentration and dilution, whereas Bipolar Membrane ED (BMED) also allows the production of chemicals (i.e., acids and bases).

Compared to membrane-based technologies, thermal-based processes as MED, Thermal Brine Concentrator (TBC), and MSF rely on the evaporation of water from brine, followed by its condensation. Therefore, it is possible to recover water apart from concentrating the brine further. Humidification Dehumidification desalination (HDH) and EPs rely on the natural evaporation of brine, allowing only the brine to concentrate and the minerals to precipitate as a mixture of different salts. With membrane-less technologies, Salinity Gradient Solar Ponds (SGSPs) can be applied to target energy from waste brines. Within this group, it is of great importance to use ion-exchange (IX) and solvent extraction (SX), which allow the selective removal (or recovery) of a dissolved ion. Finally, salts can be recovered by crystallization technologies, which exploit controlled supersaturation to precipitate dissolved ions into solid crystalline minerals.

3.1. Membrane-based technologies

3.1.1. Pressure-driven

3.1.1.1. Nanofiltration (NF). NF (molecular weight-cut off: 200–1000 Da, trans-membrane pressure: 4–30 bar) is a pressure-driven membrane process that exhibits traits of both UF (1–1000 kDa, < 5 bar) and RO (<200 Da, 10–70 bar) membranes. NF membranes have a high rejection rate for multi-charged ionic species (over 90 %), while single-charged ions can pass through the membrane to a large extent. There is ongoing debate about the structure of NF membranes; some propose that they have a dense configuration, similar to RO membranes (featuring a free-volume rather than fixed pores), while others argue they contain fixed pores akin to UF membranes. In the first scenario, the transport of species across the membrane relies on differences in diffusivities through the active layer. In contrast, in the latter case, size or steric hindrance serves as the primary exclusion mechanism [39]. Commonly, NF processes can be applied from BW (0.5–1.0 g/L TDS) to brines (60-80 g/L TDS), and the literature covers different case studies, ranging from laboratory to pilot plant scale. For simplicity, Table 1 presents examples of NF applications to SW and SWRO brines.

NF has been widely applied for pre-treating SW before any other desalination technology, whether membrane-based or thermal-based. The main purpose of such an application remains in the possibility of removing the typical scalant species, which provides the possibility of increasing water recovery in the following desalination unit [18,40,41,44–49]. For example, Hamed et al. [40] reported a 53-57 % water recovery for the NF unit at 24 bar when treating SW. The permeate (32 g/L NaCl, 154 mg/L Ca^{2+}, 225 mg/L Mg^{2+}, 75 mg/L SO_4^{2-} and 47 mg/L alkalinity) was later treated with RO, which allowed for the recovery of 45 % of water. The last stage, based on MSF treating 61 g/L TDS at a top brine temperature of 130 °C, provided a 68 % water recovery with no evidence of mineral deposits for 970 h of operation. Additionally, Kaya et al. [41] compared the performance of NF270 and NF90 for pre-treating SW in a RO desalination facility. Results showed that NF270 provided higher fluxes than NF90 (65.8 and 19.0 L/(m^2·h), respectively at 30 bar). Nevertheless, NF90 reported high rejection

Table 1
Application of nanofiltration for treating SW and SWRO brines. n.d.: no data

Water composition	Operating conditions	Membranes tested	Achieved results		Reference
			Rejections	Flux (L/(m^2·h))	
SW (pretreatment before RO and MSF)	24 bar 53-57 % permeate recovery	n.d.	• Sulphate: 97.7 % • Calcium: 68.6 % • Alkalinity: 54.3 % • TDS: 26.4 %	n.d.	Hamed et al. [40]
SW (pretreatment before RO)	30 bar	NF90 (DuPont)	• >95 % for SO_4^{2-}, Ca^{2+} and Mg^{2+} • 45-56 % for Na^+, K^+, and Cl^-	19.0	Kaya et al. [41]
		NF270 (DuPont)	• >97 % for SO_4^{2-}, Ca^{2+} and Mg^{2+} • 15-22 % for Na^+, K^+, and Cl^-	65.8	
SW (pretreatment before RO)	8 - 30 bar	DK (Veolia)	• > 95 % for SO_4^{2-} and for Mg^{2+} • > 85 % for Ca^{2+} • > 92 % for Sr^{2+} • <40 % for Na^+, K^+, and Cl^- • <10 % for B	11.5–89.3	Morgante et al. [18]
SWRO desalination brines	30 bar	NF270 (DuPont)	• > 97 % for SO_4^{2-} • 81 % for Mg^{2+} • 65 % for Ca^{2+} • 15-26 % for Na^+, K^+, and Cl^- • 9 % for B	102.6	Figueira et al. [42]
		Fortilife XC-N (DuPont)	• > 97 % for SO_4^{2-} • 94 % for Mg^{2+} • 82 % for Ca^{2+} • 24-35 % for Na^+, K^+, and Cl^- • 10 % for B	67.4	
		PRO-XS2 (Hydronautics)	• > 97 % for SO_4^{2-} • 94 % for Mg^{2+} • 80 % for Ca^{2+} • 28-31 % for Na^+, K^+, and Cl^- • 3 % for B	70.2	
SWRO desalination brines	18 bar 10 - 80 % permeate recovery	VNF (Vontron)	• 99.1-98.6 % for SO_4^{2-} • 96.3-94.6 % for Mg^{2+} • 88.9-81 % for Ca^{2+} • 27-6 % for Na^+, K^+, and Cl^- • 4-2 % for B	n.d.	Morgante et al. [43]
		NFX (Synder)	• 99.3-97.9 % for SO_4^{2-} • 99.1-97 % for Mg^{2+} • 96.6-89.9 % for Ca^{2+} • 30-2 % for Na^+, K^+, and Cl^- • 11-6 % for B	n.d.	

values (>95 %) for SO_4^{2-}, Ca^{2+} and Mg^{2+}, and values within 45-56 % for Na^+, K^+, and Cl^-. In contrast, NF270 showed similar rejection values for SO_4^{2-}, Ca^{2+} and Mg^{2+} (>97 %), but lower for Na^+, K^+, and Cl^- (15-22 %). Overall, the authors concluded that the combination of NF90 and SW30 (RO membrane) was better in terms of final permeate quality. Similarly, Morgante et al. [18] tested polymeric NF membranes (NF90, NFS, NFX, VNF and DK) with SW under flat-sheet configuration, revealing the outstanding performance of Desal DK in terms of hydraulic permeability (3.5 L/(m^2·h·bar)) and selectivity of monovalent over multivalent elements. More precisely, rejections exceeded 95 % for Mg^{2+}, 85 % for Ca^{2+} and 92 % for Sr^{2+}, while the ones for single-charged ions remained below 40 % (Na^+, K^+, and Cl^-). In this case, B rejections remained lower than 10 % because of its presence as a neutral species, namely $H_3BO_{3(aq)}$.

In addition, NF has been postulated as pretreatment for the SWRO desalination brines, to fractionate the different elements, before an MLD or ZLD scenario, allowing also to increase the concentration of multi-charged ions [42,43,50–56]. Gilabert-Oriol et al. [53] evaluated the performance of two selective NF membranes (SWRO-100 and SWRO-150) to obtain a NaCl-rich permeate from SWRO brine at a fixed recovery of 58 %. The SWRO-100 showed the possibility to reject 96 % Mg^{2+}, 85 % Ca^{2+} and 98 % SO_4^{2-}, whereas rejection values for Na^+ and Cl^- remained around 10 % and 20 %, respectively, at 26 bar. Similar values were achieved for the SWRO-150 working at 23 bar, but slightly lower for Mg^{2+} (94 %), Ca^{2+} (80 %), and Na^+ (5 %). Finally, a permeate, containing 77 g/L NaCl was treated in the SWBR-200 RO membrane, which allowed the stream to be concentrated up to 95 g/L, working at 70 bar with a permeate recovery of 26 %. The performance of the conventional NF270 was evaluated with respect to two advanced NF membranes (PRO-XS2 and Fortilife XC-N) that maximize membrane selectivity [42]. All the membranes provided high rejections for SO_4^{2-} (>97 %), whereas significant differences were found for Ca^{2+} (65 % for NF270, 80 % for PRO-XS2 and 82 % for XC-N at 30 bar) and Mg^{2+} (81 % for NF270, 94 % for PRO-XS2 and 94 % for XC-N at 30 bar). In the case of single-charged elements, Na^+ and Cl^- rejections remained below 25 % at 30 bar. In addition, a decrease in rejections, and therefore membrane selectivity, was reported working at high permeate recovery values [56]. Recently, Morgante et al. [43] tested the VNF and NFX to treat SW and SWRO brine in concentration mode. The NFX rejected effectively both Mg^{2+} (>97 %) and Ca^{2+} (>90 %), whereas single-charged ions permeated freely (<30 %). As a result, after 80 % of permeate recovery at 20 bar, concentration factors of 4.9 and 1.9 were achieved for multi-charge and single charge elements when treating the SWRO brine. The VNF presented a similar behaviour but exhibited slightly lower rejection values. A final economic analysis revealed that NFX is the preferred choice if $Mg(OH)_2$(s) is recovered from the concentrate (purity higher than 97 %).

In addition, the combination of NF with other technologies has been evaluated when treating BW, to remove the double charge ions and increase water recovery [57–62]. For instance, Song et al. [58] reported TDS rejection values of 30 % and 20 % for DK (14 bar) and DL (12 bar), respectively. More in detail, SO_4^{2-} was rejected by more than 95 %, whereas the carbonate rejection took values of 80 % and 75 % for DK and DL. With regard to the cations, Mg^{2+} and Ca^{2+} were rejected by 65 % and 40 %, respectively. Elazhar et al. [62] evaluated the integration of NF and RO in a 2-pass process, reporting that NF270 achieved a 60 % water recovery with rejections of 45 % for Mg^{2+}, 40 % for Ca^{2+} and 42 % for Cl^-. The blending of the NF permeate with the RO permeate allowed for meeting drinking water standards, resulting in an overall water recovery of 94 %, with a specific energy consumption (SEC) of 0.055 kWh/m^3 of drinking water.

Moreover, the implementation of NF within ZLD and MLD scenarios has been evaluated in the literature at pilot plant scale [48–51]. For instance, Al-Amoudi et al. [48] proposed a treatment train to reach NaCl saturation from SW. The first unit is devoted to the NF unit (16 m^3/h), which allowed the production of a NaCl-rich permeate that was later concentrated by RO-based technologies. With a different focus, Morgante et al. [49] proposed recovering $Mg(OH)_2$(s), $Ca(OH)_2$(s), NaCl (s), and water by integrating NF, a reactive crystalliser, MED, EPs, and BMED. The authors tested Synder NFX 4040 membranes treating 2.46 m^3/h in a 2-pass configuration. The authors reported the possibility of recovering 69 % water, exhibiting rejections higher than 97 % SO_4^{2-}, Ca^{2+} and Mg^{2+}, with values below 20 % for Na^+, K^+, and Cl^-. In addition, NF has been evaluated as pretreatment for BMED [50] and ED [51] from SWRO desalination brines, with the main target to remove both Ca^{2+} and Mg^{2+}.

However, one of the main drawbacks of NF is fouling, which is usually prevented in NF by pre-treating the feed solution with UF or MF to remove colloids, suspended particles and microorganisms, whereas scaling is usually prevented by adding anti-scalants or by pre-treating the solution to remove hardness. Membrane cleaning can be divided into physical and chemical methods. Physical methods, often used to remove fouling, involve backwashing or ultrasonic-assisted cleanings. Chemical cleaning, using sodium hypochlorite or citric acid, relies on reactions with the foulants, but they can compromise membrane stability in the long term [63]. For instance, Su et al. [60] reported the need to perform chemical cleanings using 2 % citric acid and NaOH (pH = 10) during BW treatment. Acidic cleanings were reported to be the most effective, suggesting that scaling potential (mainly related to Ca^{2+}) was more severe than fouling. Similar findings were reported by Wafi et al. [61] when treating saline groundwater, revealing scaling related to $CaCO_3$(s) for both NF and RO, which implied the use of chemical cleanings. Telzhensky et al. [64] reported the possibility of reaching water recoveries of 60-64 % when treating SW without the occurrence of scaling associated to gypsum. However, the SW must be acidified to pH values of 6.7-6.9 to avoid the precipitation of aragonite. Song et al. [65] studied fouling behaviour in a 3-stage NF when treating a RO brine within a ZLD scheme. The authors reported that fouling affected differently in each stage, being: i) organic fouling at the first stage, which was removed by alkaline cleanings; ii) scaling (mainly $CaCO_3$(s)) took place at the fouling layer of the second stage, which required a combination of an acidic and alkaline cleanings; and, iii) an irreversible silica and ferric scaling at the last stage. When analysing the inlet brine, four main foulants were detected: biopolymers (10–50 kDa), humic acids (0.8-1.5 kDa), hydrolysates of humic acids (0.5-0.8 kDa), and neutral organics (<0.25 kDa). Therefore, the complexation of ferric iron by humic acids was the cause of the irreversible fouling detected in the last stage.

Another drawback of the technology is its low selectivity when separating target ions using NF. For instance, Telzhensky et al. [64] aimed at separating Mg^{2+} from SW for further processing. Among the membranes evaluated, Desal DL showed good selectivity, rejecting Mg^{2+} and Na^+ by 84 and -2 %, respectively, at 14 bar and 50 % water recovery. However, when evaluating the effect of permeate recovery from 10 to 78 %, a significant decrease on rejections was observed for all the ions, from 28 % to 6 % for Cl^-, from 33 % to 3 % for K^+, from 4 % to 3 % for Na^+, from 100 % to 38 % for Ca^{2+} and from 100 % to 71 % for Mg^{2+}. This decay in rejections with the water recovery caused lower molar ratios of Cl^-/Mg^{2+} and Na^+/Mg^{2+}. Similarly, Hubach et al. [66] evaluated how to selectively separate Mg^{2+} from Li^+ when treating SW and SWRO brines. Among the membranes evaluated, NFAL provided the highest selectivity lithium to magnesium (10.5 at 30 bar and 12.5 at 20 bar). In addition, it was reported that Mg^{2+} and Ca^{2+} rejections were independent on applied pressure (being 90 % and 85 %, respectively), but the ones for Li^+ were dependent and ranged from -10 % at 20 bar to 20 % at 30 bar. Moreover, Xu et al. [52] concluded that NF separated NaCl in an optimal way due to its low energy use and higher separation capacity. However, if NaCl must be concentrated, ED is the preferred choice.

One option commonly adopted to improve the membrane selectivity is the application of Dia-Nanofiltration (Dia-NF), where low-TDS water is fed to the inlet of the NF to improve the rejections of multi-valent ions. For instance, Nativ et al. [67] evaluated the use of Dia-NF to treat SW or

SWRO brine to remove the monovalent ions as much as possible, leaving pure Mg^{2+} in the concentrate. During tests, the diluting solution was added to the feed tank, keeping a constant volume along the test, and data was related to cycles, which correspond to the volume of diluted solution referred to the initial brine. In the case of SW, working at 70 % recovery and 15 bar, after 3 cycles, the brine had a final concentration of 3.35 g/L Mg^{2+}, with a low presence of Na^+ (0.39 g/L) and Cl^- (5.09 g/L). In addition, as both Ca^{2+} and SO_4^{2-} were concentrated (0.76 g/L and 9.92 g/L, respectively), the dosage of anti-scalants was required. Similar results were achieved in the case of the SWRO brine, where after 2.10 cycles at 15 bar and 60 % recovery, the resulting brine contained 5.22 g/L Mg^{2+}, 0.05 g/L Na^+, 8.32 g/L Cl^- and 13.69 g/L SO_4^{2-}. In another work, Nativ et al. [68] evaluated the integration of Dia-NF and ED to produce a Mg^{2+} rich solution from SW. As the initial pretreatment step, the SW was treated with NF to reach a recovery ratio of 75 % prior to Dia-NF. In the Dia-NF stage after 3 cycles, it was possible to keep constant the concentrations for Mg^{2+} (5.18 g/L), Ca^{2+} (1.27 g/L) and SO_4^{2-} (12.74 g/L), whereas the concentrations of Na^+ and Cl^- decreased to 2.21 g/L and 11.46 g/L, respectively. Truong and Chong [69] reported that when treating SW, a RO-DiaNF is preferred over a DiaRO-NF as it provides higher Mg^{2+} recovery (up to 10 %), higher selectivity Mg^{2+}/Na^+ (up to 30 %), and lower scaling risk (gypsum saturation index below zero). In a later work [70] they concluded that a 4-stage DiaNF-RO design was the optimum one, which allowed for reaching a maximum selectivity Mg^{2+}/Na^+ of 12 with a SEC of 5.72 kWh/m^3. A minimum of SEC could be achieved (5.41 kWh/m^3), which resulted in a selectivity of 7.

As a conclusion, NF has emerged as a versatile and effective membrane technology for water treatment and desalination, being exploited as a pretreatment step for SW before more energy-intensive desalination processes. This is supported by the high rejection of multivalent ions, which helps mitigate the risk of scaling and corrosion in subsequent treatment stages, thereby enhancing overall system efficiency and water recovery rates. However, its performance is significantly influenced by solution composition and membrane properties, which may impact its performance. Similar to other membrane processes, scaling might limit its operation performance. Despite that, NF has a huge potential for brine management, allowing for the selective separation of NaCl, which can be later used for salt or chemicals (via BMED) production, apart from concentrating target elements that can be later recovered (i.e. Mg^{2+}).

3.1.1.2. Reverse osmosis (RO)-based technologies

3.1.1.2.1. High-pressure reverse osmosis. RO is the preferred technology for desalination, as demonstrated via the comprehensive analysis reported in Section 2. However, its application is limited when treating high salinities (>75 g/L). Recently, membrane suppliers have been offering the possibility of using High-Pressure RO (HPRO), which allows for operation at high pressures (up to 140 bar). However, most of the published works show that the technology is at an early stage, being mostly related to modelling [71–74].

For instance, Davenport et al. [71] outlined the potential of HPRO to desalinate brines. The authors reported a SEC of 7.3 kWh/m^3 to concentrate a brine from 50 to 250 g/L using HPRO, which is significantly lower than that of a 2-stage MVC (24 kWh/m^3). Nevertheless, the simulations revealed the need to operate at pressures up to 300 bar, which remains challenging due to the limitations of membrane materials and module design. Considering this limitation, operating at 150 bar and combining it with an MVC will result in a SEC of 12 kWh/m^3. Similarly, Anvari et al. [72] studied whether it is feasible to reach a brine containing 250 g/L NaCl from pre-treated SW with NF (32 g/L NaCl) by using a three-stage process combining RO, HPRO and ultra-HPRO (UHPRO). The simulation results showed that HPRO, operating at 120 bar, could concentrate the brine up to 100 g/L. If this brine is treated with a single stage of UHPRO at 200 bar, it is possible to achieve 200 g/L at a competitive cost (<10 kWh/m^3). With a similar approach, Touati and Mulligan [73] evaluated the management of RO brines using HPRO with a 2 or 3-stage system to reach 90 % and 95 % of water recovery, respectively. SEC was minimized with a 3-stage configuration (4.62 kWh/m^3). Moreover, the permeate recovery of the first RO stage was a critical parameter when determined the levelized cost of water (LCOW). The lowest value was achieved with a 2-stage system (0.72 USD/m^3) after fixing the water recovery in the first stage to 68 % (90 % overall water recovery).

Nevertheless, there are some major concerns about the application of HPRO, especially when high salinities must be reached, which can imply operating pressures within 300 and 400 bar [72]. One of the main concerns is the membrane compaction at such high pressure, which can deform the polymeric networks, leading to a denser and impermeable film. Moreover, it is of high relevance to study transport mechanisms at such pressures, especially that of salt permeability, as it is expected to increase at high salinity due to lower electrostatic repulsions [71]. Similar outcomes were pointed out by Wu et al. [74], who reported that water permeance decreased when increasing pressure from 14 to 207 bar. Membrane analyses revealed that apart from a permanent thickness reduction of the poly-sulphone support (38-60 %), their skin layer pores also collapsed. Additionally, the high-porosity permeate carrier damaged the membrane at high pressure, resulting in higher salt passage. In fact, it was reported that the polyamide film was torn apart in some areas. Moreover, the design of new spacers must also consider the need to reduce polarization effects at such high salinity [72].

In conclusion, the need for a more robust membrane structure to prevent compaction and skin layer pore collapse, as well as to redesign the permeate carriers to avoid membrane damage, is highlighted. From an economic perspective, other RO-based processes, such as Low Salinity Rejection RO (LSRRO) and Osmotically Assisted RO (OARO), can offer lower costs due to the lower operating pressure, despite needing a more complex process design and operation.

3.1.1.2.2. Low salinity rejection reverse osmosis. LSRRO is a novel RO process designed to reach hypersaline brines (i.e. close to NaCl saturation), which, due to their low salinity rejection, can produce a permeate stream with high TDS. Similarly to RO, the membranes used are made of polyamide, but the synthesis process is modified to vary the salt permeability, thus enabling lower salt rejections. This reduces the osmotic pressure difference across the membrane, requiring a lower hydraulic pressure. As a result, they can operate at a similar pressure to conventional SWRO processes, thereby enabling lower SEC. Commonly, the permeate from the LSRRO stage is used to dilute the feed from the previous stage, whereas the retentate is fed to the next stage [26]. Similar to the last case, the technology is at an early stage, with most of the work related to modelling efforts, although the LSRRO has been evaluated at the pilot plant scale.

The effect of osmotic pressure differences and concentrations on NaCl rejections when using LSRRO to concentrate NaCl solutions up to saturation was studied by Bargeman [75]. Both parameters affected the rejections, with lower values observed at larger NaCl concentrations, whereas high osmotic pressure differences resulted in higher rejections. For example, with a 0.1 wt% NaCl and an osmotic pressure difference of 30 bar, it can be possible to achieve rejections of 30 %, which would increase to 90 % if osmotic pressure difference increased to 70 bar. Moreover, rejections of 10 % and 20 % are expected for osmotic pressure differences of 30 and 70 bar, respectively, when working with 20 wt% NaCl. Overall, the simulations performed demonstrated the possibility of exploiting the dependence of NaCl rejection to transition from 70 g/kg or 180 g/kg to saturation.

Most studies have evaluated the application of LSRRO to reach hypersaline brines from a theoretical perspective [26,76–78]. For instance, Wang et al. [26] proposed a multi-stage treatment to reach a salinity higher than 234 g/L without using high pressures (<70 bar). Although the results showed the need for at least three stages to reach NaCl saturation, implementing a fourth stage allowed for a reduction in SEC. For example, SEC values were 2.92 and 15.74 kWh/m^3 (0.1 and 1 mol/L

NaCl, respectively) with a 3-stage configuration and decreased to 2.39 and 7.98 kWh/m^3 (0.1 and 1 mol/L NaCl, respectively) with a 4-stage configuration. Similarly, Atia et al. [76] optimized the LCOW from a techno-economic perspective when integrating RO and LSRRO. Three different scenarios were evaluated, differing in the feed salinity and the target water recovery (35 g/L and 70 % recovery, 70 g/L and 55 % recovery, and 125 g/L and 35 % recovery). The RO, acting as the first stage, provided rejections higher than 98 % with fluxes ranging from 11.5 to 14.9 L/(m^2·h) (85 bar), depending on the salinity. The brine from the RO unit was then treated with the LSRRO, showing rejections varying from 51 % (1 stage, 35 g/L feed solution) to 20.5 % (4 stages, 125 g/L feed solution), and permeate fluxes higher than the RO (14.8-17.9 L/(m^2·h), 65 bar). Additionally, the levelized costs of water were found to be 0.70, 1.89, and 7.41 USD/m^3 for 35, 70 and 125 g/L TDS, respectively. In addition, Naderi Beni et al. [77] developed a stage process that integrates LSRRO membranes to desalinate high-saline streams (>70 g/L). The use of batch-LSRRO offered the possibility to reduce the SEC of conventional LSRRO by 38-73 %. For example, a 4-stage batch LSRRO showed SEC ranging from 1.07 to 6.96 kWh/m^3 to concentrate 0.1-1 mol/L solutions to 4 mol/L. Zhao et al. [78] evaluated the integration of LSRRO membranes in RO desalination facilities. For the case of BW, water recovery could be increased from 71 % to 86 % (15 bar, 5 g/L TDS), implying an increase up to 1.0 kWh/m^3, although it can be decreased to 0.88 kWh/m^3 at 82 % recovery. For SWRO facilities, water recovery can be increased from 48 % to 74 % (60 bar, 35 g/L TDS), resulting in an increase in SEC from 2.96 kWh/m^3 to almost 5 kWh/m^3.

An experimental study on LSRRO at the pilot plant scale developed by Van Houghton et al. [79] investigated the effect of salinity, ranging from concentrated BW (36 g/L) to hypersaline brines (133 g/L), using a 3-stage LSRRO unit. The pilot plant results indicated the potential to achieve a concentration of 148 g/L when treating the BW. As a result, a 64 % water recovery was achieved with average permeate fluxes in the range 14-22 L/(m^2·h) at 75 bar. When treating the hypersaline brine, a water recovery of 195 g/L (32 % water recovery) was achieved, but with lower permeate fluxes (in the range of 9-15 L/(m^2·h) at 75 bar).

LSRRO offers a significant advantage over conventional methods in concentrating saline streams, utilising energy more efficiently. Apart from that, the fact of operating at lower pressure avoids membrane deformation. However, further knowledge is needed to enhance the implementation of LSRRO units. Specifically, concentration polarization at high salinity could diminish the efficiency of the process, increasing OPEX, apart from causing scaling at the membrane surface.

3.1.1.2.3. Osmotically assisted reverse osmosis. OARO has recently emerged as an alternative solution to conventional methods for concentrating brine near saturation. The process, apart from applying pressure to drive water flux (<20 bar), overcomes the high pressures required in RO processes by using a dilute solution on the permeate side, thus reducing the osmotic pressure difference [80]. Similarly, various studies aim to facilitate the transition towards implementing the technology. Although some published works rely on the use of mathematical tools to find the most efficient OARO configuration, the technology has shown promising results at both laboratory and pilot plant scales.

Different studies evaluated OARO for concentrating solutions at the lab-scale [81–83]. Nakagawa et al. [81] tested two types of cellulose triacetate hollow fibre membranes from Toyobo (H90 and H180). Tests were performed with 1 mol/LM NaCl at 15 bar, where the solution circulated through both the shell and bore sides. H90 exhibited a higher flux than H180 (1.41 vs 1.17 L/(m^2·h)), but H180 showed a higher concentration factor after 3 h (1.042 vs 1.022 for H90). A ten-stage concentration test was performed with H180 at 15 bar, showing the possibility of concentrating solutions of 2 and 1 mol/L by a factor of 1.06 and 1.12, respectively. Nakao et al. [82] developed cellulose triacetate asymmetric hollow fibre membranes, which were initially characterised and then tested at the lab-scale. The most promising membranes, designated as MA-31/10 (module A) and MB-31/10 (module B), were evaluated at long-term operation using modules with an active area of 500-600 m^2 for more than 700 h with a solution containing 95 g/L NaCl. Module A exhibited a significantly higher water permeance (0.021 L/(m^2·h·bar)) compared to module B (0.009 L/(m^2·h·bar)). However, after 700 h of operation, these values decreased by 30 % and 5 % for modules A and B, respectively. These differences in performance were related to a higher inner stability of module B. Ju et al. [83] performed experiments at the lab-scale with RO brine and evaluated different parameters (applied pressure, feed and draw solution concentrations). When using a brine of 50 g/L as both feed and draw solutions, increasing the pressure from 5 to 20 bar allowed for an improvement in flux from 3.3 to 12.8 L/(m^2·h). However, flux decreased over time due to the decrease of effective pressure related to the dilution of the draw solution. When evaluating the effect of feed concentration, the authors reported a flux decay from 6 to 4 L/(m^2·h) when using a feed and draw solutions of 50 g/L and 30 g/L, respectively. However, when working at higher concentrations (feed and draw solutions of 130 g/L and 110 g/L, respectively), the flux decreased from 0.51 L/(m^2·h) to 0.34 L/(m^2·h). Such differences with the previous tests were related to concentration polarization. Only one study was found at the pilot plant scale, where Al-Amoudi et al. [48] evaluated the concentration of a NF-RO SW brine by combining HPRO and a 2-stage OARO to reach 170 g/L. The brine from the RO (approximately 80 g/L) was concentrated to 108-110 g/L at 112 bar using the HPRO (3 m^3/h feed, 25 % recovery). Following the OARO, it was possible to concentrate it further to 168-177 g/L.

One of the crucial points is to define the configuration for OARO, aiming to maintain a constant driving force to ensure a stable flux over time [80]. Different studies performed simulations to optimise the operating conditions and design, maximising recovery and decreasing energy consumption [83–85]. For example, Bartholomew et al. [84] evaluated the effect of concentration, pressure, number of stages and membrane area on water recovery and energy consumption. When introducing a saline sweep (200 g/L), it is possible to achieve water recoveries of 34 % during the treatment of 125 g/L (1.3 L/(m^2·h), and SEC of 8.6 kWh/m^3 of produced water). In contrast, a conventional RO only offers a 4 % water recovery at 65 bar when treating 75 g/L TDS. The applied pressure could reduce the membrane area and SEC. For example, the SEC decreased from 11.1 to 7.8 kWh/m^3 (from 55 to 75 bar) at 35 % water recovery. Compared to MVC, the SEC is expected to range from 11 to 25 kWh/m^3 in the range of 35 to 150 g/L. Shamlou et al. [85] studied different configurations of the OARO differing in the brine reflux, being cascading osmotically mediated RO (COMRO), brine reflux-OARO (BR-OARO), consecutive loops-OARO (CL-OARO), and split feed-OARO (SF-OARO). The simulations demonstrated that a single-stage BR-OARO achieved high recoveries at 20 bar, outperforming all other configurations in terms of SEC (approximately 5.2 USD/m^3 for treating a brine with 10 % salinity at 50 bar).

One open discussion is whether to use LSRRO or OARO to concentrate solutions close to saturation. For instance, Atia et al. [86] compared LSRRO, COMRO and OARO to approach 250 g/L from a brine (70 g/L TDS). In terms of SEC, OARO presented the lowest value (10.31 kWh/m^3), followed by COMRO (12.77 kWh/m^3) and LSRRO (28.90 kWh/m^3). From an economic performance, OARO showed the lowest LCOW (5.14 USD/m^3), followed by LSRRO (6.63 USD/m^3) and COMRO (7.90 USD/m^3). Ultimately, the authors concluded that COMRO may be suitable for low-salinity brines (20-35 g/L TDS), whereas OARO and LSSRO offer a better trade-off at high-salinity levels (>70 g/L). Wang et al. [87] reported that a LSSRO is preferred for moderate salinity brines (<35 g/L, with a SEC of 2.5 kWh/m^3, 30 % lower than OARO), whereas OARO is preferred at higher salinities (>70 g/L, 3.6 kWh/m^3, 40 % lower than LSRRO). Despite both technologies can reduce SEC compared to MVC (20-25 kWh/m^3), LSRRO is preferred over OARO due to membrane availability and lower capital costs.

OARO shows potential for large-scale implementation in ZLD applications. The low SEC compared to traditional methods, as highlighted by MVC, underscores its potential. However, further developments are needed to improve membrane performance and optimise different

configurations.

3.1.2. Concentration-driven

3.1.2.1. Forward Osmosis (FO). Forward Osmosis (FO) is a concentration-driven membrane process that enables desalination at a lower cost compared to traditional processes (i.e. RO). The process relies on a membrane that separates the saline solution (termed as feed solution, FS) from a highly concentrated solution (named draw solution, DS), allowing water to flow due to an osmotic gradient. In comparison to well-established methods, it provides the possibility to reduce membrane fouling and work at a lower energy cost due to the absence of a high operating pressure. However, the design of spacers to reduce concentration polarisation and the selection of the DS are critical parameters, as their properties can directly impact the process [88]. The technology has been widely studied at laboratory scale across different salinity ranges, moving from BW to salinities up to 120 g/L TDS. It should be mentioned that the technology has been used either to valorise wastewater effluents (as the FS) using the brine as the DS before its discharge to the sea, or to concentrate RO brines (used as the FS).

FO has been widely studied in the laboratory for pre-treating SW before the RO unit, or to treat the brine resulting from the desalination unit [89–99]. These studies highlighted the importance of the FS and DS concentrations, as they directly impact the osmotic pressure difference. For instance, Bamaga et al. [89] observed that increasing the DS concentration enhanced water flux, but also reduced membrane permeability and increased reverse normalised salt flux (1.4–1.5 g/L). Contrary, in the case of fixing the DS concentration (75 g/L NaCl as DS), using SW as the FS produced lower fluxes than tap water (6.7 L/(m^2·h) and 11 L/(m^2·h), respectively). Similarly, Eusebio et al. [92] reported fluxes ranging from 1.1 to 6.2 L/(m^2·h) as the DS salinity increased from 50 to 200 g/L, although high concentrations led to membrane scaling and pore blocking. The same conclusions were reported by Akther et al. [93], who also confirmed the higher reverse salt flux at high DS concentrations. Additionally, they reported lower fluxes for the SWRO brine than SW as the FS at a constant DS concentration. Temperature is another influential factor, as it affects viscosity and diffusion rates. Ahmed et al. [91] demonstrated that increasing temperature from 15 to 40 °C improved water flux (from 6.9 to 9.3 L/(m^2·h)) due to higher mass transfer and osmotic pressure difference. However, Akther et al. [93] found that the effect of temperature was modest (~6.5 % increase from 23 to 40 °C), mainly due to the substantial impact of internal and external concentration polarization. The membrane characteristics and orientation are also an important key to the performance. For example, Akther et al. [93] showed that membrane orientation (e.g., AL-DS mode) influenced mass transfer and flux behaviour. About membrane characteristics, Tang and Ng [95] compared different membranes and found that a cellulose acetate (CA)-based RO membrane achieved the highest flux (19.2 L/(m^2·h)), which was related to its hydrophilicity and thickness, which minimised internal concentration polarization. Apart from that, different studies evaluated the effect of hydrodynamics, showing that increasing the treatment flowrate mitigated external concentration polarization and increased water flux (from 5.1 to 9.4 L/(m^2·h)), but this also led to a higher reverse salt flux (from 1.4 to 2.9 g/(m^2·h)) [93]. Nevertheless, increasing flow is not sufficient to enhance mass transfer and reduce polarisation effects, and new well-designed spacers are essential for this purpose [94]. Other studies explored the impact of applying pressure to improve performance. As an example, Bhadrachari et al. [99] tested several types of membranes (CTA, TFC-CTA, Aquaporin, *Z*-Nano) under pressures up to 1.5 bar. Although fluxes increased significantly (e.g. Z-Nano from 17.7 to 35.6 L/(m^2·h) at 1.5 bar), salt rejection declined sharply from 100 % to 50 %, revealing a trade-off between flux and selectivity under applied pressure. Finally, some lab-scale tests aimed at integrating FO with other technologies to improve water recovery. For instance, Im et al. [97] proposed a multi-stage FO-RO–FO process for SW that can achieve 60 % of water recovery at 25 bar. Son et al. [98] used wastewater as FS to concentrate SWRO and MD brines, achieving high initial fluxes (around 51 kg/m^2·h) and low specific reverse salt flux (0.13 g/kg).

In addition, FO has been proposed as a pretreatment of thermal-based desalination technologies [100,101]. FO allows the removal of scale-forming ions (as Ca^{2+}, Mg^{2+}, and SO_4^{2-}), which mitigates scaling on the surfaces of heat exchangers in MSF and MED units. This reduction enables operating at higher Top Brine Temperatures, which are currently limited to 112 °C and 65 °C for MSF and MED, respectively. Moreover, it directly reduced the thickness of the $CaCO_3$(s) scale layer from 74 μm (without FO) to 39 μm (32 % recovery at FO), thereby improving heat transfer and efficiency while reducing the need for cleaning [100]. For instance, Thabit et al. [101] used FO to pre-treat SW (43 g/L TDS) before feeding it into MSF, with the reject brine from the MSF (81 g/L TDS) serving as the DS. The results showed that increasing the flowrate reduced concentration polarisation and improved water flux, moving from 8.1 L/(m^2·h) at 0.8 L/min to 12.2 L/(m^2·h) at 2 L/min. Although salt accumulation on the membrane surface was observed, it was easily removed with simple distilled water cleaning. Apart from that, it was demonstrated that increasing the temperature of the DS from 25 to 40 °C resulted in a water flux increase from 16.9 to 22.3 L/(m^2·h), attributed to lower water viscosity and greater diffusivity across the membrane, as well as an increase in the osmotic pressure difference. Nevertheless, despite the benefits of implementing FO, membrane degradation can occur when working with hot brines [102]. For instance, CTA membranes have shown an increase in reverse salt flux (3 times the initial flux) after being immersed in MED brines at 40 °C, whereas water fluxes barely varied (18.4 L/(m^2·h) and 20.9 L/(m^2·h) for CTA and TFC membranes, respectively). Analysis of the CTA membrane revealed that the active layer suffered deacetylation and chain breakage, but the anti-fouling properties increased due to the formation of hydroxyl groups. In the TFC membrane, it was reported the cleavage of the amide bond and the de-grafting of the polymer (i.e., poly-sulfobetaine methacrylate (pSBMA)) from the active layer, resulting in a loss of the anti-fouling properties.

Other applications of FO that might be of interest are for BW [103–105]. In the case of BW, Martinetti et al. [103] reported fluxes of 12 and 9 L/(m^2·h) for BWs with 7.5 and 17.5 g/L TDS, respectively, using 50 g/L NaCl as DS. However, scaling (e.g., SiO_2(s), $CaSO_4$:$2H_2O$(s)) and membrane degradation (CTA-based) due to alkaline cleaning were reported. Lee et al. [104], when comparing FO, MD and RO, found that FO showed less flux decline than RO during early recovery stages, although both declined significantly beyond 45 % recovery due to $CaCO_3$(s) scaling. On the contrary, MD showed the most stable performance, even up to 65 % recovery.

One of the advantages of the FO process is its low tendency to fouling phenomena, compared to pressure-driven membrane processes as RO [106–108]. For example, Kim et al. [106] reported a 17 % decrease in flux after 650 min of operation during the treatment of saturated $CaSO_4$·H_2O(s) solutions, whereas RO faced severe scaling. The differences were related to the fact that FO uses hydrophilic membranes and low pressures that reduced crystal adherence. In addition, Chen et al. [107] reported that the selection of the spacer and the membrane properties are critical during operation. For example, a mesh spacer can provide favourable conditions during scaling, i.e., the crystals formed on the mesh may progressively aggregate and grow, causing surface crystallisation. With regard to membrane properties, a CTA membrane showed a low, gradual scaling process and no sharp flux decline without a spacer, whereas the rough surface of a TFC membrane promoted crystal aggregation under the same conditions. During the integration of FO for SW and brine desalination (acting as DS) and wastewater reclamation (acting as FS), Boo et al. [108] reported that flux decline related to scaling was relatively insignificant, while organic fouling caused a dense and compact layer. However, using high-concentration DS (5 mol/L NaCl) increased concentration polarisation, causing scaling at the

membrane. To mitigate fouling, the authors suggested hydrodynamic strategies, including increased cross-flow velocity, redesign of spacers, and pulsed flow operation.

Different studies have evaluated the economic feasibility of integrating FO within desalination schemes [109–112]. For example, Yangali-Quintanilla et al. [109] explored FO using treated wastewater (as the FS) and SWRO brine (as the DS). The results showed that FO contribution to CAPEX could be reduced by increasing membrane flux, which can result in a 2M USD savings for a 10000 m^3/d plant. In addition, integrating FO could significantly reduce OPEX, moving from 0.83 to 1.01 USD/m^3 (conventional desalination) to 0.62-0.96 USD/m^3 (integrating FO). Guizani et al. [112] estimated a SEC of ~1 kWh/m^3 (that can be decreased to 0.81 kWh/m^3) when FO was used as RO pretreatment. Similarly, Feng and Chung [111] reported that SW dilution by FO provided economic benefits in a desalination facility due to lower OPEX (related to lower pressure at the RO), although the high investment for FO could limit the feasibility. Darwish et al. [110] proposed FO to pre-treat MSF cooling water using the final brine as DS. Although FO reduced scaling potential and allowed higher recoveries at the MDS, the large FO membrane area requires a balance between desalination capacity and CAPEX before its implementation. Naderi Beni et al. [113] studied FO pretreatment combined with RO/OARO for DS reconcentration. The authors highlighted the effect of non-woven spacers, which improved flux (1.97 L/(m^2·h) vs 1.73 L/(m^2·h)) and reduced levelized water costs (5.83 USD/m^3 vs 7.31 USD/m^3). Apart from that, the analysis carried out showed that membrane permeability and replacement rates had significant impact on the levelized cost.

The current state-of-the-art of FO has shown that the technology has strong potential for desalination and brine management. The benefits of the technology included the possibility of reducing scaling and operating at low fouling tendencies, as well as improving energy efficiency when combined with RO, MSF, and MED. However, challenges on membrane durability under harsh conditions and optimising membrane materials to balance water flux and salt rejection must be solved before its implementation on a larger scale.

3.1.2.2. Pervaporation. Pervaporation is a membrane separation process that integrates permeation and evaporation, combining principles of both thermally driven and membrane-based technologies [114–117]. The driving force behind this process is the chemical potential gradient, i.e. partial pressure across the membrane. While the feed side is maintained at ambient pressure, the permeate side operates under vacuum. Selective transport occurs via the solution-diffusion mechanism, wherein specific components are adsorbed, diffuse through, and are desorbed from the membrane while others are retained. During transport, the permeate remains in the vapour phase before undergoing subsequent condensation. Given that each pervaporation membrane exhibits distinct selectivity, the diffusion rate of individual components varies, enabling the separation of feed components into a purified permeate and a concentrated waste stream.

Pervaporation represents a promising alternative for desalination of high-salinity waters, particularly when conventional RO becomes ineffective due to extreme salinity levels. It stands out due to its capability to handle feed solutions with concentrations exceeding 100 g/L [118]. This process offers several advantages, including high desalination efficiency, independence from salt concentration or osmotic pressure limitations, and superior antifouling properties [114,115,119]. Despite its exceptional salt rejection (>99.5 %) and relatively low SEC (~2 kWh/m^3) [115,120], current commercial pervaporation membranes exhibit low water permeance, constraining their applicability in desalination. However, advancements in membrane materials with enhanced water permeance could position pervaporation as a viable and efficient alternative for treating highly saline water.

The membrane is the key component in pervaporation desalination, determining both selectivity and performance. While some inorganic membranes, commonly zeolites [121], are used, pervaporation desalination is predominantly conducted with polymeric membranes [122]. These membranes are classified as hydrophilic or hydrophobic [26]. Hydrophobic membranes are used for separating organic compounds from aqueous solutions, whereas hydrophilic membranes facilitate water transport while rejecting salts or other compounds, making the latter ideal for desalination applications [117,123]. Among hydrophilic materials, polyvinyl alcohol (PVA), polyethylene (PE), polyether amide, polyether ester, cellulose, block polymers, and polyester exhibit salt rejection and water purification capabilities, making them suitable for pervaporation desalination [121,124].

Li et al. [114] reviewed sixty-five studies on pervaporation desalination, examining various membrane materials and composite structures. PVA was found to still remain as the primary material for pervaporation desalination membranes due to its hydrophilicity and excellent film-forming processability. To enhance its performance, PVA has been modified by incorporating various additives, such as glutaraldehyde, carbon nanotubes, maleic acid, or sulfonic acid. These modifications increased crosslinking within the PVA structure, thereby reducing swelling [125–127]. Additionally, the use of sulfonated materials has been reported to improve water flux, enhance hydrophilicity, and increase membrane stability [128,129]. Graphene oxide, zeolites, and silica are widely used as well, reporting results with a large variability depending on material and feed composition [115]. A material comparison was carried out considering average permeance as indicator [114]. As previously exposed, PVA membranes had the best performance, followed by silica/silicate, graphene oxide-based membranes and finally zeolite, with values of 256 kg/(m^2·h·bar), 116 kg/(m^2·h·bar), 89 kg/(m^2·h·bar) and 23 kg/(m^2·h·bar), respectively.

On the other hand, temperature also plays an important role in pervaporation desalination, as the permeation flux increases with increasing temperature [116,121,130]. Typically, pervaporation desalination is operated at relatively high temperatures, usually over 60 °C [114]. Therefore, to operate under optimal technical conditions, it will be necessary to heat the feed streams, which increases the energy consumption of the process, raising its associated costs and potentially limiting its applicability. Moreover, not only the economic feasibility but also the environmental feasibility may be compromised if there is no availability of renewable energy sources.

There is a lack of studies on the energy consumption of pervaporation desalination due to the variability of results, mainly influenced by the membrane selected and the operating temperature. The energy consumption of pervaporation should consider both electrical and thermal energy consumption, with the latter representing the highest energy demand [114]. Xie et al. [131] reported that the electrical energy consumption of pervaporation ranges from 0.1 to 0.25 kWh/m^3. Although this range is lower than the electrical energy consumption of RO, the thermal energy consumption was not included in the calculation. Kaminski et al. [130] indicated that the pumping energy required for pervaporation is comparable to that of MD in desalination processes. Furthermore, Thomas et al. [124] compared the SEC of different desalination technologies and estimated that pervaporation and MD have similar SEC values of about 7.7 kWh/m^3, whereas the SEC of SWRO is between 3.0 and 4.0 kWh/m^3. Although pervaporation seems to be less suitable for desalination when treating SW, it could be a more viable option for feed streams with higher salinity. Wang et al. [132] reported an electrical SEC (vacuum pump and feed circulation) of 0.65 kWh/m^3 and thermal SEC of 52.7 kWh/m^3 when operating with 10 g/L solutions at 85 °C, achieving a water flux of 23 L/(m^2·h). Prihatiningtyas et al. [133] evaluated the thermal energy requirements of three different configurations of a pervaporation desalination plant with a capacity of 5000 m^3/day, a feed concentration of 90 g/L NaCl, and an operating temperature of 70 °C. Reported SEC ranged from 40.7 to 50.7 kWh/m^3, with the lowest value observed in the photovoltaic (PV) system with a series configuration using two modules. These findings highlight the need for further energy consumption analyses in pervaporation

desalination, particularly focusing on the feasibility of integrating renewable energy as a thermal source.

Despite existing pervaporation pilot-scale projects [134,135], pervaporation desalination remains at a low maturity level (Technology Readiness Level (TRL) 4) [136] with a lack of pilot scale or demonstration scale data [137]. Future research should focus on membrane fabrication and modification to achieve higher water flux without compromising selectivity, improve efficiency by reducing energy consumption, and optimize operating conditions or explore novel system configurations.

3.1.2.3. Reverse Electrodialysis (RED). Reverse Electrodialysis (RED) is an electrochemical process for generating electricity by exploiting the salinity gradient energy (SGE) between two solutions, the so-called high concentrated (HC) and low concentrated (LC) solutions[138]. The system uses a stack of alternating cation exchange membranes (CEMs) and anion exchange membranes (AEMs) to separate the two solutions. Ions from the HC solution migrate through the membranes towards the LC solution due to the concentration gradient. CEMs allow only cations to pass through, while AEMs allow only anions. This ion migration creates a potential difference across each membrane pair, which adds up over the stack to produce a usable voltage. Electrodes at either end of the stack convert the ionic current into electrical current, completing the circuit.

Works related to SGE harnessing by means of RED have been contextualized in the water industry sector, both desalination and wastewater treatment. In this sense, effluents from the water industry sector could provide a renewable energy source that could range a theoretical value ranging from 0.4 kWh/m^3 to 0.8 kWh/m^3 if SW or brines, and river water or wastewater effluents are considered as HC and LC streams, respectively [139]. In comparison to other commercially available renewable energy sources such as wind or solar, RED could be continuously exploited [140]. Investigations into the harnessing of SGE through RED have primarily addressed the optimization of operating conditions, encompassing velocities inside the channel (usually between 1 and 3 cm/s) [141], temperature (typically kept as high as possible) [142], and composition and concentrations of input streams [143,144]; and the selection of appropriate stack components, including membranes, spacers, and electrode systems [145–148], have resulted in achieving power density values of up to 1.77 W/m^2 working at room temperature with SW/wastewater [145]. Current research endeavours are directed towards enhancing commercially available ion-exchange membrane performance, selecting appropriate electrodes and electrolytes, optimizing spacer design to balance minimising electrical resistance and pressure drop, and identifying novel solution pairings to maximize available SGE. The potential of SGE-RED was investigated using diverse SWs (varying salinity and temperature) and wastewater treatment plant effluents, predicting a potential energy recovery ranging from 7 to 60 Wh/m^3 of reclaimed water [149]. The potential of using RO brine as a HC stream for SGE-RED was investigated by Tristan et al. [150] in a global assessment of SWRO desalination plants. Their results showed that net specific energy values of 0.08–0.15 kWh/m^3 and net power densities of 2.0–3.7 W/m^2 could be obtained.

The use of real water sources, including both natural and wastewater, necessitates pretreatment steps to ensure water quality and minimize the impact of fouling, as these sources typically contain natural organic matter and/or multi-charge ions [151–153]. To date, membrane fouling remains one of the primary challenges in RED systems; however, this issue has been relatively understudied [154–157]. Performance worsening has been reported due to the presence of multi-charge ions (commonly Mg^{2+}, Ca^{2+}, and SO_4^{2-}) [157–159] and dissolved organic matter [160–164], which contribute to increased membrane resistance and fouling. To address these issues, fouling mitigation and prevention strategies are being developed and implemented, including periodic feedwater switching (polarity reversal), chemical cleaning, ultraviolet (UV) lamp treatment, and even membrane modifications [164–166].

The economic feasibility of SGE-RED has been minimally explored, with limited studies addressing the calculation of the levelized cost of energy (LCOE). Currently, the LCOE of RED is estimated to range from 0.2 to 0.5 USD/kWh, which is still uncompetitive compared to well-established renewable energy sources, such as wind and solar photovoltaics, which have LCOEs between 0.1 and 0.15 USD/kWh [166]. However, reductions in membrane costs and the realization of higher power densities anticipated in the near future could potentially lower the RED LCOE to a more competitive value of 0.1 USD/kWh [162,166].

RED can be effectively integrated into industrial facilities as either a standalone system or as a component of ZLD or MLD schemes. This integration provides dual benefits: i) energy recovery and ii) waste minimisation, which are crucial in industries aiming for high resource efficiency and lower environmental impact. Consequently, RED technology has been implemented in diverse projects.

Although there are some existing RED pilot plant investigations reported in the literature, more research is required to boost the scaling-up and implementation of RED, and to fully understand the technology. Some examples of pilot-scale demonstration studies are summarised in Table 2.

One of the earliest attempts to scale up RED process was undertaken by Verman et al. [167]. They compared the performance of a lab-scale stack comprising 50 cells with a membrane area of 10 × 10 cm^2 (1 m^2 total membrane area) to that of a pilot-scale stack also containing 50 cells, but with a larger membrane area of 25 × 75 cm^2 (18.75 m^2 total membrane area). This pilot-scale stack represented the largest reported in the scientific literature at the time. The hydrodynamic characteristics of the stack were determined to be of paramount importance for the maximisation of power density, owing to the strong dependence of performance on solution residence time. The increased flow path length in the pilot-scale stack resulted in elevated hydrodynamic losses, thus compromising RED performance. A pilot-scale RED plant, representing the first of its kind, was constructed and operated in Italy as part of the REAPower project [173]. This installation comprised 125 cell pairs and boasted a total membrane area of 50 m^2. The power output achieved using natural solutions reached approximately 40 W, translating to a specific power density of 1.6 W/m^2 per cell pair. Notably, testing with artificial NaCl solutions yielded a 60 % increase in power output, reaching an estimated value of 65 W (2.7 W/m^2 per cell pair). The performance of the unit was monitored over a five-month period, and no significant performance degradation due to scaling, fouling, or ageing phenomena was observed [168]. Further research led to the recovery of almost 700 W from synthetic brine and BW [169]. Compared to ideal conditions, operation with real solutions led to a power output reduction of up to 50 %, underscoring the negative influence of real solutions on RED performance.

Subsequent to these initial works, numerous efforts to scale up RED technology have been documented; however, the achievable power density in large-scale RED systems remains constrained within the range of 0.4 to 2.7 W/m^2 per cell pair [166]. Nam et al. [171] achieved a power output of 96 W, corresponding to a power density of 0.76 W/m^2 per cell pair using a pilot-scale RED system assembled with 1000 cell pairs, corresponding to a total membrane area of 250 m^2, using municipal wastewater effluent (1.3–5.7 mS/cm) solution and SW (52.9–53.8 mS/cm) as LC and HC solutions, respectively. Analyses revealed that pressure drops at the fluid inlets, caused by spacer clogging, had the most significant negative impact on power output. Furthermore, inorganic fouling, i.e. scaling, due to precipitate formation was observed as an unavoidable consequence of the water dissociation reaction driven by the substantial potential generated within the stack's cathode chamber. D'Angelo et al. [170] investigated the feasibility of employing pilot-scale RED (comprising 500 cell pairs with an electrode area of 44 × 44 cm^2) fed with natural BW and concentrated brine from saltworks for the simultaneous production of energy and wastewater

Table 2
Summary of RED pilot-scale demonstration studies.

Project	Novelty	HC / LC	Stack size	Main Results	Location	Ref.
–	Comparison of Lab-scale stack and Pilot-scale stack Study of hydrodynamic characteristics	Synthetic SW (30 g/L NaCl) / Synthetic River Water (1 g/L NaCl)	Lab-scale stack: 50 cells, 1 m^2 total membrane area Pilot-scale stack: 50 cells, 18.75 m^2 total membrane area.	Gross power densities: up to 0.83 W/m^2 Net power densities: up to 0.4 W/m^2	–	[167]
REAPower	Claimed first pilot-scale RED plant of its kind	Brine (saltworks) 4-5 mol/L $NaCl_{eq.}$ / BW 0.03 mol/L $NaCl_{eq.}$	125 cell pairs, 50 m^2 total membrane area	Artificial solutions: power output of 65 W, 2.7 W/m^2 per cell pair Natural solutions: power output of 40 W, 1.6 W/m^2 per cell pair	Marsala (Italy)	[168]
REAPower	largest 3 module configuration facility reported so far	Brine (saltworks) / BW	2 modules 500 cell pairs/module 194 m^2 total effective area / module	Artificial solutions: power output of 700 W Natural solutions: power output of 330 W	Marsala (Italy)	[169]
REAPower	Combination of energy generation and wastewater treatment	Brine (saltworks) / BW	500 cell pairs 194 m^2 total effective area	1.6 W/m^2 per cell pair Removals of 30 % of Acid Orange 7 (at electrode solution)	Marsala (Italy)	[170]
–	First demonstration of a pilot-scale RED fed with wastewater effluent and SW Analysis of inorganic and organic solutes	SW (52.9–53.8 mS/cm) / Municipal wastewater effluent (1.3–5.7 mS/cm)	1000-cell-pair stack (total membrane area: 250 m2),	Maximum power: 96 W Power density: 0.76 W/m^2 cell pair	Jeju (Korea)	[171]
–	Analysis of the influence of temperature (10-35 °C), spacer thickness (200 μm and 600 μm), and flowrate (2-6 L/min)	Synthetic SW (53 ± 0.5 mS/cm NaCl aq) / Synthetic River Water - Wastewater (1.3 ± 0.5 mS/cm NaCl aq.)	2 modules (spacer thickness: 200 μm and 600 μm) 200 cell pairs/module 40 m^2 total effective area / module	Maximum power output 38.6 W (0.96 W/m^2) at 35 °C, 200 μm, and 6 L/min	Not reported	[172]
Life-3E	Integration of renewable energy generation with water reclamation	SW (33275 mg/L TDS) / UWWTP secondary effluent (466 mg/L TDS)	2 modules 115 cell pairs/module 20.125 m^2 total effective area / module	Peak power densities of 1.39 W/m^2 (synthetic solutions) and 0.95 W/m^2 (real waters)	Comillas (Spain)	[139]

treatment. The system's sustained operation over several months, without a discernible decline in power output, demonstrated the long-term operational stability of RED with consistent membrane performance, indicating minimal structural modification. The influence of temperature on RED performance was assessed using two pilot-scale RED stacks, each comprising 200 cell pairs and a total active membrane area of 40 m^2 [172]. The stacks differed in spacer thickness, with 200 and 600 μm spacers. Elevated temperatures positively impacted RED performance in both configurations; however, this effect was more pronounced in the stack utilizing the 200 μm spacers.

The European Life-3E project: Environment-Energy-Economy [174] focuses on integrating renewable energy generation with water reclamation. Specifically, the project posits that SGE-RED can provide power for tertiary wastewater treatment processes in coastal urban wastewater treatment plants (UWWTPs), thereby mitigating energy costs associated with water regeneration and reuse. As part of this initiative, a pioneering pilot-scale RED system, featuring a membrane area of 20.125 m^2, was established at a coastal UWWTP in Comillas, Spain. This system achieved peak power densities of 1.39 W/m^2 and 0.95 W/m^2 when operated with synthetic solutions and under real environmental conditions, respectively [139].

Given the preceding discussion, it can be concluded that the widespread implementation and adoption of SGE-RED technology face several challenges, notably those related to membrane cost and, critically, membrane fouling [138,175,176]. Addressing these challenges is crucial for realising the full potential of SGE-RED for sustainable energy production [177–182]. Nevertheless, these issues do not preclude the applicability of the process.

3.1.2.4. Pressure retarded osmosis (PRO). Pressure retarded osmosis (PRO) presents a viable alternative for harnessing SGE, alongside RED. PRO exploits an osmotic pressure differential to drive water transport from a dilute FS across a semi-permeable membrane into a concentrated DS maintained under pressure, though below its osmotic threshold. The osmotic driving force results in pressurization of the permeate stream while diluting the draw solution, allowing the extracted hydraulic energy to be converted into mechanical and electrical power via a turbine-generator system. A critical factor influencing the efficiency and economic feasibility of PRO is the semi-permeable membrane, as its characteristics determine attainable power density [183].

PRO exhibits strong potential for integration within existing desalination infrastructure. This potential arises from the availability of both natural salinity gradients, such as river water mixing with SW, and anthropogenic gradients, including desalination brine and treated urban wastewater, as feed sources [184]. Traditionally, PRO has been explored to harness energy from river-SW mixing; however, due to the relatively low salinity gradient in these systems, energy production is limited to approximately 0.15 kWh/m^3 of the total mixed solution [185].

To enhance energy output, researchers have investigated PRO integration with RO, forming the RO–PRO system. In this configuration, the concentrated brine waste from RO serves as the high-salinity DS, while impaired water (e.g., wastewater effluent) is used as the low-salinity feed. This system facilitates hydraulic energy recovery, reducing RO energy consumption and mitigating environmental impacts by diluting concentrated brine prior to discharge. Two notable RO–PRO pilot systems have been reported: a Japanese prototype utilising treated sewage as the impaired water source, which faced significant membrane fouling challenges [186], and a U.S. pilot-scale system that demonstrated a predicted net specific energy production of 0.8 kWh/m^3 for 50 % RO recovery, leading to an estimated 30 % reduction in SEC [187,188]. Sensitivity analyses identified water permeability as a key factor in optimising energy recovery, with experimental validation confirming the feasibility of pressure exchange between PRO and RO subsystems.

Despite its potential, several challenges hinder PRO

commercialisation. Membrane fouling remains a significant issue, as observed in pilot studies [186]. Inconsistencies in power densities, attributed to wetting irregularities and entrained air within the membrane envelope, also present obstacles [189]. Experimental power densities range from 1.1 to 2.3 W/m^2, significantly lower than the predicted maximum of 10 W/m^2 [188]. Addressing these issues requires advancements in membrane design, with an emphasis on improving water permeability and refining system configurations to achieve stable and efficient energy recovery.

Key technical challenges include: (i) internal concentration polarization control, (ii) membrane fouling mitigation, and (iii) integration with other processes [190]. Effective internal concentration polarisation management is crucial for PRO viability, with proposed solutions involving the development of membranes with thinner, more porous, and less tortuous support layers, along with optimisation of FS and DS flowrates and pressures. The advancement of high-performance PRO membranes with enhanced water permeability, selectivity, and minimal internal concentration polarisation is critical for system efficiency [191]. Membrane fouling can be mitigated by applying suitable water pretreatments that enhance feed quality through the removal of species promoting scaling (e.g., Ca^{2+} and Mg^{2+}) and organic fouling (e.g., natural organic matter), and by maintaining operation within appropriate pH and temperature ranges. Additionally, membrane properties, including surface charge and hydrophobicity, significantly influence fouling resistance. Strategies for fouling control involve chemical and physical cleaning methods and membrane surface modifications [192].

Beyond the RO–PRO combination, developments have also been made in the pilot-scale deployment of standalone PRO plants, which are summarised in Table 3.

The first large-scale PRO osmotic power pilot plant was launched by Statkraft in Norway in 2009 [193]. This facility employed freshwater as the FS and SW as the DS. With a projected output of 12 TWh/year, approximately 10 % of Norway's total electricity demand, the facility operated at 10 kW, achieving an initial membrane energy density of 1 W/m^2. However, economic feasibility remains a barrier, as PRO membranes must attain 5 W/m^2 for viable commercialisation [194]. Statkraft ultimately discontinued the project in 2014 due to financial constraints [195].

One of the limitations faced by the Statkraft project was the low salinity of the DS. Studies suggest that PRO has a better performance outlook when using high-salinity brines (>1.2 mol/L $NaCl_{eq.}$), i.e., brines with higher salinity than those produced in SWRO desalination processes [200–202]. In this regard, several ongoing initiatives continue to explore PRO's potential. The SeaHERO project in Busan, Korea, integrates PRO within a renewable energy hybrid SWRO system designed to treat 45500 m^3/day of SW while reducing SEC (<4 kWh/m^3) and fouling by 50 % [196]. This facility employs three PRO units to recover mixing energy, from i) treated urban wastewater and SW, ii) treated urban wastewater and SWRO brine, and iii) treated urban wastewater and denser SWRO brine, yielding outputs of 1.5, 3.0, and 4.2 MJ/m^3, respectively. Similarly, Japan's Mega-ton Water System Project, the world's largest SWRO facility (1 million m^3/day), utilizes PRO to enhance efficiency, targeting a 20–30 % energy reduction [197]. This system processes 100000 m^3/day of treated urban wastewater and brine for energy generation and raw SW pre-pressurization. The prototype, incorporating Toyobo's CTA membranes (13.3 W/m^2), currently generates 4–8 kW, with future plans for systems capable of 100 kW output.

Since 2021, SaltPower has been developing a 20 kW commercial osmotic power pilot plant in Denmark, leveraging high-salinity brine (120–310 g/L) from a geothermal facility [198]. This facility employs PRO membranes from Toyobo and integrates geothermal heat with salinity gradient energy for combined heat and power generation. The LCOE for this osmotic power system was estimated at 0.18 USD/kWh, decreasing by 41 % to 0.10 USD/kWh when integrated with geothermal energy. This assessment underscores the competitiveness of PRO relative to conventional electricity generation technologies. Recently, the commissioning of Japan's first osmotic power plant, located in the city of Fukuoka, has been reported in the media [199]. The facility is expected to generate approximately 880000 kWh per year by using the salinity difference between SWRO brine and treated urban wastewater, which will contribute to powering a desalination plant that supplies freshwater to the city and surrounding areas.

3.1.3. *Electrically-driven*

3.1.3.1. Electrodialysis (ED). Electrodialysis (ED) is a membrane-based separation process that employs an applied electrical potential to facilitate the selective transport of ions through ion-exchange membranes. This process effectively separates ions from the solution, resulting in the generation of two distinct streams with differing salinity levels: a concentrated stream and a diluted stream. The underlying principle is electromigration of ions through the membranes, facilitated by a series of alternating CEMs and AEMs. These selectively permit the passage of cations and anions, respectively, while blocking the opposite charge species [203,204].

ED emerged as a viable desalination technology in the mid-20th century in contrast to traditional methods such as RO and thermal processes. However, it was not until the late 20th and early 21st centuries that interest in ED was renewed, driven by increasing global water scarcity. This technology has gained appeal in water treatment processes due not only to its use in desalination but also to its ability to recover valuable resources from saline waste streams. Moreover, studies have underscored the role of ED in circular water economies, highlighting its potential for water recycling and its capacity to reduce the environmental impacts associated with desalination [15,205].

The primary application of ED in the desalination industry is the production of freshwater. Although less commonly employed than RO, ED offers several advantages over this technology. These include reduced pre- and post-treatment requirements, which extend membrane lifespan, greater operational flexibility due to its higher tolerance to temperature variations and selective ion removal, and improved water

Table 3
Outlook of pilot-scale standalone PRO plants.

Project (Location)	Feed and draw solutions	Energy capacity	Novelty and findings	Ref.
Statkraft (Norway)	Freshwater / SW	10 kW (1 W/m^2)	First large-scale PRO pilot Discontinued due to non-economic feasibility	[193–195]
SeaHERO (South Korea)	Treated wastewater / SW, SWRO brine	1.5, 3.0 and 4.2 MJ/m^3	Integration of PRO within a renewable energy hybrid SWRO system aiming to achieve 50 % fouling reduction and < 4 kWh/m^3 energy consumptions	[196]
Mega-ton (Japan)	Treated wastewater / Brine	4–8 kW actual / 100 kW projected	Used for energy generation and rawSW pre-pressurization	[197]
SaltPower (Denmark)	Freshwater / Geothermal brine (120–310 g/L)	20 kW / LCOE: 0.18 → 0.10 USD/kWh	Integration of geothermal heat with salinity gradient energy for combined heat and power generation LCOE of 0.18 USD/kWh	[198]
Fukuoka (Japan)	Treated wastewater / SWRO brine	880000 kWh/year	Japan's first osmotic power plant	[199]

recovery rates [206,207]. Although ED achieves desalinations efficiencies of 45-90 %, its high SEC, ranging from 1 to 12 kWh/m^3 of freshwater remains as a challenge [208,209]. While ED can be applied to a variety of feed streams, it is particularly effective for desalinating BWs whose TDS content ranges from 3 to 20 g/L. The LCOW for ED has been demonstrated to be more competitive than that of RO for feed salinities lower than 3 g/L, with a reported value of 0.21 USD/m^3 [210]. ED could overtake RO at higher feed salinities by reducing the cost of ion-exchange membranes.

However, it is noteworthy that in Japan ED has also been implemented as an alternative for table salt production. The country lacks rock salt deposits, and salt production through SW in salt fields is not viable due to the extensive land requirements and the often unfavourable climatic conditions. Since 1971, traditional salt field methods have been replaced by ED processes that concentrate SW or SWRO brines up to 200 g/L NaCl prior to evaporation, achieving production levels of nearly one million tons of table salt per year. The operating conditions, as well as different operation modes, have been extensively reported by Tanaka [211–217].

On the other hand, Reig et al. [218] evaluated at pilot scale the capability of ED to concentrate SWRO brines for use in the chlor-alkali industry. The NaCl concentration was successfully increased from 70 g/L to 245 g/L, while simultaneously reducing the concentration of multivalent ions (Ca^{2+}, Mg^{2+}, SO_4^{2-}) due to the selectivities of the membranes employed, Neosepta CEMs (CIMS) and AEMs (ACS). Although high NaCl concentrations were achieved, the process was limited by high energy consumption, considering the optimum operating point when working in continuous mode at 0.35 kA/m^2 with 185 g/L NaCl, achieving a SEC of 0.12 kWh/kg NaCl.

Despite its advantages, ED faces several challenges, including membrane fouling, energy consumption, and limitations in treating highly saline solutions. Research efforts have focused on improving membrane materials, optimizing system configurations, and integrating hybrid desalination approaches to overcome these barriers.

The integration of ED with renewable energy sources has been extensively studied in the literature as a strategy to mitigate indirect CO_2(g) emissions associated with energy consumption, thereby reducing the environmental impact of these processes [219,220]. Fernandez-Gonzalez et al. [221] reviewed the state-of-the-art in renewable ED, highlighting its superior adaptability to intermittent energy supply compared to other desalination technologies, such as RO. Consequently, ED can be seamlessly integrated with wind and PV energy sources[222]. In particular, PV-ED has been identified as a more sustainable alternative to PV-RO when treating BW, with projected costs ranging from 0.15 to 0.40 €/m^3 by 2050. The technical feasibility of desalination of BW using PV-ED was investigated through experimental and mathematical modelling works [223,224]. SECs in the range of 0.7–1.4 kWh/m^3 and 0.9–1.7 kWh/m^3 were reported for irrigation and drinking water uses, respectively. LCOW in the range of 0.14–0.23 €/m^3 for irrigation uses and 0.17–0.32 €/m^3 for drinking water uses was calculated. A lab-scale PV-ED desalination system with corrugated membranes achieved 35 % salt removal in 15 min, operating at 60-70 % ED current efficiency fully powered by the PV panel [225]. Moreover, the significant potential of PV-ED and wind-ED for small off-grid systems has been emphasized. Bian et al. [226] selected a PV-ED system for village-scale applications in rural India due to its superior efficiency, requiring only half the specific energy, thereby halving power system costs, compared to small-scale RO systems. Additionally, PV-ED significantly reduces water wastage, lowering it from 60 % to less than 10 % for groundwater salinity levels typically observed in India. Malek et al. [227] conducted laboratory experiments on a wind-ED desalination system without energy storage. The results showed that the SEC of the process remained relatively stable despite fluctuations in energy supply, indicating that the system is electrically robust and a reliable off-grid desalination solution for remote, water-stressed regions.

Desalination efficiency in ED can be enhanced by implementing multiple sequential stages, known as multi-stage ED. This approach was studied to simultaneously desalinate concentrated brine from SW desalination plants while reconcentrating it for coarse salt recovery. By optimizing current density and the volume ratio between dilute and concentrate solutions, a three-stage ED system achieved a brine concentration of 27 %, a 68 % water recovery rate, and a 72 % desalination rate [228]. A further study [229] evaluated the performance of single-, two-, and three-stage ED systems. The single-stage ED achieved a concentrated solution with 11.4 wt% salt content at a SEC of 0.18 kWh/kg NaCl. In contrast, the two-stage and three-stage ED systems increased the salt concentration to 18 % and 21 %, respectively, with corresponding SECs of 0.31 kWh/kg and 0.45 kWh/kg.

Moreover, ED has proven effective in desalination applications where selective ion removal is required. Unlike RO, which removes all dissolved species indiscriminately, ED can be used to target specific ions such as nitrates, sulphates, and transition metals, making it advantageous in customized water treatment or blue mining applications. The use of mono selective ion-exchange membranes, both cation and anion could favour the possibility to separate single charge to double charge ions. Therefore, beyond freshwater production, ED has demonstrated significant potential in the desalination sector for resource recovery from brines.

The growing interest in lithium recovery from salt-lake brines is driven by rising lithium prices, increasing demand for battery production, and geographic constraints on its mining, classifying it as a critical material. A key challenge in electro-membrane and membrane processes is the separation of lithium from magnesium, as both ions have similar radii in aqueous solutions [230]. Guo et al. [231] reduced the [Mg^{2+}]/[Li^+] ratio by 2.35, achieving a lithium recovery of 77 % with a SEC of 0.094 kWh/g Li. Improved results achieved a [Mg^{2+}]/[Li^+] ratio reduction by 19, with a lithium recovery rate of 95 % and an exceptionally low SEC of 0.0019 kWh/g Li [232]. Additionally, it was demonstrated that the presence of K^+ and Ca^{2+} did not negatively affect the selectivity or efficiency of the ED process. However, later studies concluded that brine composition significantly affects selectivity, recovery rate, and SEC [233]. Na^+ significantly impaired ED performance, as the recovery rate, current efficiency, and separation coefficient dropped sharply from 71 % to 40 %, 11 % to 2 %, and 9 to 2, respectively, when the [Na^+]/[Li^+] ratio increased from 1 to 20 [234]. Ying et al. [235] achieved a lithium recovery of 90 % and decreased Mg/Li mass ratio from 10 to 0.6 using a multi-stage ED.

Recently, rare earth elements (REEs) recovery by means of ED from secondary sources, within a circular economy paradigm, has been explored in the literature, due to limitations associated with the primary extraction of mining ores. Li et al. [236] evaluated Sc^{3+} ion recovery from wastewater, demonstrating that the ED process is highly promising, achieving 99.5 % removal with a SEC of 0.26 kWh/m^3. Nevertheless, the effectiveness of ED in separating multi-component REE solutions is challenging, as REE have identical valence electrons. To address this issue, the use of chelating agents has been proposed [237,238].

ED is increasingly being incorporated into ZLD and MLD frameworks. In these applications, ED is used to concentrate brines before further treatment by thermal or crystallisation processes. Several large-scale projects within the EU and beyond have demonstrated the feasibility of ED-based ZLD strategies. A clear example is REvivED water, a project funded under the EU's Horizon 2020 programme, that aimed to contribute to overcoming the drinking water challenge by establishing ED as the new standard for desalination of SW [239]. The expected results and impacts from the project were achieving a reduction of the energy consumption compared to current state-of-the-art energy technologies but remaining cost efficient. Within the project different pilot or industrial-scale ED systems were built, including: i) small stand-alone PV-ED BW desalination systems for rural areas (installed at Somaliland, Tanzania, Djibouti and India), ii) industrial-scale SW desalination by multi-stage ED, iii) multi-stage ED couple with RED to reduce energy

consumption in SW desalination, and iv) the integration of ED-RO.

3.1.3.2. Bipolar membrane electrodialysis (BMED). Bipolar Membrane Electrodialysis (BMED) enables the generation of acids and bases from saline solutions by applying an electric field. The stack is the core element of this technology, which is ensembled with several repeating units of AEMs and CEMs alongside bipolar membranes (BPM). AEM and CEM facilitate selective ion transport, allowing anions and cations, respectively, to migrate across the membrane. In contrast, the BPM induces water dissociation yielding protons and hydroxide ions.

In this context, BMED could be incorporated into the desalination industry by converting brines, primarily composed of NaCl, into valuable NaOH and HCl [240,241]. These products could then be: i) utilized on-site for pretreatment or cleaning stages, facilitating self-consumption; ii) applied in other processes within integrated systems, such as ZLD or MLD schemes; or iii) commercialized, provided that the required market standards for purity and concentration are met.

Specifically, the recovery of HCl and NaOH from SWRO desalination brines via BMED has been extensively investigated in the scientific literature. In lab-scale studies, BMED has demonstrated the production of 0.8 mol/L HCl and 1.0 mol/L NaOH from synthetic softened SWRO brines (1.0 mol/L NaCl without Ca and Mg) under a current density of 1000 A/m^2, using a system configured with two membrane triplets (Ralex AMH and CMH membranes and Neosepta BP1) and a 100 cm^2 active area (Elektrolyse Project) [242]. Yang et al. [243] reported the generation of 0.7 mol/L HCl and 1.0 mol/L NaOH from SWRO brines (0.65 mol/L NaCl) after softening with NaOH and CO_2(g) to remove Mg and Ca, achieving a SEC of 9.0 kWh/kg HCl. In contrast, Reig et al. [244] obtained 1.99 mol/L HCl and 2.14 mol/L NaOH from pre-concentrated SWRO brines (3.42 mol/L NaCl) with a three-triplet membrane stack (64 cm^2 active area, PCCell, Germany), reporting a SEC of 3.8 kWh/kg HCl. Similarly, Leon et al. [245] produced 1.77 mol/L HCl and 1.25 mol/L NaOH from a 2.0 mol/L NaCl solution using a five-triplet stack (280 cm^2, Suez, France), achieving a SEC of 3.29 kWh/kg NaOH. Recent efforts have focused on scaling up BMED, with a pilot plant featuring 0.16 m^2 active area per membrane and a configuration of 40 triplets, enabling the investigation of various operational parameters and stack configurations [246,247].

Although BMED has demonstrated significant potential for brine valorisation, several challenges hinder its broader adoption. Key limitations include: a) restricted product concentrations (<2 mol/L or approximately 8 wt%), which are substantially lower than commercial concentrations (33-50 wt%) [248] and necessitate substantial volumes of freshwater for production; and b) high electrical energy requirements, potentially leading to indirect CO_2(g) emissions. Several strategies have been proposed to address these challenges which are discussed next and summarized in Table 4.

Novel operational schemes have been developed and proposed to enhance product concentrations and minimise freshwater consumption. One approach, involving an oversized brine-to-product volume ratio of 20:1, enabled the attainment of 3.3 mol/L HCl and 3.6 mol/L NaOH [249]. This brine volume oversizing concept, based on maintaining a stable feed concentration, suggests that continuous (single-pass) operation in this set-up could yield even higher product concentrations. However, achieving such high product concentrations necessitates the application of high current densities (1000 A/m^2), resulting in elevated SEC values of 41 kWh/kg HCl [249] or 23 kWh/kg NaOH [250]. Later, Fu et al. [251] yielded concentrations of 4.7 mol/L of HCl and 6.2 mol/L of NaOH by an integrated ED-BMED system and mimicking a continuous operation mode. NaCl brines at 3.5 wt% (~0.6 mol/L, 54 mS/cm) were concentrated to 15 wt% (~2.6 mol/L, 200 mS/cm) before being introduced into the BMED system. The integrated ED-BMED process exhibited a better energetic performance compared to standalone BMED, consuming 8.69 kWh/kg NaOH. Further studies by the same group led to the production of 9.2 mol/L NaOH by processing saturated NaCl solutions (26.5 wt%, 5.43 mol/L) and applying an online neutralization technique to promote water dissociation via equilibrium shifting [252]. Recently, Leon et al. [253] obtained 5.31 mol/L NaOH from 6.0 mol/L NaCl brines with a salt-to-base volume ratio of 10:1, achieving a reduced SEC of 2.92 kWh/kg NaOH.

In contrast, Filingeri et al. [254] investigated new operating conditions by using a high-salinity stream (2 mol/L NaCl) instead of freshwater as the feed for the acidic and alkaline compartments. The results showed that the presence of NaCl in the alkaline compartment had minimal impact on performance, achieving a favourable balance between energy consumption and a reduction in water consumption (up to 50 %). However, introducing NaCl into the acidic compartment led to a 19-33 % decrease in NaOH product concentration, accompanied by a 15-33 % increase in energy consumption. Additionally, when NaCl was fed into both compartments, the target concentration of 1.0 mol/L NaOH could not be reached. This approach could be particularly beneficial in applications where product concentration and purity are not critical, such as in self-consumption scenarios.

Reducing energy consumption in BMED remains a considerable challenge, but the shift to decarbonized energy sources is essential for progressing towards a more sustainable process. Despite recommendations for integrating BMED with renewable energy, research in this topic has been minimally explored. Encouraging progress has been achieved by integrating BMED with PV solar energy (PV-BMED), showing promising results. Lab-scale studies on PV-BMED (TRL 4) have demonstrated

Table 4
Summary of novel strategies proposed to address BMED challenges.

Challenge	Approach and innovation	Feedwater	Product concentration (mol/L)	SEC (kWh/kg)	Scale	Ref.
Target higher product concentration	Brine volume oversizing (20:1 brine to product)	Simulated SWRO brine (1 mol/LNaCl)	Up to 3.3 HCl / 3.6 NaOH	41 kWh/kg HCl / 23 kWh/kg NaOH	Lab	[249,250]
Target higher product concentration	ED-BMED integration to pre-concentrate BMED feedstream	Pre-concentrated NaCl brines 3.5 wt% (~0.6 mol/L) to 15 wt % (~2.6 mol/L)	4.7 mol/L of HCl and 6.2 mol/L of NaOH	8.69 kWh/kg NaOH	Lab	[251]
Target higher product concentration	Application of an online neutralization technique	Saturated NaCl solutions (26.5 wt%, 5.43 mol/L)	9.2 mol/L NaOH	4.61 kWh/kg NaOH	Lab	[252]
Target higher product concentration	Brine volume oversizing (10:1 brine to product)	6.0 mol/L NaCl brines	5.31 mol/L NaOH	2.92 kWh/kg NaOH.	Lab	[253]
Reduction of freshwater consumption	Use of high-salinity stream (2.0 mol/L NaCl) as the feed for the acidic and alkaline compartments	2.0 mol/L NaCl	0.50 mol/L of HCl and 0.65 mol/L of NaOH	2.78 kWh/kg HCl / 1.95 kWh/kg NaOH (at concentrations of 0.5 mol/L)	Lab	[254]
Reduction of indirect CO_2 emissions	Integration of renewable energies (PV)	Simulated SWRO brine (1 mol/LNaCl)	Up to 3.3 HCl / 3.6 NaOH	41 kWh/kg HCl	Lab	[249]

technical performance equivalent to that achieved with grid-based power sources [249,255]. The strength of this integrated approach lies in its environmental benefits, achieving a tenfold reduction in CO_2(g) emissions [249,250,256,257]. Recent mathematical simulations evaluating PV-BMED scale-up indicate that PV does not adversely affect technical performance [258]. While the initial costs of PV installation present an investment challenge, they are offset by reduced reliance on grid electricity, resulting in an estimated 20 % decrease in the levelized cost of NaOH compared to grid-supplied BMED. Although these promising findings support further integration of BMED with renewable energy, continued efforts remain necessary to advance this approach.

Although the application of BMED in the desalination industry has predominantly focused on acid and base production, its potential for recovering minor or trace elements, such as lithium or rare earths, has also been explored [259–262]. However, these approaches remain at a lower level of technological maturity.

The growing interest in this technology for applications in ZLD and MLD systems is reflected in several European projects. These projects received funding to construct and demonstrate the feasibility and operational viability of such systems at a pilot scale. Notable examples include the Water Mining [263], SEArcularMINE [264], and Sea4Value [265] projects, each focusing on the recovery of different raw materials, including critical raw materials, from SW or desalination brine concentrates. Specifically, BMED in Water Mining and SEArcularMINE is employed to produce NaOH, which is subsequently used for the precipitation and recovery of magnesium as $Mg(OH)_2$(s), as seen in some recent works of the literature [49,247,254,266–268]. In the Sea4Value project, BMED is applied for the selective recovery of boron [269]. Conversely, in the Indesal project [270], BMED is used for the production of NaOH and HCl to meet the quantity and concentration requirements of the desalination plant.

BMED can also find applications in energy-related fields, either in harnessing energy from pH gradients through BMRED or in energy storage through the development of acid-base flow batteries (ABFB) [271]. BMRED is the opposite process to BMED. In BMRED, pH gradient energy is recovered by the controlled neutralisation of two streams with different pH, typically an acidic and an alkaline solution. In ABFB charging (BMED) and discharging (BMRED) cycles are performed in a closed-loop device. Although BMRED and ABFB are still at a low TRL, they are attracting attention of the scientific community, with an increasing number of publications in recent years [272].

At the current state of the art, the application of BMRED technology itself or within ABFB batteries is still limited by some challenges, such as: i) the complex assembly processes due to requirements of asymmetric electrolytes (acids and bases); ii) relatively limited stability and durability because of ion leakage and ion crossover, that leads to the depletion of acid and base solutions; iii) high internal electrical resistance generated by the assemble of multiple cells, and, in particular BPMs; iv) the relatively elevated cost of BPMs compared to AEMs and CEMs; and v) restricted options for electrode reactions [273]. The scaling-up of ABFB technology has been demonstrated through a pilot plant of 1.0 kW rated power, which has been installed and operated on the island of Pantelleria (Italy) [274–276]. The pilot plant was configured with four stacks (hydraulically parallel) of an active area of 0.5 × 0.5 m^2 and 56 triplets each. In this sense, the system was designed considering that each stack could provide a power output of 250 W and an average power density of 6 W/m^2 of membrane [276].

3.1.4. Temperature-driven

3.1.4.1. Membrane distillation/membrane crystallisation (MD/MDC). Membrane brine concentrators have been reported to have the potential to revolutionize MLD by reducing specific energy consumption and capital costs by up to 50 %, while concentrating brines to values higher than 250 g/L [277]. Among such technologies that are capable of simultaneously concentrating brine salts and increasing water recovery, Membrane Distillation (MD) stands out as a promising option [278]. MD is a thermally driven phase separation process in which water evaporates through the pores of a hydrophobic membrane due to a transmembrane vapour pressure gradient induced by a feed/distillate temperature difference. The water vapour then condenses once in contact with the permeate side. Although the membrane pores are larger than water molecules, liquid water does not pass through due to high surface tension. Due to such mechanism, compared to other membrane processes, MD can theoretically reject 100 % of the non-volatile molecules [278]. MD can be configured in several ways, with the most common being Direct Contact Membrane Distillation (DCMD). Table 5 reports the operating principles of each configuration, alongside their advantages and main drawbacks [279].

MD is well-suited for desalination of high salinity brines because it operates in the vapour phase, meaning the presence of ions has a negligible effect on the water partial vapour pressure [280]. Furthermore, MD can operate in a wide range of temperatures up to 80 °C, above which operation results to be challenging due to the mechanical degradation of the membranes [281]. Typically, the feed solution in MD is heated at temperature values ranging from 40 to 60 °C, thus allowing the possibility to exploit waste heat or renewable energy and thereby eliminating the drawback of high thermal energy consumption and reducing substantially the operating costs [282]. Further advantages of MD include: (i) operation at low pressure and (ii) the low fouling propensity of the membranes, extending the lifetime of the latter and requiring limited pretreatment. Overall, given such advantages, MD can potentially substitute RO and MED for water production, especially when treating higher salinity solutions (i.e., ~250 g/L of NaCl) [283]. However, despite over five decades of research, MD has not yet reached to achieve large-scale commercialization due to operational complexities (i.e., unsatisfactory membrane performance, scaling and high

Table 5
Main MD configurations that can be used for freshwater production from SW or brine.

Configuration Type	Operating Principle	Advantages	Disadvantages
Direct Contact MD (DCMD)	Hot feed and cold permeate are in direct contact with opposite sides of the membrane; vapour passes through membrane pores and condenses.	Simple design; widely studied; good for lab-scale.	High heat loss due to direct contact; lower energy efficiency.
Air Gap MD (AGMD)	Non-circulating air gap between membrane and condensation surface reduces heat loss; vapour passes through membrane and air gap before condensing.	Reduced conductive heat loss; better thermal efficiency than DCMD.	Increased mass transfer resistance; lower flux.
Permeate Gap MD (PGMD)	Liquid permeate replaces air gap to reduce mass transfer resistance and improve flux.	Higher flux than AGMD; improved energy efficiency.	More complex design; potential for membrane wetting.
Vacuum MD (VMD)	Vacuum applied on permeate side to enhance vapour transport and separation.	High flux; good for volatile compound separation.	Requires vacuum system; risk of membrane pore collapse.
Sweeping Gas MD (SGMD)	Carrier gas sweeps vapour from membrane surface to external condenser.	Avoids direct condensation; suitable for volatile recovery.	Complex gas handling; lower energy efficiency.

energy consumption) [284–286] and is currently limited to small-to-medium scale plants. Indeed, among the very few companies specialized in MD, the global leader, Aquastill B·V, has nowadays industrialized small (10 m^3/d) to medium scale (1000 m^3/d) MD plants to treat SW (~35 g/L TDS) or industrial wastewater (~5 g/L TDS) exploiting waste heat, thus reaching TRL 8-9 [287]. In parallel, several pilot studies have been carried out exploiting several configurations of MD, different to DCMD. Elcik et al. investigated the performances of two pilot-scaled MD plants for desalinating respectively SW and concentrated brine in Jeddah, Saudi Arabia, demonstrating a 52 % water recovery rate with a vacuum multi-effect MD system and a 98.9 % salt rejection rate using AGMD [288]. However, challenges such as membrane module weight and system performance limited further testing. Similarly, Triki et al. integrated solar-powered VMD into an RO plant, achieving a water recovery increase from 37 % to 88 %, reducing brine volume fivefold while maintaining low production costs (3.78 USD/m^3).

It is worth mentioning that many of the initial MD pilot studies focused on solar-driven SW desalination, harnessing thus solar energy via PV panels or solar collectors with heat storage systems and reducing the overall energy consumption of the technology [289–292]. However, several other attempts to enhance the performances of MD have been made through the fabrication of novel materials. An example is the use of hydrophilic fabrics instead of hydrophobic membranes. These mitigate membrane wetting and fouling but require periodic salt removal, limiting commercialization. Ju et al., on the other hand, synthesized superhydrophobic Polytetrafluoroethylene (PTFE) membranes via electrospinning and calcination, achieving 40 L/(m^2·h·bar) permeability and 99.99 % salt rejection at 60 °C with 200-h stability [293].

Due to the appealing potential of treating high salinity solutions, several studies have focused on the treatment of brine, enhancing the efficiency of SW desalination [294]. Adham et al. built a state-of-the-art MD bench scale set-up to treat real thermal desalination brines from Qatar with a salinity of 70 g/L. Results showed that high fluxes (20 L/(m^2·h)) and high quality permeate (< 10 μS/cm) could be achieved, demonstrating that MD can increase overall water recovery from thermal desalination plants coupled with power plants within the Middle East [295]. It was within that region that to evaluate the technical feasibility of MD at pilot scale for thermal brine desalination in the Middle East, a consortium consisting of the ConocoPhillips Global Water Sustainability Center, Qatar University, and Qatar Electricity and Water Company was formed [296]. Schwantes et al. tested an innovative pilot-scale AGMD (the air-gap distillate was actively evacuated by an air jet) treating a brine with a salinity up to 253 g/kg NaCl. Concentration nearly up to saturation through the novel AGMD was successfully achieved [297]. Therefore, in the case of high salinity brine treatment, the TRL of MD is limited to 6.

Despite these technological developments exploiting the attractive advantages, MD yet faces further significant challenges when treating brines. A major hurdle that prevents large-scale implementation is membrane pore wetting, caused by organic compounds and that degrades membrane performance over time, losing selectivity. Rajwade et al. found foam fractionation to be an effective pretreatment strategy for mitigating membrane wetting in urban RO brine treatment [298]. Another challenge consists of the high energy consumption. Single-stage MD requires substantial energy input [299]. Multi-stage MD designs, such as those investigated by Chung et al., can improve efficiency, achieving performance levels comparable to MSF with lower capital costs [296,299]. Furthermore, in common with other membrane-based technologies, MD can suffer from scaling and concentration (and temperature) polarization [300], limiting the flux and energetic efficiency. Indeed, Yan et al. observed that MD effectively achieved high desalination rates but suffered from reduced thermal efficiency at high brine concentrations [301].

A recent technological advancement of MD is Submerged Membrane Distillation (SMD) which reduces energy consumption and offer higher thermal efficiency. The membrane module is submerged in the feed solution tank, resulting in a lower heat loss. Choi et al. demonstrated that submerged DCMD was able to concentrate brine solution to over a volume concentration factor of 2.1. However, SMD was strongly affected by feed temperature losses because of the Polyvinylidene Fluoride (PVDF) membrane tendency to form pore crystallization [302]. In order to avoid the phenomenon of temperature polarization, a further advancement of MD in recent years has been Photothermal Membrane Distillation (PMD) in which localized heating effects of photothermal particles incorporated in the membrane lead to the suppression of temperature polarization, thus enhancing evaporation flux [303]. To such scope, Politano et al. incorporated silver nanoparticles in PVDF membranes and was able to desalinate SW, achieving a permeate flux and conductivity equal to 25.7 L/(m^2·h) and 590 μS m^{-1}, respectively.

While historically used for water desalination, MD is gaining traction in the last decade for resource recovery from concentrated brines, thus approaching the MLD concept [304]. Examples include MD-SWRO Hybrid Systems. Such systems have the potential to maximize water production and reduce energy consumption [305], however, Naidu et al. demonstrated MD's ability to recover high-purity rubidium from SWRO brine, reducing overall treatment costs [306]. By adding FO to the SWRO-MD system, Son et al. demonstrated that a 2.2 brine concentration factor was achievable while mitigating calcium fouling [98]. Within the framework of resource recovery, EU-funded projects have been initiated in the past decade. An example is the MEDINA project that explored the combination of RO and VMD to enhance recovery and reduce brine discharge [307].

Furthermore, resource recovery from desalination brine has been achieved through a technological evolution of MD, namely Membrane Distillation Crystallisation (MDC). MDC is a hybrid of MD and crystallisation in which brine reaches saturation and subsequently supersaturation to facilitate the production of crystals that are gathered in an external crystalliser via controlled cooling or evaporation of the solvent. An advantage of MDC is the possibility to control the crystal size distribution. Quist-Jensen et al. employed MDC to NF retentate and RO brine [308]. Numerical simulations predicted that it was possible to recover multivalent ions such as barium, strontium, and magnesium from NF retentate whereas lithium can only be extracted from RO brine. KCl may be extracted from both NF retentate and RO brine. Zhang et al. used MDC to extract NaCl with 99.08 % purity, highlighting MD's potential for controlled crystallization. [309]. All in all, MDC seems promising for resource recovery and it has been reported by Macedonio et al. that desalination costs can be covered solemnly by the sale of the recovered salts even if waste heat is not available [310]. However, MDC is currently limited to the lab-scale.

3.2. *Membrane-less technologies*

3.2.1. *Temperature-driven*

3.2.1.1. Multi-Effect Distillation (MED). Multi-Effect Distillation (MED) is a thermal desalination technology that operates in a series of evaporators under progressively reduced pressures and temperatures, thereby enabling efficient heat recovery [311,312]. Each "effect" consists of a heat exchanger where SW is sprayed onto tubes heated by steam or hot water, producing water vapour that condenses and transfers heat to the next stage. Operating typically at 60–70 °C and under pressures from 0.1 to 0.35 bar, MED achieves energy-efficient distillation through reuse of latent heat [313].

For heat recovery and increasing the energy efficiency of MED, thermal vapour compression (TVC) is commonly employed [311]. In this process, a portion of the vapour from the last or an intermediate stage is extracted and compressed using a steam jet ejector to a higher pressure and temperature level. This compressed vapour is then reused as the heating steam in the first stage. The motive steam pressure entering the jet ejector in TVC plants ranges between 2.5 and 20 bar

[313]. In addition, mechanical-vapour compression (MVC) can be applied to single- and multiple-effect evaporators [311]. In this case, the generated vapour in the evaporator is compressed by a volumetric compressor to increase its pressure and thus its condensation temperature. This vapour can then be used as the heating steam in the same or in proceeding stages. This configuration is favoured in small-scale SW desalination systems due to the use of electrical energy and an electric SEC [314].

The primary objective of MED is to produce freshwater from saline feedwater. As mentioned and confirmed in the analysis conducted in Section 2, MED is widely implemented in large-scale SW desalination (TRL 9), particularly in the Middle East, with capacities reaching 600000 m^3/d of freshwater [311]. MED-TVC is often integrated to enhance energy efficiency and capacity. For example, Mahmoud et al. evaluated the performances of a pilot-scaled MED-TVC (freshwater production of 24 m^3/d) in Jubail, Saudi Arabia, successfully increasing the top brine temperature from 65 °C to 95 °C without scale formation [315]. Results of a subsequent techno-economic analysis revealed that using TVC allowed to reduce steam consumption by 34 % and the water production cost by 16 %.

In general, industrial-scale MED plants are typically in the >10000 m^3/day range treating standard SW (35–45 g/kg TDS) and can concentrate the latter up to 65 g/kg [311]. Some systems integrate MED with renewable heat sources for improved sustainability [316].

MED has also been evaluated in ZLD and near-ZLD contexts where the main objective is to concentrate the brine. Experimental and modelled applications have demonstrated the ability of MED to handle feed salinities up to 260 g/kg [316,317]. Coupled systems (e.g., MED with solar power) have shown potential to process up to 357 g/L [318], indicating suitability for hypersaline brine treatment. Several studies [25,319] model its performance in brine concentration loops, where MED can concentrate brines to levels (e.g., >260 g/kg) that enable subsequent mineral extraction (e.g., NaCl, Mg, and Ca salts) in downstream processes [25]. However, MED for direct brine treatment is still limited to the pilot scale/large demonstration scale, featuring in integrated desalination projects across the Middle East and Mediterranean, often supported by public-private partnerships and R&D programs. More specifically, within the Water Mining project, Scelfo et al. tested a pilot-scale MED (capacity = 1.7 m^3/h) integrated in a MLD chain, valorising the SW retentate of an upstream NF unit [320]. The MED unit was fully powered by waste heat at 70-80 °C from diesel engines. A recovery ratio above 80 % was achieved, producing a final brine with a conductivity of 240 mS/cm, very close to NaCl saturation, thus being excellent for food-grade sea salt production in EPs.

Key limitations include high CAPEX due to complex multi-stage systems and the need for corrosion-resistant materials, especially for brine concentration [321]. Future improvements target cost reduction through novel corrosion-resistant and low-cost materials (e.g., polymer-lined metals or ceramics) [321,322].

3.2.1.2. Thermal brine concentrators (TBC). Thermal brine concentration often utilizes one or more evaporators and is frequently combined with MVC [321]. In this set-up, incoming feedwater is initially heated using heat exchangers that recover thermal energy from the outgoing distillate stream. The warmed feed is then combined with a circulating slurry of concentrated brine in the sump of the evaporator unit. Within the concentrator, the slurry travels downwards through vertical tubes, forming a thin liquid film along the interior tube surfaces where evaporation occurs. To prevent scaling on heat transfer surfaces, gypsum seed crystals are frequently introduced, which help maintain precipitating salts in suspension [323]. The vapour generated during evaporation is compressed and then condensed on the outer surfaces of the tubes, releasing latent heat that drives further evaporation of the descending brine. The resulting distillate is used once again to preheat incoming feedwater. The thin-film configuration enhances heat transfer efficiency, lowering both the compression ratio and energy consumption [324]. Nevertheless, the MVC thermal brine concentration still demands considerable amounts of high-quality electrical energy [323]. This method is widely used in ZLD applications, although brine concentration typically reaches a limit of around 250 g/L due to the risk of glauberite precipitation [324]. Furthermore, the high salinity and chloride content of the brine require construction materials with superior corrosion resistance, such as titanium or stainless steel, driving up the system's capital costs [321]. The TRL of the TBC is 9. However, improvements can be made by enhancing the corrosion resistance of the used tubing materials by using thermally conductive polymer composite tubes [322]. Moreover, also the addition of pretreatment processes (e.g. NF) to reduce the risk of scale formation is suggested to increase the maximum possible concentration [56].

3.2.1.3. Multi Stage Flash (MSF). Multi Stage Flash (MSF) distillation is one of the most widely implemented thermal desalination technologies, particularly in the Middle East [311,325]. The process operates on the principle of "flashing" SW into steam by reducing the pressure in successive stages, allowing for efficient evaporation and freshwater production [311].

In an MSF system, SW is first preheated in a series of heat exchangers before entering a brine heater, where it is raised to a high temperature (typically 90 °C to 120 °C) using steam from an external source [325]. The heated water then flows into a series of flash chambers, each operating at a lower pressure than the previous one. Due to the pressure drop, a portion of the heated water instantaneously vaporizes, or "flashes" into steam. This steam is then condensed onto the heat exchanger tubes, recovering the latent heat and preheating incoming SW. The remaining brine continues through multiple stages, flashing successively until it is discharged as concentrated brine [325].

One of the key advantages of MSF is its robustness and ability to handle large-scale water production. MSF plants can produce thousands of cubic meters of freshwater per day, making them suitable for large-scale urban and industrial applications [311]. The maximum reached salinity in industrial used MSF plants is 65 g/kg.

However, MSF has significant drawbacks, primarily related to its high energy consumption. The process requires large amounts of thermal energy, making it heavily dependent on fossil fuels unless integrated with waste heat recovery systems [311]. Additionally, the high operating temperatures lead to challenges such as scaling and corrosion, which necessitate frequent maintenance and chemical treatment of the feedwater [325]. Therefore, its primary use is limited to freshwater production from SW and its application for brine concentration has not been investigated.

3.2.1.4. Humidification Dehumidification (HDH). Humidification Dehumidification Desalination (HDH) is a small-scale, decentralized technique that uses a carrier gas to produce clean water from saline water [326]. The HDH process essentially mimics the cycle of rainfall in nature. More specifically, heated saline water humidifies air in a direct contact heat exchanger (humidifying column), where air moves upwards whilst hot saline water falls downwards [327]. The heated, humidified air is then transferred to a dehumidifying column through cross connected ducts, where the condensed water (at a surface temperature which is lower than the dew point of ambient air) is collected as freshwater.

Among the operating parameters that influence the most the final performances of HDH, there are: (i) the air flowrate and (ii) the salinity of the feed solution. The air flowrate significantly can impact the amount of freshwater produced where the larger flowrates promote larger productivity. Meanwhile, as for the salinity of the feed solution, the higher it is, the higher is the thermal energy consumption, causing lower productivity. Nevertheless, despite lower productivity, it has been demonstrated that the quality of clean water produced is not

compromised [328]. Thus, one first advantage of HDH is the ability to treat high salinity (exceeding 100 g/L) even though HDH systems have been commonly used to treat BW and SW (up to 35 g/L).

Additional advantages over other thermal distillation technologies include: simple design, low maintenance and operating costs, low investment, the potential to be powered by sustainable energy sources (i.e., solar and geothermal), ability to operate at low pressure and compatibility with low-temperature heat sources [329]. HDH systems can also utilize waste heat from condensation to heat the feed water, enhancing efficiency.

Among the drawbacks, conventional dehumidifiers require a large condensing area due to the additional thermal resistance caused by high concentrations (60-95 wt%) of non-condensable gases in the air. Bubble column dehumidifiers can solve such issue, reducing the condensing area and cost [330]. However, bubble coalescence can decrease the gas-liquid contact area and reduce mass and heat transfer [331]. Heat loss and therefore low productivity (with maximum 35 % recovery when treating SW) are the main reasons that have limited the potential of HDH to be commercialised for large-scale SW desalination, thus presenting a current TRL of 4-6. To reach commercialisation, more experimental investigations are required on HDH driven by renewable energy at a larger scale, along with the exploration of new designs, insulators and packaging to reduce heat loss and increase productivity.

Conventional desalination technologies such as RO, MED and MVC are suitable for large-scale freshwater production (100-50000 m^3/d) but are costly for small-scale production and impractical in areas with limited maintenance facilities and energy supply [332]. Therefore, HDH is a more appealing alternative to produce freshwater at smaller capacities.

Various heat configurations (e.g., air-heated, water-heated and dual-heated) have been explored, with air-heated cycle showing the most promise. However, most studies on air-heated HDH systems are theoretical, with few experimental studies on small lab-scale set-ups. Compared to other desalination technologies, there has been limited research on HDH in the past two decades, primarily at the lab-scale.

Among the larger-scale systems (pilot-scale), Ghazal et al. investigated a solar humidification prototype where air travels upwards as bubbles, combining air heating, water heating, and humidification in one compact unit [331]. Experiments in North Cyprus showed that, with an average solar radiation intensity of 700 W/m^2 and an air mass flowrate of 12.6 kg/h, the water evaporation rate was 0.75 kg/h per square metre.

In 2025, Shaikh et al. studied a pilot-scale flat-plate solar air collector-powered HDH unit in Kerala, India [326]. With an average solar intensity of 712 W/m^2, the system achieved a maximum distillate yield and gain output ratio of 17.34 kg/d and 0.65, respectively. Wood apple shell packing outperformed commercial packing in terms of distillate yield, gain output ratio and humidifier performance potential factor.

Eslamimanesh et al. conducted an economic analysis comparing HDH to small-scale RO for treating SW from the Persian Gulf [333]. They found that the production costs of water for both technologies were comparable, but HDD was more suitable when energy costs were not a major concern or when renewable energy sources were used. Both technologies achieved production costs of 6.4 USD/m^3.

Elhenawy et al. proposed a novel solar hybrid AGMD and HDH using photovoltaic panels for electricity. With a SW flowrate of 600 kg/h, the gain output ratio reached 5.33 in the summer with a specific thermal energy consumption (STEC) ranging from 60 to 310 kWh/m^3 at a global radiation of 718 W/m^2 [334]. The LCOW was 14.32 USD/m^3.

All in all, most HDH research focuses on lab-scale or small pilot-scale production of freshwater from solutions with a salinity comparable to that of SW. In the case of desalination brine management, some mathematical studies have explored the potential of HDH to concentrate brine by direct contact with hot, dry air to the level of supersaturation. The desalination brine crystallises salt as vapour is transported to the condenser for the recovery of distillate and condensation heat. Using HDH-based crystallization would bring various benefits such as low scaling and fouling potential, along with low costs. A techno-economic analysis demonstrated that the HDH-based crystalliser presented an energy consumption that was 56 % lower than that of a traditional evaporative crystalliser [335]. In 2024, only Shamet et al. integrated a multi-stage HDH system with a crystalliser for ZLD of SW desalination brine [336]. HDH was used to treat desalination brine at the lab-scale, addressing issues like membrane fouling/scaling encountered in membrane-based technologies. The highest gain output ratio of 2.2 was achieved with a series configuration, and the crystalliser increased water productivity by 26.4 %. In this set-up, the SEC and STEC were 3.21 and 1050 kJ/kg, respectively. Using waste heat, the parallel configuration allowed for free freshwater distribution, whilst salt crystals could be sold at 58 USD per tonne.

It is however to be mentioned that despite HDH not being implemented at a commercial scale for SW and desalination brine treatment, HDH is currently commercially available for a specific application: treating highly salinised produced water from hydraulically fractured oil and gas wells.

3.2.1.5. Evaporation/solar ponds (EPs/SPs). Evaporation ponds (EPs) are attractive for desalting water and recovering salts from brines due to their simplicity in manufacturing and low operational costs. An EP is a large, shallow body of saltwater solution where brine evaporates using solar energy, leaving concentrated salt solution or crystals at the bottom. This method is one of several conventional brine disposal techniques (TRL 9), with disposal costs ranges of 3.3 - 10.1 USD/m^3, making it to date the most expensive method [337]. Assuming a high evaporation rate of 0.1 L/(h·m^2), capital costs of an EP can reach 40 million USD for a concentrate flow of 3800 m^3/d [55].

In EPs, the solar energy conversion is less than 2 %, making the process slow and inefficient and thus requiring large footprints. As water evaporates from brine, the heat capacity of the remaining water increases, further slowing the process [304]. EPs require intercepted solar energy per kg of distillate equal to several times the latent heat, whereas other distillation systems (e.g. MSF or MED) require only a fraction (1/3 - 1/9) of the latent heat, limiting EPs to small capacities. On the other hand, advantages of EPs include easy construction, low maintenance and minimal mechanical equipment. It is to be noted however that ponds must be prepared with impervious lining to avoid the contamination of underlying aquifers and double lining may be recommended if the brine contains significant amounts of toxic materials.

EPs can handle very high salinity levels (up to 160–350 g/L TDS), but their efficiency decreases as salinity increases. Typical brine concentrations treated in EPs are within the range 20–50 g/L TDS. When treating high salinities (i.e., 160 g/L TDS), evaporation rates can drop up to 50 %.

The main valuable salt that is generally recovered from EPs is NaCl (generally the first salt to precipitate), followed by potassium and magnesium chlorides. The achievable purity of the recovered salts depends on several factors such as the feed composition and crystallisation control. Typically, from SWRO brine, NaCl purity can reach values between 95 and 99 % after appropriate washing. As for KCl, values span in the range 90-98 % purity meanwhile for magnesium-based compounds values are within the 85-95 % purity range [338]. At even higher concentration levels, it is also possible to recover lithium carbonate. In the latter case, EPs have been widely used in lithium-rich regions like the Atacama Desert in Chile and Salar de Uyuni in Bolivia [339]. However, lithium recovery from brine is more complex and often involves chemical precipitation and solvent extraction after evaporation via EPs.

Several examples exist today in which EPs at a large-scale have been integrated with a desalination facility to reach MLD, treating brine and recovering salts.

In Eilat, Israel, the brine from the SWRO plant (capacity 10000 m^3/

d) was blended with SW (to avoid scaling in the downstream piping) and fed into a series of EPs [340], eliminating the need of a brine discharge line. This configuration increased salt production by 30 % compared to salt production from SW alone, with high product. It is to be noted that EPs are significantly convenient in Gulf countries due to strong solar radiation, low precipitation, low-cost desert land, easy transportation to ports and good accessibility to Asian nations, which are large consumers of salt. However, some additional issues concerning the use of EPs include dissolved organic matter interfering with salt crystallisation, reducing sodium availability for salt production and poor salt crystal shape.

Within the framework of the Water Mining Project, Morgante et al. integrated a series of EPs at the end of an MLD process for SW valorisation implemented at a large demonstration scale in Lampedusa, Italy [49]. Within the MLD process, the outlet of the MED unit fed the EPs at a flowrate of 180 L/h. 3 ponds in total were employed: (i) Pond A to concentrate the brine up to saturation, (ii) Pond B crystallization occurred, and, (iii) Pond C served to collect the precipitated salt. An NaCl purity greater than 99 % was achieved, well above the minimum required purity limit for food applications. During the SEArcularMINE project, Campione et al. simulated the approach of integrating a SWRO desalination plant with natural saltworks in Trapani [341]. Results showed that by feeding the saltworks with RO brine and not SW, the saltworks could operate with less than 53 % of its initial area. On the other hand, the coupling of RO and saltworks allowed to theoretically increase the salt productivity by 70 %, leading to an increase of 50 % productivity of the saltworks during the whole operational year.

In a techno-economic assessment, Ayou et al. evaluated the feasibility of water and salt production via the integration of small-scale grid-connected PV-RO (11.6 m^3/day of potable water production capacity) and EPs [342]. By using the RO brine to feed the ponds, it was possible to reduce the required size in the conventional salt evaporation ponds, reaching an area of 66.5 m^2, producing 1.2 tons of salts. It is better in terms of productivity than the conventional EPs which need 300 m^2 surface for 10-ton salt production.

Another type of EPs is Wind-Aided Intensified Evaporation (WAIV) where the ponds employ hydrophilic materials and wetting methods to increase the evaporative capacity per area by a factor of 10 or more [55]. Unlike traditional EPs, this alternative has not yet reached commercialisation and is currently limited to pilot-scale testing (TRL 6). Katzir et al. tested a bench pilot WAIV unit (~ 1 m^2 evaporation area loaded on 0.17 m^2 footprint) that was operated on two different desalination brines (RO and ED) [343]. In the case of ED brines, the pilot could concentrate up to 23 % TDS. Furthermore, the process showed preferential enrichment of magnesium ions over calcium and sodium.

Compared to conventional EPs, an additional advantage of WAIV is the reduced footprint since vertical structures are employed and minimal fouling can be observed on such vertical structures. However, disadvantages that have limited the upscale of WAIV are: (i) high set-up costs due to structural materials compared to EPs and (ii) handling precipitated salts from vertical surfaces can be more complex [343].

Apart from the conventional use where salts precipitate due to water evaporation, ponds can be employed as salinity gradient solar ponds (SGSP) to generate electricity from solar energy [304]. Advanced alternatives to SGSPs are membrane ponds and gel ponds.

SGSPs consist of: (i) a thin convective surface layer of low salinity water that has a temperature close to ambient temperature, (ii) stable non-convective transparent zone with density, salinity and temperature gradients and (iii) a convective (or storage) bottom layer of high salinity water and high temperature [327]. Thus, solar ponds can be used to capture and store solar thermal energy for various purposes treating salinities up to 250 g/L (industrial brine). As a stand-alone technology for heat storage, SGSPs present already a TRL of 8-9, being commercially demonstrated in several countries (e.g., Israel, India [344], USA, Australia [345], China [346], Iran [347] and Spain [348,349]). However, in the case of thermal coupling in desalination facilities (i.e., with MD or MED), TRL is reduced to 6-7 whilst small-scale pilot plants (TRL 5) exist within the scenario of brine treatment [350].

Monjezi et al. demonstrated that thermal energy from a solar pond of 10000 m^2 could regenerate the DS for a FO plant for SW desalination, with a low electricity consumption of 0.46 kWh/m^3 [351]. Financial viability and technical feasibility analyses for constant and reliable heat extraction from these SPs are yet required. Al-Othman et al. used a SP with a total depth of 4 m to heat SW for a simulated MSF desalination plant mainly driven by parabolic trough collectors in Sharjah, UAE, with 76 % of the power required could be provided by parabolic trough collectors and the remaining 24 % by a SP surface area of 0.53 km^2 [352].

Within the field of RO brine treatment, Manzoor et al. used an experimental SGSP with a 4.65 m^2 surface area to extract and apply heat on a lab-scale DCMD under the arid climatic conditions of Islamabad, Pakistan. Results identified an optimum flowrate of 7.5 L/min based on minimal drops of 2-2.5 °C in the Lower Convection Zone (LCZ). The LCZ was able to pre-heat the concentrated brine that was then sent to an MD unit that operated a low temperatures (~37 °C in the summer and 28.5 °C in the winter) [353].

Sayer et al. explored gel solar ponds as an alternative of the SGSPs [354]. Gel solar ponds can supply thermal energy to applications requiring low-grade temperatures, with similar temperatures in the low convective zone as SGSPs. However, gel ponds are more expensive but can address challenges posed by SGSPs, such as salt diffusion affecting pond stability and evaporation, reducing water quantity in the upper convective zone. Other disadvantages of using SGSP are the enormous quantity of salt required for the construction of a SGSP, being a potential source for pollution and heat extraction from the SGSP might disturb the interface between layers of the pond and cause oscillation and hence convection. Despite the greater cost and labour, gel ponds can be seen as a viable alternative if the gel layer is made of cheap and environmentally friendly polymers.

Abdusalam et al. integrated a SP and EPs via a heat exchanger and pump, to facilitate the transfer of hot brine from the SP to the EP and vice versa. This enhanced the evaporation rate as heat exchangers supplied more heat and they observed a significant improvement in the evaporation rate [355].

Overall, due to the high ecological footprint and large land availability, many countries have tried to minimize the use of EPs [356]. The little economy of scale has led the EPs to be used only for small volume concentrates [357]. In Table 6, an overview of the pond-based technologies employing solar energy is reported.

3.2.2. *Chemically-driven*

3.2.2.1. Crystallisation. In any mineral/salt recovery scheme exploiting any kind of feed water source (i.e., BW, SW or or desalination brine), the crystallisation step is crucial for recovering minerals in the solid form. There are two main conventional methods to achieve this: (i) thermal crystallisation and (ii) chemical crystallisation. Despite the specific method, it is to be noted that in general the TRL of crystallisation increases with the increase of the salinity of the feed water source. Indeed, whilst direct SW mining is less common due to the dilute concentrations of target minerals and the complexity of selective recovery (TRL 3-5), more efforts have been made for higher salinity feed solutions such as desalination brine (up to TRL 6).

Thermal Crystallisation: In this method, heat is applied to the brine solution to evaporate the water, concentrating the ions. The concentrated solution is then cooled, promoting the crystallisation of salts [358]. Poirier et al. proposed a multi-crystallisation separation process at the lab-scale that can recover calcite, anhydrite, halite, and epsomite, achieving near-ZLD and resource recovery. Specifically, a water recovery of 99.2 % and a brine volume reduction of 98.9 % were achieved [359].

Table 6
Comparison of the pond-based technologies employing solar energy for SWRO brine treatment.

Technology	Feed (TDS)	Potential surface area [m^2] to process 100 m^3/d of brine	Scale (TRL)	Resource recovered	Advantages	Disadvantages	Ref.
EPs	SWRO brine	1000 - 2000	9	NaCl (>99 %), KCl (90–98 %), Mg salts (85–95 %), Li_2CO_3	Simple design, low maintenance, high purity salt	Large footprint, slow evaporation, climate-dependent	[340]
WAIV	SWRO brine	100 - 400	6	NaCl, Mg-enriched salts	Higher evaporation rate than EP, smaller footprint	High set-up cost, salt handling complexity	[343]
SGSPs	SWRO brine	1000 - 2000	8-9 as standalone, 6-7 for desalination coupling	Thermal energy	Energy recovery, commercial deployment	Large salt requirement, layer stability issues	[372] [348,349]
Gel ponds	SWRO brine	1000 - 1500	5	Thermal energy	Stable thermal gradient, reduced evaporation loss	High cost, complex construction	[354]

An alternative is freeze crystallisation, where the brine solution is directly cooled below the freezing point of water, excluding the salts from the produced ice, which sink due to density differences. The brine is then further processed to recover the salts [360]. EFC (Eutectic-Freezing Crystallisation) has several advantages over conventional separation techniques, including low energy consumption, high-quality products, no scaling or fouling (due to low temperatures) and no need for additional chemicals [361]. Randall and Nathoo conducted a thermodynamic assessment on resource recovery via freezing from RO brine, SW, and stored urine [362]. They showed that salt recovery from RO brine and SW is possible using EFC technology, which can retrieve water and salts in pure form with low energy requirements compared to traditional evaporation-based processes. However, one issue is the formation of an ice scale layer on the heat exchanger surface during long steady-state operations [363,364]. To reduce ice scaling, Lewis et al. investigated novel heat exchangers made of materials with low surface energy, achieving successful results. Additionally, using a novel continuously stirred column crystalliser led to high supercooling and long induction times, overcoming the issue of ice scaling. Despite such efforts, EFC is still limited to a very low TRL in brine treatment. Indeed, it can be challenging to design and operate effectively due to the complexity of the elements involved. In addition, EFC also presents further drawbacks such as: (i) slower crystal growth than evaporation, (ii) applicable to salts with known eutectic points and favourable crystallisation behaviour and (iii) significant cooling energy is required, offsetting energy savings along with high capital costs.

Wang et al. [365] developed a conical solar–thermal–radiative evaporator for sustainable desalination and salt recovery, leveraging broadband solar absorption for efficient energy use. The photothermal converter transformed solar energy into infrared light, enhancing water absorption. A bottom transport structure enabled anti-gravity water flow via passive capillarity and active negative pressure evaporation. The optimized system achieved an evaporation rate of 1.25 kg/(m^2·h) and 89 % solar efficiency under one sun. During a continuous 40-h treatment of 10 wt% saline solution, it maintained a stable rate of 1.15 kg/(m^2·h) while continuously collecting salt from the edges, enabling simultaneous recovery of freshwater and salt.

Among the multiple salts that can be recovered from brine via thermal crystallization, Bouazza et al. introduced a novel approach for recovering kainite, a mineral with substantial industrial applications and notorious for its nucleation difficulties, from RO brine. This approach involved discontinuous evaporation through a temperature-altering technique, adjusting temperatures from 69 °C, 55 °C, 35 °C, and 25 °C, each subsequently reduced to 15 °C. Results demonstrated the success of kainite recovery, proving the potential of this technique and contributing to sustainable water management [366].

Finally, a novel lab-scale thermal crystallisation technique was explored by Santoro et al. This consisted in photothermal crystallization using 3D vertically oriented graphene sheet arrays as potential photothermal membranes. Superior light-to-heat conversion was achieved, and NaCl(s), KCl(s), and $MgSO_4$(s) were successfully recovered from hypersaline solutions [367].

Chemical Crystallisation: This method does not use heat but requires a chemical reactant to promote the precipitation of a specific salt. Chemical precipitation is usually simple, cheap, and easy to commercialise [368]. The pH at which the chemical reaction occurs is crucial, as at different pH values different salts can precipitate, potentially compromising the purity of the final product. Depending on the chemical reactant and the feed solution composition, there is a risk of recovering low-purity products.

In the case of magnesium recovery from brine, Vassallo et al. bypassed this issue by investigating a lab-scale Crystalliser with Ion Exchange Membrane (CrIEM), a membrane reactor that uses low-cost alkaline reactants such as calcium hydroxide to promote the selective permeation of OH^-, leading to the precipitation of magnesium hydroxide on the other side of the membrane [369]. In chemical/reactive crystallisation, the relative concentration of the alkaline reactant is also important, as it can influence the final properties of the recovered product. Morgante et al. observed that a higher initial Mg^{2+} concentration (1.0 M) in the feed brine led to the production of larger and stronger agglomerates of $Mg(OH)_2$(s) particles than those produced by a lower initial concentration (0.24 mol/L) [370]. After applying ultrasound and a dispersant agent, micro-sized $Mg(OH)_2$(s) agglomerates/aggregates were measured in the case of 1.0 M Mg^{2+} solutions, while nano-sized and micro-sized particles were detected for the 0.24 mol/L case. The recycling strategy was crucial to overcome filterability and sedimentation issues in large-scale production of $Mg(OH)_2$(s) suspensions, especially for those precipitated using NaOH solutions.

Several EU-funded projects have inserted crystallisation steps within MLD chains to recover valuable solid-salts from SW, desalination brines or saltwork bitterns. It has to be noted that the main component that has been attempted to recover from such sources was magnesium. This is mainly due to the concentration, being the second most abundant cation in SW. In the Water Mining project, a large-scale integrated demonstration plant was built and operated in Lampedusa island treating SW. With the integrated scheme, magnesium and calcium were recovered in the form of hydroxides using NaOH in a large-pilot scale reactive crystallizer, Multiple-Feed Plug Flow Reactor (MF-PFR), reaching purities of 98 % and 80 %, respectively [49]. The same technology was also used in the SEArcularMINE project, treating saltwork bitterns and reaching higher purities of magnesium due to the low presence of calcium in the initial bitterns [264]. Nowadays this technology is under technological validation through the MareMag LIFE project [371]. More specifically, the MF-PFR at a TRL of 7 will be used to recover magnesium hydroxide

from residual brine from sea-salt production from the Kitros saltworks in Greece, using (i) renewable energy and (ii) chemicals from a BMED unit.

Additionally, it is worth mentioning that recovering valuable solids via crystallisation has also the parallel effect of enhancing water recovery in MLD/ZLD treatment chains. Indeed, O'Connell et al. observed that water recovery can reach up to 98.6 vol% [7]. Crystallisation can improve water recovery and increase economic efficiency when disposal is expensive but comes with energy burdens. The LCOW is lower when water recovery is driven by crystallisation compared to high-recovery concentrators. However, SEC decreases for concentrators compared to crystallisers. In the specific case of land availability being an issue, crystallisation becomes essential and preferred to conventional EPs.

However, the typical crystallisation step generates a fine slurry of crystals, requiring filtration and drying steps to obtain a dry product, adding complexities. Recently, Nielsen et al. introduced the concept of vacuum per-crystallisation, separating saline solutions to yield distilled water and dry crystals in a single step [372]. Warm feed solution passes through a membrane without retaining the dissolved components. The liquid permeating through the membrane is evaporated through vacuum to precipitate the dissolved solids as crystals. In this specific case, identifying suitable membrane features and operative conditions to ensure crystal detachment from the membrane surface is crucial. In their study, only membranes with a permeation rate comparable to the evaporation rate under vacuum worked well.

A final alternative to conventional chemical crystallization is Solvent-Driven Fractional Precipitation (SDFP) or Anti-solvent crystallization in which targeted solutes are selectively precipitated from multicomponent solutions upon the addition of an external organic solvent. For instance, selective precipitation of KCl(s) from mixed salt solutions upon alcohol and ammonia addition have been recently reported. SDFP was dominant in the early development of the potassium fertilizer industry where organoamines were deliberately added to hypersaline brines to selectively precipitate KCl(s) from a NaCl-rich solution [373]. Such process presents two notable advantages over traditional approaches: (i) they are not constrained by the practical limitations of membrane systems and (ii) they avoid the high latent of vapourisation of water during extraction and regeneration. However, data on the effect of temperature of the multi-phase equilibria is limited and mechanistic understanding of the molecular interactions in water-solvent-salt systems is incomplete. Thermodynamic and first-principles-based research are also required to establish the mechanism of fractional crystallisation. Thus, all such aspects have currently limited the implementation of SDFP at the laboratory scale.

Table 7 compares all different types of crystallisation processes that have currently treated desalination brine and that have been discussed throughout this study.

3.2.2.2. Precipitation. One of the main problems that faces desalination processes, either membrane-based or thermal-based technologies, is the formation of calcium deposits. In fact, gypsum formation limits the application of MSF to a 50 % water recovery during SW desalination. This water recovery could be improved with lower calcium concentrations; for example, a 20 % lower calcium concentration in SW can make it feasible to operate an MSF evaporator with up to 75 % water recovery [374]. Calcium sulphate is also a common scalant in membrane-based processes [375], but it can also precipitate as carbonate ($CaCO_3$(s)) and even as phosphate ($Ca_3(PO_4)_2$(s) or $Ca_5(OH)(PO_4)_3$(s)) in pressure-driven membrane processes [376]. Commonly, scaling related to calcium minerals is prevented by modifying the feed water characteristics, aiming to reduce its concentration, through the use of coagulation, ion-exchange, and acidification, among other methods. Other strategies include the optimisation of the process, as well as an appropriate system design, and the addition of anti-scalants. As a summary, Table 8 collects the main results obtained when removing calcium by precipitation.

The most widely used method to remove calcium from SW and desalination brines is based on its precipitation as carbonate. Calcium removal as carbonate has been studied either as SW pretreatment or focusing on the resulting brine, with the aim to recover other minerals of interest or to implement ZLD or MLD strategies. However, in case Mg^{2+} must be recovered, it must be highlighted that its presence directly affects the calcite crystal growth, which is mainly related to its incorporation into the calcite seed surfaces [383]. Such an effect becomes significant if Mg^{2+} recovery is pursued. For instance, Drioli et al. [377], when proposing the recovery of different salts from SWNF brine, reported that calcium removals varied from 56 % to 86 % depending on the initial pH values, revealing the formation of vaterite at pH < 9 and calcite at pH > 9. Nevertheless, some of the Mg^{2+} co-precipitated (approximately 8-10 %) due to its incorporation into the carbonate phase. In a similar case study, Casas et al. [378] proposed calcium and magnesium recovery from different types of brines (potash mine collector brine, SWRO brine and ED-SWRO brine). Calcium removal was increased at higher pH values, temperatures and carbonate content. In fact, calcium removals within the range of 94-96 % were obtained at pH > 10; however, when the temperature was increased to 65 °C, precipitation occurred at lower pH values. The presence of anti-scalants was detrimental to calcium precipitation, causing a reduction on its removal due to the adsorption of the anti-scalant onto the nucleating crystals. Similarly, the formation of vaterite was identified at Mg^{2+}/Ca^{+2} ratios higher than 3, whereas calcite was formed in the other cases. On the other side, Ayoub et al. [379] proposed softening of SW before the desalination process, using a $NaOH/Na_2CO_3$ ratio of 2:1. Although the pH was found to be significant on their removals, temperature barely influenced at pH higher than 11. As a matter of fact, Ca^{2+} and Mg^{2+}

Table 7
Comparison of crystallization-based technologies to recover valuable salts from desalination brine.

Technology	Principle	Target resources	Advantages	Disadvantages	TRL	Ref.
Thermal crystallisation	Evaporation followed by cooling	NaCl, $MgSO_4$, KCl, Kainite	High water recovery (up to 99.2 %)	High energy demand, scaling, fouling	6-9	[358] [358]
EFC	Cooling below freezing point to exclude salts from ice	NaCl, $MgSO_4$	Low energy required, high purity products, no scaling	Ice scaling, slow growth, high capital costs	3-5	[358] [358]
Photothermal crystallisation	Light-to-heat conversion via advanced membranes	NaCl, KCl, $MgSO_4$	Efficient solar energy use, continuous salt collection	Material cost, lab-scale only	4-5	[358] [358]
Chemical crystallisation	Addition of reactants to precipitate salts	$Mg(OH)_2$, $Ca(OH)_2$	Simple, scalable, selective recovery	Purity control, co-precipitation	6-7	[358] [358]
CrIEM	Selective OH- permeation through membranes for salt precipitation	$Mg(OH)_2$	High selectivity, low-cost reactants	Membrane cost, scaling	5-6	[358]
MF-PFR	Continuous reactive crystallization	$Mg(OH)_2$ $Ca(OH)_2$	High purity, pilot-scale validated	Requires integrated chemical supply	7	[358] [358]
SDFP	Addition of organic solvents to selectively precipitate salts	NaCl, KCl	Avoids membrane/evaporation constraints	Limited mechanistic understanding, lab-scale	3-4	[358]
Vacuum per-crystallisation	Membrane-based separation under vacuum	NaCl, $MgSO_4$	Simultaneous water and salt recovery	Requires matched membrane/evaporation rates	4-5	[358]
MDC	Combines MD with crystallisation	NaCl, $MgSO_4$, RbCl	Enables MLD, uses waste heat	Scaling, membrane durability	6-7	[358] [358]

Table 8
Calcium removal from SW and SWRO brines.

Method	Feed water	pH / Temperature / Reagents	Ca removal (%)	Co-precipitation of other ions (%)	Reference
Calcium carbonate (calcite)	SWNF retentate (1.24 g/L Ca^{2+}, 4.30 g/L Mg^{2+})	pH = 9.90 15 °C $NaHCO_3/Na_2CO_3$	89 %	8-10 % molar of $MgCO_3$ in the solid	[377]
Calcium carbonate (calcite)	SWRO brine (0.83 g/L Ca^{2+}, 2.62 g/L Mg^{2+})	pH = 10.6 25 °C Na_2CO_3	96 ± 2 %	70 % Mg^{2+}	[378]
	SWRO brine (0.83 g/L Ca^{2+}, 2.62 g/L Mg^{2+})	pH = 10.7 65 °C Na_2CO_3	94 ± 1 %	82 % Mg^{2+}	
Calcium carbonate	SW (0.52 g/L Ca^{2+}, 1.53 g/L Mg^{2+})	pH =10.5 25 °C 2 NaOH: 1 Na_2CO_3	76.34 ± 0.74 %	83.9 ± 1.49 % Mg^{2+} 66.7 ± 4.20 % B	[379]
	SW (0.52 g/L Ca^{2+}, 1.53 g/L Mg^{2+})	pH =10.5 30 °C 2 NaOH: 1 Na_2CO_3	81.92 ± 0.33 %	83.0 ± 0.1 % Mg^{2+} 70.1 ± 2.50 % B	
Calcium carbonate	Synthetic brine (0.86 g/L Ca^{2+}, 2.79 g/L Mg^{2+})	pH = n.d. 70 °C $NaHCO_3$ (HCO_3^-/Ca^{2+} molar ratio of 4)	91 %	7 % Mg^{2+}	[380]
		pH = n.d. 25 °C Na_2CO_3 (CO_3^{2-}/Ca^{2+} molar ratio of 1.2)	98 %	33 % Mg^{2+}	
Dolomite ($CaMg(CO_3)_2$)	SW (0.41 g/L Ca^{2+}, 1.29 g/L Mg^{2+})	pH = 10.2–9.2 25 °C CO_2(g)	97 %	91 % Mg^{2+}	[381]
Calcium sulphate	Synthetic brine (1.62 g/L Ca^{2+}, 5.34 g/L Mg^{2+})	pH = 7 60 °C	19.8 ± 0.2 %	Not detected by EDS	[382]

removals were 77 % and 85 %, respectively, at pH 10.5 and 20 °C, and increased to values higher than 99 % at higher pH values. Sorour et al. [384] evaluated Ca^{2+} removal as carbonates from SW and brines, reporting removals higher than 90 % at pH 9.2-9.3, but with losses of 10 % for Mg^{2+}. In another study, Sorour et al. [385] reported Ca^{2+} removals of 97 % and 93 % for SW and RO brines at a final pH of 9–9.2, with 23 % of Mg^{2+} co-precipitating. More specifically, Wang et al. [6] found that temperature was the most significant factor in removing calcium as carbonate from both SW and brine, reporting a decrease in solubility when the temperature increased from 25 °C to 95 °C at equimolar Na_2CO_3/Ca^{2+} ratios. When evaluating the reaction kinetics, removals of 75-85 % (depending on salinity) were reported after 40 min at 85 °C, but Mg^{2+} co-precipitated as well (approximately 7 %). A final study on Na_2CO_3 dosage revealed the possibility to increase removals to 85-90 % when working with a stoichiometric excess (ratio of 1.2). When implementing a ZLD process for brine treatment, Molinari et al. [380] proposed the Ca^{2+} removal as a first step. Firstly, the authors tested different reagents with solutions containing 0.86 g/L Ca^{2+}. The use of citrate (molar ratio citrate/calcium of 2, temperatures of 30 and 60 °C) revealed very slow kinetics (10 % removal) after 30 h. However, removals of 60 % (after 75 h at 30 °C) and 75 % (after 20 h at 60 °C) were attained with a solution containing 3.8 g/L Ca^{2+} using citrate. Since Mg^{2+} co-precipitated (25 %, initial concentration of 2.4 g/L) when using Na_2CO_3, the use of $NaHCO_3$ was preferred, despite the higher Ca^{2+} removals (98 %, molar ratio of 1.3). During the treatment of the brine with $NaHCO_3$, the authors reported that the presence of Mg^{2+} decreased Ca^{2+} removal due to a competition effect, whereas the presence of NaCl (instead of $MgCl_2$) resulted in a slight decrease in Ca^{2+} removal. The effect of the pH was found to be more significant at 60 °C, causing a decrease in removal from 78 % to 65 % when the pH changed from 9.5 to 9.0. In contrast, at room temperature, the removals matched (around 52 %). In addition, the authors reported a Ca^{2+} removal of 90 % at 60 °C and pH 9, working at molar ratios Na_2CO_3/Ca^{2+} higher than 4. Nevertheless, in all cases, approximately 10 % of Mg^{2+} was co-precipitated, which was attributed to the formation of $MgCO_3$(s) nanocrystals. In a later work [386], Ca^{2+} removals around 85 % with Mg^{2+} losses below 5 % were reported at 35 °C using diluted Na_2CO_3 solutions. Additional tests revealed that anti-scalants (2 mg/L) barely affected the precipitation, whereas Sr^{2+} could form $SrCO_3$(s). Continuous mode tests showed removals of 85 % for Ca^{2+} and 5 % for Mg^{2+}, resulting in calcium carbonate purities higher than 97 %. Chang et al. [387] proposed a fluidised bed homogeneous crystallisation technology for producing dolomite from brines. Batch tests showed the effect of pH on Ca^{2+} and Mg^{2+} removal, revealing the need to work at high pH values. For instance, 99.9 % of Ca^{2+} was removed at a pH higher than 9 (accompanied by 70 % Mg^{2+} removal), whereas a pH of 10 was required to remove 89 % of Mg^{2+}. Solids were determined to be a mixture of $CaCO_3{\cdot}H_2O$(s) (monohydrocalcite) and $MgCO_3{\cdot}3H_2O$(s) (nesquehonite). During the tests with the fluidised crystalliser, it was possible to remove 91 % of Ca^{2+} and 76 % of Mg^{2+} at pH 9.5, a Na_2CO_3 molar ratio of 2 and 40 min of hydraulic retention time. The analysis of the solids revealed the presence of $CaCO_3.H_2O$(s) and $MgCO_3.3H_2O$(s) with a dolomite-like structure.

Additionally, the removal of $CaCO_3$(s) from BW has been investigated. For instance, Rom and Klas [388] studied the aeration of a concentrate (4350 mg $CaCO_3$(s)/L total hardness, being 2200 mg/L calcium hardness). When treating the brine at the highest aeration rate (1.05 L/min) and seed concentrations (10 g/L), a removal rate of 1.05 g $CaCO_3$/(L·h) was achieved, with a minimum hydraulic retention time of 1.5 h. Cherif et al. [389] proposed calcium removal before magnesium recovery from a desalination brine. Two solutions were considered, a NF brine and a RO brine (after treating the NF brine). When treating the NF brine (224 mg/L Ca^{2+}), it was possible to remove completely calcium as calcite at pH 11.32, but a removal of 69 % was obtained a pH 9.78 with the RO brine (416 mg/L Ca^{2+}).

Other methods evaluated were related to fixing CO_2(g) with SW, precipitating both Ca^{2+} and Mg^{2+} as carbonates. For example, Wang et al. [381] reported a pH decrease when bubbling 15 % CO_2(g) in SW, causing removals of Ca^{2+} and Mg^{2+} of 97 % and 91 %, respectively. The analysis of the solids revealed that they were composed of dolomite [$CaMg(CO_3)_2$(s)] and magnesite [$MgCO_3$-nH_2O(s)]. Considering the proposed process, it could be possible to fix 1.34 m^3 (or 2.65 kg) of CO_2(g) per one m^3 of SW, assuming 90 % removals for Ca^{2+} and Mg^{2+}. In a similar study, Mahmud et al. [390] proposed CO_2(g) sequestration using Mg^{+2} free desalination brines. Independently of the salinity,

removals higher than 99 % were achieved at NaOH dosages of 5 g/L, whereas the CO_2(g) flowrate had no significant effect. Optimum conditions were found at 5 g/L NaOH, 2 L CO_2(g)/min and 75 g/L salinity, allowing to uptake 5.4 g CO_2(g)/L.

Other calcium removal options are based on the precipitation of gypsum. For example, Almasri et al. [391] proposed a two-stage treatment process for brine, based on a first removal of gypsum, followed by the removal of calcium sulfoaluminate. In the first stage, it was possible to reduce the sulphate concentration from 100 to 12.1 mmol/L when using twice the stoichiometric dosage of calcium chloride. By adding lime and sodium aluminate (in a proportion of 1/0.67 to the initial sulphate), it was possible to decrease the sulphate concentration to 6 mmol/L at pH 11. XRD analysis of the solids collected in this second stage identified a mixture of ettringite and monosulfate. Moreover, Choi et al. [382] proposed the crystallisation of calcium sulphate from SWRO brine. The authors reported that the pH (within the range of 5 and 9) did not affect the precipitation of $CaSO_4$(s). However, it was revealed that higher temperatures improved calcium removal, moving from 22 % (at 50 °C) to 32 % (at 80 °C). Additionally, the presence of Mg^{2+} decreased the removal of Ca^{2+} from 29 % to 19 %. Finally, when studying the effect of a back electrolyte, the authors reported that the ionic interferences of Na^+ and Cl^- caused a reduction in the removal efficiency.

3.2.3. Extractant affinity

3.2.3.1. Ion-exchange (IX) / adsorption. Ion-exchange (IX) and adsorption processes are used to selectively extract dissolved solutes (<300 mg/L, according to providers) from aqueous solutions. Although both present similar characteristics, IX is based on the exchange of ions with those contained in the functional groups of the sorbent. In contrast, adsorption involves weaker interactions (i.e., van der Waals forces) [392,393]. Both technologies are applied on a large scale, primarily focused on removing hardness in the chlor-alkali industry before the electrolytic cell (approximately 305 g/L NaCl, 2 mg/L Ca^{2+} and Mg^{2+}), or in the removal of hardness from potable water [394,395]. Due to the benefits of the process, in terms of selectivity and low CAPEX and OPEX, both technologies have been evaluated for the recovery of different elements at lab-scale. However, the process remains challenging because of their low concentrations.

Boron, a small-sized and uncharged species, can easily permeate during an RO-based desalination process. In fact, drinking water standards fixed boron concentration to 1 mg/L in the EU and 2.4 mg/L by the WHO, whereas its concentration in the SW ranges from 3.5 to 6 mg/L. Boron removal is commonly targeted by implementing a multi-pass RO configuration, which increases both CAPEX and OPEX [396]. Most of the studies related to boron using chelating IX are focusing on its removal from either SW or the RO permeate, rather than assessing its recovery. For instance, IX using *N*-methylglucamine resins for boron removal from SW was evaluated by Jung and Kim [397], where the CRB05 showed efficiencies of 95 %, being easily regenerated using 0.05 mol/L H_2SO_4 (85 ± 5 %) or 0.25 mol/L HCl (87 ± 5 %). Similarly, Hameed et al. [398] proposed the use of a *N*-methylglucamine resin (e.g. Amberlite IRA 743) for SW pretreatment and studied the effect of initial concentration, pH, temperature and adsorbent dosage, revealing the possibility of extracting more than 90 % of boron. Instead of focusing on SW, Figueira et al. [399] evaluated the *N*-methylglucamine resins (S108, CRB03, CRB05) from SWRO brines. Batch tests revealed that sorption followed Langmuir isotherms, with boron capacities of 11 mg/g for S108, 12 mg/g for CRB05 and 15 mg/g for CRB03. Tests under column mode with the CRB03 showed that the resin was saturated after 130 BV (starting concentration of 50 mg/L). Following desorption using 4 % HCl, it was possible to concentrate boron by a factor of 30. Still focusing on boron recovery, but applied to bitterns (120-360 mg/L B), Vallès et al. [400] investigated the performance of the same resins using lab-scale columns, reporting the possibility of extracting boron. They found that CRB05 (9.1–12 mg B/g resin) was the preferred choice. Following regeneration with 1 mol/L HCl, a concentration factor of 9.6 was reported. In addition, the authors reported that these resins were also effective in extracting some trace elements, as Ga, Ge and Co. Moreover, the use of B-chelating resins was also proposed before recovering $Mg(OH)_2$(s), to avoid boron adsorption on the produced crystals. As a matter of fact, the implementation of such process allowed to reach purities of 95 ± 2 % for $Mg(OH)_2$(s) during the treatment of lithium rich brines [401]. Similarly, this strategy was applied to bitterns, which resulted in the possibility of recovering pure $Mg(OH)_2$(s) (>98 %) with low B-content (<0.10 mg B/g), matching the specifications for refractory industry. Additionally, if an evaporative crystallisation for B recovery is performed with the IX eluate, 95 % purity of H_3BO_3(s) could be attained [402].

Another element of interest that can be targeted using sorption is lithium, whose concentration in SW ranges from 0.1 mg/L (North Sea) to 0.22 mg/L (Atlantic Ocean), whereas in continental brines it can range from 20 to 1500 mg/L [403]. Due to the high availability of Li^+ in SW, several authors have proposed the use of spinel-type manganese oxide adsorbents as an efficient way for its recovery instead of IX resins due to their low selectivity [404,405]. Commonly, a lithium manganese oxide (LiMnO(s)) is first developed. After that, Li^+ is extracted using acidic media, leaving an ion sieve sorbent that can selectively extract Li^+ from SW. For instance, Xiao et al. [406] demonstrated that the LiMnO(s) material exhibited high selectivity for Li^+, but the presence of co-existing cations reduced the sorption capacity towards Li^+, especially when Mg^{2+} was present. Nevertheless, after elution with 1 mol/L HCl, the concentration of competing cations remained below 10 mmol/L, whereas Li^+ concentration could be increased up to 280 mmol/L (32.0 mmol/L in the feed solution). Similarly, Park et al. [407] reported that co-existing cations also affected the Li^+ extraction when using manganese oxide. Moreover, the authors reported that the sorption followed the Langmuir isotherm model, with a maximum sorption capacity of 11.9 mg Li^+/g in SW. The same findings were observed by Chen et al. [408] who developed a material with a Li^+ adsorption capacity of 5.6 mmol/g, which was reduced to 2.5 mmol/g in the presence of other ions. Na^+ and K^+ were slightly extracted (adsorption capacities of 0.035 and 0.017 mmol/g, respectively), whereas both Ca^{2+} and Mg^{2+} were removed to a larger extent (adsorption capacities of 0.394 and 0.425 mmol/g, respectively). A material developed by Yoshizuka et al. [409] based on manganese oxide and tested with SW and brine showed that the presence of cations did not influence Li^+ adsorption capacity, showing that other cations (Na^+, K^+, Mg^{2+}, and Ca^{2+}) were hardly adsorbed. However, when studying desorption, the acid concentration was found to be significant in terms of material integrity, revealing that at concentrations higher than 0.75 mol/L HCl, the manganese oxide dissolved into the solution.

The low availability of rubidium, which is commonly present in low quantities in some minerals (e.g., lepidolite or zinnwaldite), has driven research towards its recovery from either SW or brines, where it is present in concentrations ranging from 0.180 mg/L to 0.3 mg/L. The most studied sorbents are based on potassium hexacyanoferrate. In a first stage, Naidu et al. [410] developed different potassium hexacyanoferrate sorbents with different metals (KMFC), showing that Rb sorption capacities were in the order of KCuFC > KNiFC > KCoFC > KFeFC. After that, the KCuFC was later encapsulated within polyacrylonitrile, showing a reduction in Rb^+ sorption with increasing NaCl content, moving from 0.30 mmol Rb^+/g (in the absence of NaCl) to 0.20 mmol Rb^+/g (2.5 mol/L NaCl). However, when testing the SWRO brine capacity dropped by 80-85 % due to the predominance of K^+. Tests with packed-bed columns using 0.06 mmol/L of Rb^+ reported a capacity of 1.01 mmol/g, and after saturation, 95 % of Rb^+ was desorbed with 0.2 mol/L KCl. The competition of K^+ for the active sites in the sorbent could be diminished by using a natural clinoptilolite zeolite to remove it before Rb^+ extraction [411]. In fact, Rb^+ sorption capacity increased from 1.81 ± 0.04 mg/g to 7.83 ± 0.02 mg/g after removing 65 % of the initial K^+ from the SWRO brine. In addition, the authors assessed the use of MD (at

65 % permeate recovery) coupled with Rb^+ extraction for treating the SWRO brine [306]. The tests with the brine allowed for the extraction of 96.6 % of Rb^+ (initial concentration of 5 mg/L). Following saturation, the sorbent was regenerated with either 0.2 mol/L KCl or NH_4Cl, allowing the recovery of 97-98 % and 95-96 % of the Rb^+, respectively. However, regeneration with NH_4Cl requires an additional step using 0.5 mol/L KCl to convert the sorbent to the potassium form. Considering that K^+ presence diminished Rb^+ uptake, Quyet Truong et al. [412] created a composite material by grafting potassium cobalt hexacyanoferrate (KCoFC) with zeolitic imidazole frameworks (named KCoFC@ZIF). The KCoFC@ZIF exhibited a higher capacity than the KCoFC, but both showed a reduction in Rb^+ uptake of 44-45 % when treated with SW due to the competition from K^+. Despite that, KCoFC@ZIF maintained a high Rb^+ uptake of 236 mg/g compared to KCoFC (28 mg/g).

Similar materials used for Rb^+ extraction are also employed for Cs^+ recovery from SW; however, most of these studies focus on the removal of radioactive caesium-137 (^{137}Cs) [413–415]. Even though most of the literature is related to ^{137}Cs, only a few works aimed to recover it from SWRO brines. For example, Gibert et al. [416] studied the recovery of Cs^+ (20 mg/L) and Rb^+ (33 mg/L) at lab-scale using the Cs-Treat, a hexacyanoferrate compound. The breakthrough points, referred to as 90 % removal efficiency, occurred approximately at 21 and 40 days for Rb and Cs (2 mL/min of brine flowrate). As a result, sorption capacities of 238 mg Rb^+/g and 44 mg Cs^+/g were reported. However, no information on the regeneration of the sorbent was provided. Another study, but focused on bitterns [459], showed the synthesis of a Cu-hexacyanoferrate compound (CuHCF) to recover both Rb^+ and Cs^+. During tests under column mode, it was necessary to reach 1100 BV to become saturated with Rb^+, whereas Cs^+ breakthrough needed 8000 BV to reach saturation. Such performance resulted in sorption capacities of 10 and 70 mg/g for Rb^+ and Cs^+, respectively. Unfortunately, the sorbent showed small recoveries (<5 %) during regeneration with 0.1 mol/L H_2SO_4 and 0.1 mol/L NaOH.

A similar case is found with strontium, with most of the studies targeting radioactive strontium-90 (^{90}Sr) [417–419]. Despite that, some works evaluated Sr^{2+} recovery from SW, which is commonly present in the range of 7–8 mg/L [420]. For instance, an alginate microsphere sorbent was developed, exhibiting a capacity of 110 mg Sr^{2+}/g, which decreased due to the presence of Na^+ [421]. During the evaluation of different polymeric resins for recovering trace elements from bitterns [459], the IX resins IRC747 and S940 exhibited some extraction of Sr^{2+} (sorption capacities of 0.1 mg/g). Such low values were related to the competence with the Mg^{2+} and Ca^{2+} that were present in the solution. Despite that, during regeneration with 1 mol/L HCl, it was possible to concentrate Sr^{2+} by a factor of 25.

A more challenging case study is related to uranium recovery from SW, which is difficult due to its low concentration (in the order of 3 μg/L). For this purpose, various materials have been developed and tested for their recovery from SW [422–424]. Related to brine treatment, different fibres have been designed for uranium adsorption but showed a low adsorption capacity (19 μg/g) [425]. A different study involved the use of amidoxime-functionalized resins to recover uranium from desalination brines (uranium concentration spiked to 19 mg/L). It was reported that the concentration at the outlet increased steeply from the beginning, reaching a plateau after 30 days of the experiment, resulting in a uranium capacity of 41 mg/g [416].

Despite the benefits of IX and sorption, the implementation of this process is still in its early stages, and further research is needed to make it both technically and economically feasible. Additional research is required to improve the material properties, particularly in terms of selectivity and minimising the extraction of other competing ions, as well as enhancing material stability.

3.2.3.2. Solvent extraction (SX). Solvent extraction (SX, also known as liquid-liquid extraction) is one of the most common methods for separation and purification that relies on the solubility of ligand-metal complexes in organic solvents. The process is based on the use of a mixture of two different solvents: (i) an aqueous phase containing the target metal and (ii) an organic phase containing the extractant. After mixing, the different metals distribute within the phases, enabling separation and purification. Once the organic phase is saturated, stripping takes place with acidic solutions to isolate the target metal [426]. Typically, solvent extraction is used for recovering metals at concentrations higher than 1 g/L, and values below this limit can compromise both technical and economic feasibility. It is worth noting that most published works on SX are related to salt-lake brines, focusing on the extraction of boron [427], the recovery of Li [426,428] or Rb [429].

The application of SX for lithium separation has been widely studied for salt-lake brines, aiming to enhance Li^+/Mg^{2+} selectivity [430]. Among the different extractants, tributyl phosphate (TBP) – $FeCl_3$ exhibits the most promising Li^+ extraction showing selectivity in the order $Li^+ > Na^+ > K^+ > Mg^{2+}$. The reason for such strong selectivity is found in the formation of the organic complex $LiFeCl_4$:nTBP [431–434]. The use of ionic liquids [435,436] or tertiary systems (including another extractant) [437,438], along with TBP, has been studied to enhance Li^+ extraction, selectivity or stripping. Several works have investigated Li^+ recovery from SW or desalination brines using SX, and all of them emphasise the need to remove divalent cations before extracting Li^+ to ensure high selectivity [439–442]. For example, Harvianto et al. [439] used a mixture of thenoyltrifluoroacetone (TTA) and trioctylphosphine oxide (TOPO) in kerosene to extract Li^+ from both SW and SWRO brine. To ensure a high selectivity towards Li^+, Mg^{2+} was removed at pH 11 using NH_3. The authors reported that extraction efficiency (0.02 mol/L TTA, 0.04 mol/L TOPO, pH 10.6) decreased when working at larger A/O ratios due to a larger volume of aqueous solution compared to the extractant. Moreover, a decrease in Li^+ concentration was reported when using brine compared to SW, likely due to the competition of other cations in solution (e.g., Na^+, K^+, and Ca^{2+}). Despite this, 65 % of Li^+ was extracted from SW after 30 min, whereas it was 55 % for the RO brine at an A/O ratio of 1. Although the authors did not study the stripping of the loaded organic phase, preliminary experiments conducted with single Li^+ solutions showed that using an inorganic acid (e.g., HCl, H_2SO_4, H_3PO_4) allowed for the stripping of 90 % of Li^+ if the pH was lower than 3. Yu et al. [440] proposed the recovery of Li^+ from SW via a two-stage SX process. Similar to the previous study, the first stage involves Ca^{2+} and Mg^{2+}, avoiding the loss of Li^+. This stage involved the use of DEHPA (Bis(2-ethylhexyl)phosphate) at pH 10 to ensure their removal, but losses of Li^+ were reported (c.a. 10 %). The second stage, based on DEHPA/HDES (hydrophobic deep eutectic solvent), showed an extraction efficiency of 27 % for Li^+, which was related to the presence of a high concentration of divalent metal ions. Nevertheless, it should be noted that in this second stage, the authors reported a Li^+ extraction efficiency of 66 % and a Li^+/Na^+ separation coefficient of 11.6 with more diluted solutions (1 mg/L Li^+, 100 mg/L Na^+, 4 mg/L K^+, 13 mg/L Mg^{2+} and 4 mg/L Ca^{2+}). Fernández-Escalante et al. [441] assessed the use of extractant mixtures of TOPO with dibenzoylmethane (DBM) or heptafluoro-dimethyloctanedione (FDOD) to extract Li^+ from SWRO brines. Using single-salt solutions (0.02 mol/L) initially, it was reported the need to ensure a pH of 12 to achieve extractions of 85 % and 93 % of Li^+ for DBM:TOPO and FDOD:TOPO, respectively, when working at an extractant concentration of 0.01 mol/L. Due to the basic pH of the solutions, it was expected that precipitation of Ca^{2+} and Mg^{2+} would occur. During tests with SWRO solutions, molar ratios of FDOD:TOPO/Li^+ higher than 50 allowed a complete Li^+ extraction, whereas a ratio of 175 for DBM:TOPO reached 90 % Li^+ extraction. A final study of pH effect on cation extraction at organic concentrations of 0.03 mol/L showed the possibility of extracting 95 % Li^+ for DBM:TOPO at pH 12, while at pH 10.9, it was possible to reach a 99 % Li extraction for FDOD:TOPO. In all cases, co-extractions of other cations remained below 1 % for DBM:TOPO and 5 % for FDOD:TOPO under the above-mentioned

conditions. Raiguel et al. [442] proposed a SX route for Li^+ recovery from a NF-treated desalination brine (3.1 g/L Mg^{2+}, 1.6 mg/L Li^+, 76 g/L Na^+, 3 g/L K^+ and 0.3 g/L Ca^{2+}). Initially, Ca^{2+} and Mg^{2+} were removed by a basic extractant (methyltrioctylammonium neo-decanoate), whereas Li^+ was later recovered using a β-diketone (Mextral 54–100) in synergism with a mixture of phosphine oxides (Cyanex 923). In the first stage, with an organic extractant concentration of 0.5 mol/L at an organic-to-aqueous ratio of 1, it was possible to remove more than 99 % of Ca^{2+} and Mg^{2+} with a Li^+ co-extraction below 0.1 % after 6 stages. After a two-stage stripping, using first water and then 0.1 mol/L HCl it was possible to regenerate the basic extractant. In the Li^+ extraction stage, the authors demonstrated extraction efficiencies of 90 % at pH 12 with a 1.5 % vol concentration for both extractants, whereas co-extractions of Na^+ and K^+ remained below 5 %. Na^+ and K^+ were scrubbed with a single stage with water, whereas Li^+ was completely stripped after a 2-stage process with 0.1 mol/L HCl.

In relation to boron removal, using 2,2,4-trimethyl-1,3-pentanediol (TMPD) as extractant is the most widely studied solution for such purpose from salt-lake brines [443–445]. With regard to SWRO desalination brines [446], TMPD provided high efficiencies (>90 %) when working at pH < 9, showing that the solvating extractant primarily chelates the neutral boric acid (H_3BO_3(aq)). Moreover, under optimum parameters, the extraction efficiency was 93 % (pH 8, 0.5 mol/L TMPD, organic-to-aqueous ratio (O/A) of 1, 5 min contact time), whereas the stripping efficiency was 91 % (0.5 NH_3, O/A ratio of 2, 5 min). In addition, other extractants, such as 2-butyl-1-n-octanol [447], monohydric alcohols [448,449] or N221 (4-dodecyl-N-tosylbenzenesulfonamide) [450] have been studied for boron removal from salt-lake brines, but no works were found for desalination brines.

4-tert-butyl-2-(α-methylbenzyl) phenol) (t-BAMBP, ROH) has proven its ability to separate efficiently both Cs^+ and Rb^+ from Na^+ and K^+ when applied to salt-lake brines [451–454]. Pang et al. [455] revealed that the alkaline metal forms a complex MOR·3ROH (M = Cs^+, Rb^+) in the organic phase, with the electrostatic attraction between M^+ and the oxygen of the phenolic hydroxyl being the dominant factor. The application of t-BAMBP on thermal desalination brines (7.1 mg/L Rb^+, 43.6 mg/L Cs^+) was studied by Chen et al. [456]. To avoid K^+ co-extraction, it was initially removed as perchlorate by 98.5 % at -5 °C and pH 2. It was proposed a process flow sheet to selectively separate Cs^+ and Rb^+. The first stage, carried out with 0.1 mol/L t-BAMBP at pH 8, O/A ratio of 0.1, and 3 min at 35 °C, allowed for the extraction of 99.8 % of Cs^+, with a Rb^+ co-extraction of 5 %. During the stripping process (1 mol/L NH_3, O/A ratio of 2 at 25 °C), 99.9 % of the Cs^+ was recovered, resulting in a stream containing 1635 mg/L Cs^+ with other cationic impurities below 10 mg/L (e.g., K^+, Rb^+, Na^+). The Cs^+-free brine was then treated in a second stage with 0.5 mol/L t-BAMBP (pH 12, O/A ratio 0.1, 15 min at 5 °C), allowing the extraction of 98.3 % of Rb^+, but with a 41.3 % extraction of K^+. The stripping at 0.5 mol/L NH_3 (O/A ratio of 2 at 35 °C) allowed the recovery of 95 % of Rb^+, thus resulting in a Rb^+-rich stream containing 292 mg/L. Other extractants, such as crown ethers, have also been applied for both Cs^+ and Rb^+ from salt-lake brines [457,458].

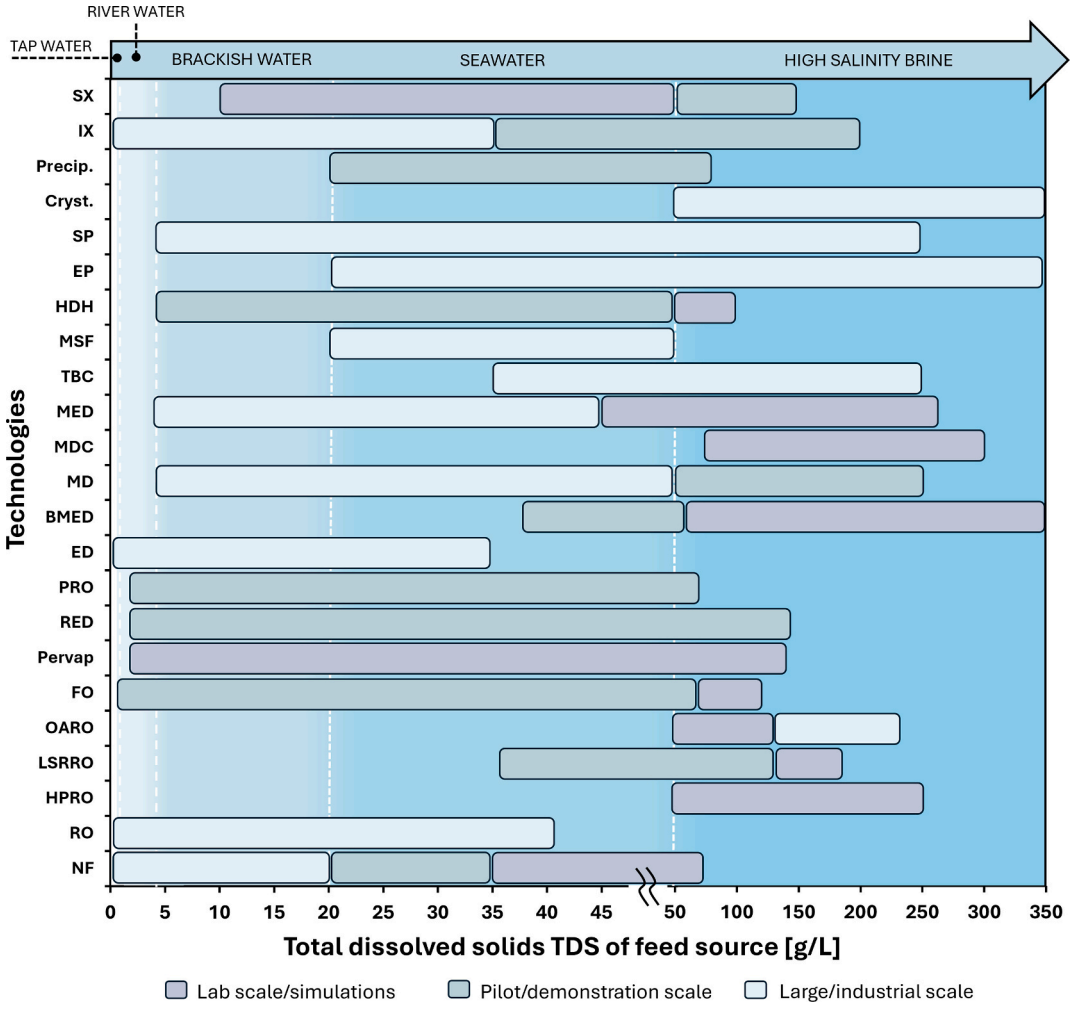

Fig. 10. Salinity range of the feedwater treated by each technology and corresponding implementation scale (Lab-scale/simulations, pilot/demonstration scale and large/industrial scale).

4. Comparative overview of technologies

As discussed in Section 3, a wide range of technologies can be applied within the desalination industry, either for direct freshwater production or for the management and valorisation of concentrate streams. To date, no standardized technological scheme exists that can be universally applied, since the suitability of each option depends on several factors, including feedwater salinity and composition, the TRL, and the specific interest in potentially recoverable resources, whether material or energetic. Likewise, country-specific conditions, such as prevailing legislation or geopolitical positioning, may either promote or constrain the adoption of particular technologies.

To summarize and enable comparison of the information presented for each technology in the different subsections of Section 3, Fig. 10 illustrates the salinity ranges of feedwater sources that each technology can effectively process apart from the current maturity development, while Fig. 11 provides a qualitative comparison of technologies employed in brine resource recovery, highlighting the maximum salinity treated, the associated TRL, the recoverable resources, and the main current limitations.

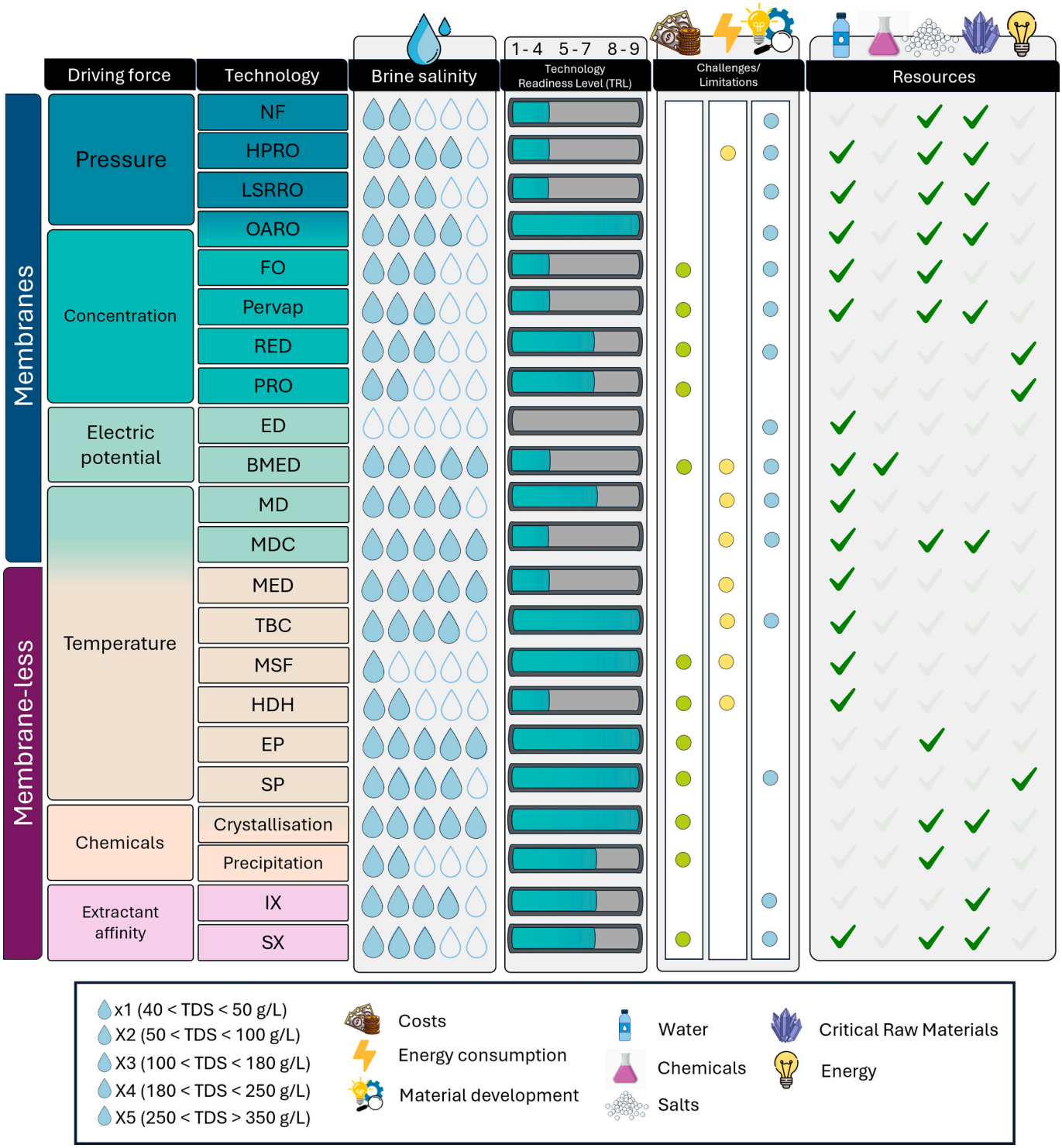

Fig. 11. Qualitative comparison of technologies employed for desalination and resource recovery.

Several technologies have already been implemented at large or industrial scales. At this level, the membrane-based technologies NF and ED are capable of treating low-salinity feedwaters, up to approximately 20 g/L and 35 g/L, respectively. In contrast, temperature-driven technologies, including MED, MD, and MSF, are generally more suitable for higher salinity SW. Technologies such as TBC, EP, SP, and crystallizers are commercially employed to treat feedwaters with salinities in the highest range (50–350 g/L). Within this same salinity range, several emerging technologies have been evaluated but remain limited to small-scale installations. These include HPRO, LSRRO, FO, pervaporation, BMED, MDC, MED, and HDH. These technologies are currently restricted to lab-scale experiments or numerical and fundamental studies. For some technologies, an increase in feedwater salinity corresponds to a decrease in implementation scale. For example, NF is less feasible at higher salinities. Other technologies are inherently limited to pilot or demonstration scales for specific salinity ranges, such as calcium removal processes, PRO, and RED. Fig. 10 provides an overview of the applicable technologies based on feedwater salinity. However, salinity tolerance is not the only differentiating factor; technologies also vary in the types of resources they are designed to recover.

Fig. 11 presents a qualitative comparison of the technologies used in brine resource recovery, which have been reported in Section 3, highlighting the maximum salinity treated, the corresponding TRL (described in Fig. S6, see Section S7 of Supplementary Material), the recoverable resources, and the current limitations. Several technologies aim to enhance desalination by recovering additional freshwater. Among these, BMED and MED can treat brines with salinities between 250 and 350 g/L, although they are currently limited to lab-scale applications. MED is constrained by high energy consumption, while BMED faces challenges related to energy efficiency, cost, and material development. MD and TBC can treat slightly lower salinity ranges (180–250 g/L) and are implemented at pilot and industrial scales, respectively. Nevertheless, both are hindered by high energy demands, and further research is needed to improve material performance. Some technologies are capable of recovering multiple resources. For instance, BMED not only recovers freshwater but also valuable chemicals such as NaOH and HCl. Notably, BMED is currently the only technology capable of chemical recovery from desalination brine. Other technologies focus on concentrating and recovering salts or CRMs. EP and crystallization are the only technologies operating at industrial scale for the highest salinity ranges. The remaining technologies for salt and CRM recovery are limited to laboratory or pilot scales and are typically applied to lower salinity brines. Finally, RED, PRO, and SP are distinguished by their exclusive focus on energy recovery. While SP is commercially deployed, RED and PRO are limited to demonstration-scale installations, with RED capable of employing higher salinity brines than PRO.

5. Industrial examples of close to full-scale seawater/brines valorisation case studies

In Section 3, various technologies are discussed that enhance desalination efficiency or enable the recovery of specific resources from desalination brine. These technologies have been implemented either independently or as part of integrated schemes aimed at achieving MLD or ZLD within the desalination sector. However, it is crucial to assess the current stage and scale of MLD and ZLD implementation to determine whether these concepts represent a tangible reality or remain aspirational. To the best of the authors' knowledge, Fig. 12 presents an overview of three SW/brine valorisation plants operating at the largest scales for multi-resource recovery. These plants generally follow a three-step process: (i) Pretreatment and/or desalination (highlighted in pink), (ii) Brine concentration (blue), and (iii) Thermal treatment (green).

Depending on the technologies employed, the brine concentration step may either serve to concentrate the brine for downstream water and salt recovery via thermal processes or directly recover specific resources. Currently the largest brine mining facility, the Maven plant (Fig. 12a) processes SW at a flowrate of 1254 m^3/h [https://www.youtube.com/watch?v=6TUzIkbjW8M]. The pretreatment includes UF for suspended solids and organic matter removal, followed by NF for ion separation. UF and NF achieve permeate recoveries of 98.6 % and 82 %, respectively, with retentates discharged to the sea, an impact considered minimal due to the high recovery rates. The NF permeate is treated via SWRO, operating at an elevated recovery of 59 % due to the robust upstream pretreatment. The resulting RO brine is further concentrated using OARO, increasing salinity from 84 g/L to 179 g/L. This concentrated brine is then processed in a falling film evaporator (FFE) and a crystalliser, yielding ultrapure water (<100 mg/L TDS) and 25.5 tons/h of NaCl. While the Maven plant exemplifies large-scale MLD implementation through freshwater and NaCl recovery, valorisation of the NF retentate remains unrealised. However, plans exist to recover magnesium and lithium compounds from this stream. The plant currently achieves an overall water recovery of 80 %, making it the most advanced example of MLD in the desalination industry. The Water Mining plant (Fig. 12b) operates at a smaller scale (2.46 m^3/h) but represents the most comprehensive multi-resource recovery system to date [49]. Pretreatment consists of a two-pass NF system with a combined permeate recovery of 69 %. Unlike the Maven plant, both permeate and retentate streams are valorised. The NF retentate is processed in a reactive crystalliser (MF-PFR) to recover $Mg(OH)_2$(s) and $Ca(OH)_2$(s) using NaOH generated internally by a BMED unit, which also produces HCl. The NF permeate is concentrated via a MED unit, achieving 70–85 % water recovery using waste heat from the local diesel power plant. Freshwater and food-grade NaCl are recovered through MED and EPs, respectively. Despite integrating technologies of varying scales, some brine is still discharged. However, simulations indicate that full integration could enable MLD. The Water Mining plant demonstrates the feasibility of multi-resource recovery, albeit at a pilot scale. The SWCC plant (Fig. 12c) shares similarities with the Maven plant [48]. After dual media filtration (DMF), 16.0 m^3/h of SW is treated via NF, achieving 85 % recovery at 19.3 bar. Due to scale mismatches, excess NF permeate is discarded. The SWRO unit operates at 75 bar, and its retentate (82 g/L salinity) is mixed with a diluted stream from the first OARO stage (70 bar) and sent to a HPRO unit operating at 112 bar and 25 % recovery, producing a concentrate of 110 g/L. This is further mixed with the diluted stream from a second OARO stage (69 bar), resulting in a final concentrate of 0.52–0.72 m^3/h with salinity up to 176 g/L, suitable for NaCl production. The NF retentate is processed via a single OARO stage to yield a divalent ion-enriched solution with salinity of 90 g/L.

From these three case studies, it is evident that the largest brine mining facilities currently focus on freshwater and NaCl recovery. While multi-resource recovery has been demonstrated, it remains confined to pilot-scale plants with feed capacities around 2 m^3/h and overall water recoveries below 65 %, thus falling short of MLD classification. Consequently, while MLD is achievable through water and NaCl recovery, ZLD remains an aspirational goal in the desalination industry.

6. Conclusions

Through the detailed assessment of the current state of desalination worldwide presented in Section 2, it is more than clear that desalination has become a well-established method across various sectors, ranging from industrial applications to urban water supply. Various feedwater sources are treated, with salinity levels spanning from tap water to highly concentrated SW, serving diverse purposes. Among the available technologies, RO currently dominates the global desalination landscape, both in terms of operational plants (5015 plants with a minimum capacity of 2000 m^3/d) and total freshwater production capacity (89.4 Mm^3/d). In addition, SW remains the primary feedwater source for desalination, accounting for the largest share of plants and consequently generating the highest volume of brine. Although often regarded as a by-product, desalination brine represents a promising unconventional source of valuable resources, including critical raw materials, salts,

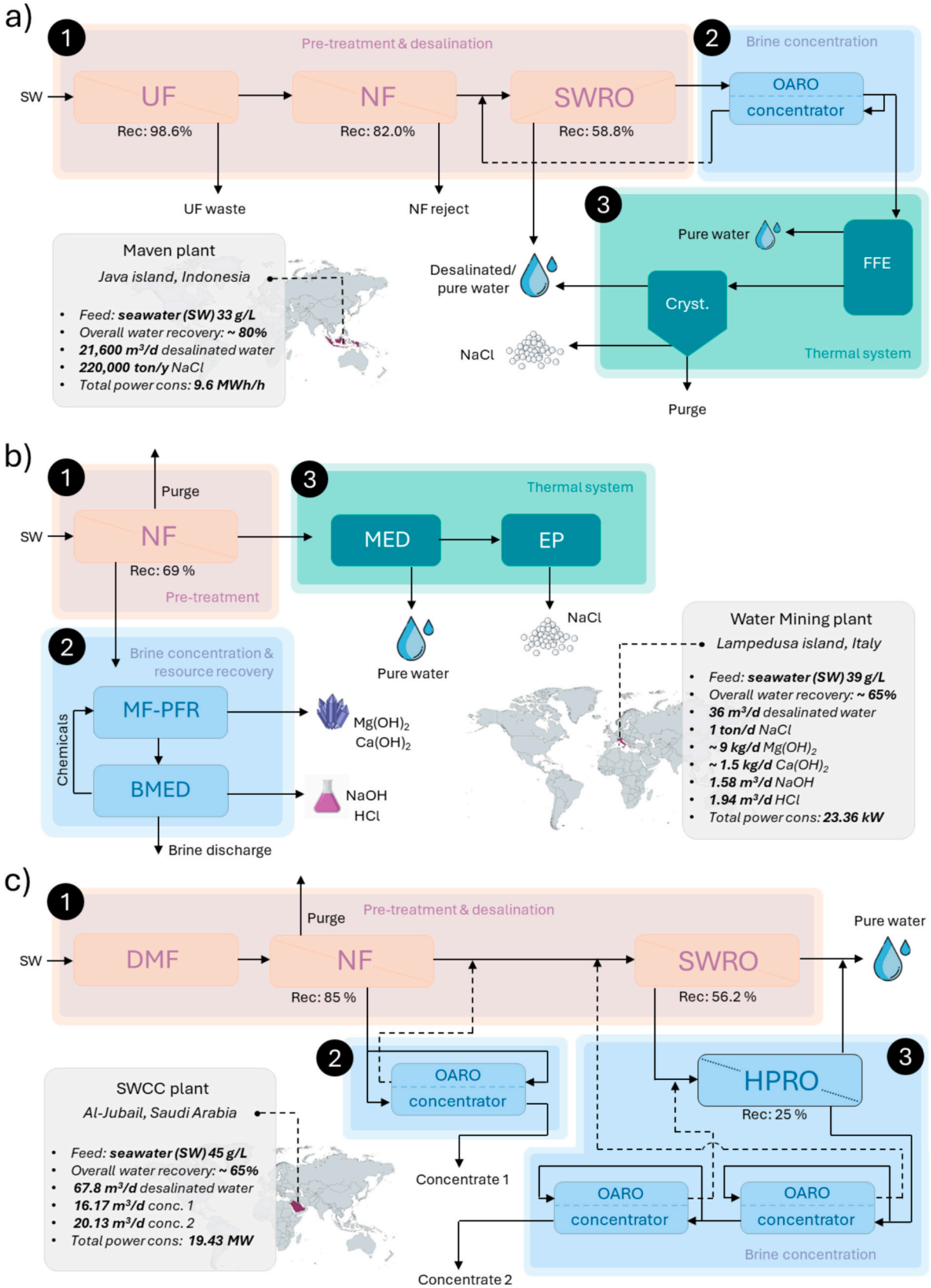

Fig. 12. Block flow diagrams of 3 industrial examples of close-to-full-scale SW/brine valorisation plants situated in a) Java Island, Indonesia, b) Lampedusa island, Italy and c) Al-Jubail, Saudi Arabia, respectively.

energy, chemicals, and additional high-quality water.

Over the past decade, a range of conventional and emerging technologies has been explored for resource recovery from desalination brine. These efforts span desalination enhancement, mineral extraction, and the generation of chemicals or energy, often within the framework of MLD and ZLD strategies. A comprehensive assessment of these technologies reveals that most of them are capable of treating desalination brines.

This review provides a comprehensive overview of the current state of desalination technologies worldwide, with a particular focus on the feasibility of resource recovery from desalination brine. It highlights the most advanced technologies for recovering specific resources and offers guidance on selecting appropriate technologies based on the target resource.

By mapping the TRL and salinity tolerance of various processes, this review serves as a valuable reference for the desalination research community. It identifies key challenges that must be addressed to advance brine mining and emphasizes the need to accelerate the development of promising technologies that remain confined to the lab-scale.

Overall, the findings underscore the significant potential of brine resource recovery, both now and in the future, as a sustainable alternative to conventional, often costly and environmentally detrimental, resource extraction methods. To date, some successful MLD schemes within the desalination sector have been implemented across the world. However, full-scale implementation is still limited to the recovery of freshwater and NaCl, whilst the recovery of more valuable minerals remains at lower TRL.

Through continued innovation and targeted research, resource recovery from brine could play a pivotal role in transforming desalination from a waste-generating process into a circular and resource-efficient solution.

Acronyms

ABFB	Acid-Base Flow Battery
AEM	Anion Exchange Membrane
AGMD	Air Gap Membrane Distillation
BMED	Bipolar Membrane Electrodialysis
BMRED	Bipolar Membrane Reverse Electrodialysis
BPM	Bipolar Membrane
BR-OARO	Brine Reflux - Osmotically Assisted Reverse Osmosis
BW	Brackish Water
CA	Cellulose Acetate
CAPEX	Capital Expenditures
CEM	Cation Exchange Membrane
CL-OARO	Consecutive Loops - Osmotically Assisted Reverse Osmosis
CrIEM	Crystallizer with Ion Exchange Membrane
DBM	Dibenzoylmethane
DCMD	Direct Contact Membrane Distillation
DEHPA	Bis(2-ethylhexyl)phosphate
Dia-NF	Dia-Nanofiltration
DMF	Dual Media Filtration
DS	Draw Solution
ED	Electrodialysis
EDI	Electrodeionization
EDR	Electrodialysis Reversal
EFC	Eutectic-Freezing Crystallization
EP	Evaporation pond
EU	European Union
FFE	Falling Film Evaporator
FDOD	Heptafluoro-dimethyloctanedione
FO	Forward Osmosis
FS	Feed Solution
GWI	Global Water Intelligence
HDH	Humidification Dehumidification Desalination
HPRO	High-Pressure Reverse Osmosis
IX	Ion-exchange
LC	Low Concentrated
LCOE	Levelized Cost of Electricity
LCOW	Levelized Cost of Water
LCZ	Lower Convection Zone
LSRRO	Low Salinity Rejection Reverse Osmosis
MD	Membrane Distillation
MDC	Membrane Crystallisation
MED	Multi-effect Distillation
MF-PFR	Multiple-Feed Plug Flow Reactor
MLD	Minimum Liquid Discharge
MSF	Multi Stage Flash
MVC	Mechanical Vapour Compression
NF	Nanofiltration
OPEX	Operational Expenditures
PRO	Pressure Retarded Osmosis
PE	Polyethylene
PGMD	Permeate Gap Membrane Distillation
PMD	Photothermal Membrane Distillation
PTFE	Polytetrafluoroethylene
PVA	Polyvinyl Alcohol
PV	Photovoltaic
PVDF	Polyvinylidene Fluoride
RED	Reverse Electrodialysis
REE	Rare Earth Elements
RO	Reverse Osmosis
SEC	Specific Energy Consumption
SGE	Salinity Gradient Energy
SGMD	Sweeping Gas Membrane Distillation
SGSP	Salinity Gradient Solar Pond
SMD	Submerged Membrane Distillation
SW	Seawater
SWRO	Seawater Reverse Osmosis
SX	Solvent Extraction
TBC	Thermal Brine concentrator
TBP	Tributyl phosphate
TDS	Total Dissolved Solids
TOPO	Trioctylphosphine oxide
TRL	Technology Readiness Level
TTA	Thenoyltrifluoroacetone
TVC	Thermal Vapour Compression
UF	Ultrafiltration
UHPRO	Ultra-High-Pressure Reverse Osmosis
UV	Ultraviolet
UWWTP	Urban Wastewater Treatment Plant
VMD	Vacuum Membrane Distillation
WAIV	Wind-Aided Intensified Evaporation
ZLD	Zero Liquid Discharge

CRediT authorship contribution statement

C. Morgante: Writing – original draft, Visualization, Methodology, Investigation, Data curation, Conceptualization. **M. Herrero-Gonzalez:** Writing – original draft, Visualization, Methodology, Investigation, Data curation, Conceptualization. **J. Lopez:** Writing – original draft, Visualization, Methodology, Investigation, Data curation, Conceptualization. **J. Imholze:** Writing – original draft, Visualization, Data curation. **V. Boffa:** Writing – review & editing, Supervision, Funding acquisition. **R. Ibañez:** Writing – review & editing, Supervision, Funding acquisition. **J. L. Cortina:** Writing – review & editing, Supervision, Funding acquisition.

Declaration of competing interest

The authors declare the following financial interests/personal relationships which may be considered as potential competing interests: Jan Imholze reports a relationship with Fichtner GmbH & Co KG that includes: employment. If there are other authors, they declare that they have no known competing financial interests or personal relationships that could have appeared to influence the work reported in this paper.

Acknowledgements

This research was supported by the MagNa project (EIT RM - 24652) financed by the European Institute of Innovation and Technology (EIT),

and by the Upcycling project (PID2023-147160OB-C21) financed by the Spanish Research Agency (AEI). Additionally, the authors acknowledge the support of the Catalan Government through the R2EM group (2021-SGR-GRC-00596). Moreover, this work was carried out within the framework of the Multiscale Center of Excellence, funded by the María de Maeztu Program for Units of Excellence (CEX2023-001300-M), supported by MCIN/AEI/10.13039/501100011033, Spain. J.L. Cortina also received through the "ICREA Academia" recognition for excellence in research funded by the Generalitat de Catalunya. Finally, we would also like to acknowledge the following grants: TED2021-129874B-I00 funded by MICIU/AEI/ 10.13039/501100011033 and by the "European Union NextGenerationEU/PRTR"; PID2020-115409RB-I00 funded by MICIU/AEI/10.13039/501100011033; and PID2023-147888OB-I00 funded by MICIU/AEI/ 10.13039/501100011033 and by FEDER/EU.

Appendix A. Supplementary Material

Supplementary data to this article can be found online at https://doi.org/10.1016/j.desal.2025.119718.

Data availability

Data will be made available on request.

References

[1] P. Loganathan, G. Naidu, S. Vigneswaran, Mining valuable minerals from seawater: a critical review, Environ. Sci. (Camb) 3 (2017) 37–53, https://doi.org/10.1039/c6ew00268d.
[2] P. Kumari, Y.S. Chang, G.J. Witkamp, J. Vrouwenvelder, L.F. Vega, L.F. Dumée, Brine valorization through resource mining and CO2 utilization in the Middle East – a perspective, Desalination 582 (2024), https://doi.org/10.1016/j.desal.2024.117598.
[3] A. Kumar, G. Naidu, H. Fukuda, F. Du, S. Vigneswaran, E. Drioli, J.H. Lienhard, Metals recovery from seawater desalination brines: technologies, Opportunities, and Challenges, ACS Sustain. Chem. Eng. 9 (2021) 7704–7712, https://doi.org/10.1021/acssuschemeng.1c00785.
[4] M. Kim, S. Kim, S. Shin, G. Kim, Production of high-purity MgSO 4 from seawater desalination brine, Desalination 518 (2021) 115288, https://doi.org/10.1016/j.desal.2021.115288.
[5] N. Mahmud, D.V. Fraga, M.H. Ibrahim, M.H. El-naas, D.V. Esposito, Magnesium recovery from desalination reject brine as pretreatment for membraneless electrolysis, Desalination 525 (2022) 115489, https://doi.org/10.1016/j.desal.2021.115489.
[6] M.A. Carneiro, E. de Kroon, B. Vital, S.P. Pereira, L.L.F. Agostinho, Electrochemical process of chlorination and energy generation as viable alternatives for SWRO brine valorization, Desalination 586 (2024), https://doi.org/10.1016/j.desal.2024.117875.
[7] M.G. O'Connell, N. Rajendran, M. Elimelech, J. Gilron, J.B. Dunn, Analysis of energy, water, land and cost implications of zero and minimal liquid discharge desalination technologies, Nat. Water 2 (2024) 1116–1127, https://doi.org/10.1038/s44221-024-00327-1.
[8] E. Jones, M. Qadir, M.T.H. Van Vliet, V. Smakhtin, S. Kang, The state of desalination and brine production : a global outlook, Sci. Total Environ. 657 (2019) 1343–1356, https://doi.org/10.1016/j.scitotenv.2018.12.076.
[9] U.S. Department of the Interior Bureau of Reclamation, Brine-Concentrate Treatment and Disposal Options Report - Part 1, 2009.
[10] I. Ersever, V. Ravindran, M. Pirbazari, Biological denitrification of reverse osmosis brine concentrates: I. Batch reactor and chemostat studies, J. Environ. Eng. Sci. 6 (2007) 503–518, https://doi.org/10.1139/S07-021.
[11] J.H. Tsai, F. Macedonio, E. Drioli, L. Giorno, C.Y. Chou, F.C. Hu, C.L. Li, C. J. Chuang, K.L. Tung, Membrane-based zero liquid discharge: myth or reality? J. Taiwan Inst. Chem. Eng. 80 (2017) 192–202, https://doi.org/10.1016/j.jtice.2017.06.050.
[12] A. Subramani, J.G. Jacangelo, Treatment technologies for reverse osmosis concentrate volume minimization: a review, Sep. Purif. Technol. 122 (2014) 472–489, https://doi.org/10.1016/j.seppur.2013.12.004.
[13] R.A.I. Bashitialshaaer, K.M. Persson, M. Aljaradin, Estimated future salinity in the Arabian Gulf, the Mediterranean Sea and the Red Sea Consequences of Brine Discharge from Desalination 3, 2011, pp. 133–140.
[14] A. Giwa, V. Dufour, F. Al Marzooqi, M. Al Kaabi, S.W. Hasan, Brine management methods: recent innovations and current status, Desalination 407 (2017) 1–23, https://doi.org/10.1016/j.desal.2016.12.008.
[15] A.S. Bello, N. Zouari, D.A. Da'ana, J.N. Hahladakis, M.A. Al-Ghouti, An overview of brine management: emerging desalination technologies, life cycle assessment, and metal recovery methodologies, J. Environ. Manag. 288 (2021) 112358, https://doi.org/10.1016/j.jenvman.2021.112358.
[16] S. van Wyk, A.G.J. van der Ham, S.R.A. Kersten, Potential of supercritical water desalination (SCWD) as zero liquid discharge (ZLD) technology, Desalination 495 (2020) 114593, https://doi.org/10.1016/j.desal.2020.114593.
[17] R. Navarro, J.L.S. Lizaso, S. Iván, Assessment of energy consumption of brine discharge from SWRO plants, Water (Switzerland) (2023), https://doi.org/10.3390/w15040786.
[18] C. Morgante, J. Lopez, J.L. Cortina, A. Tamburini, New generation of commercial nanofiltration membranes for seawater/brine mining: experimental evaluation and modelling of membrane selectivity for major and trace elements, Sep. Purif. Technol. 340 (2024) 126758, https://doi.org/10.1016/j.seppur.2024.126758.
[19] A. Shahmansouri, J. Min, L. Jin, C. Bellona, Feasibility of extracting valuable minerals from desalination concentrate: a comprehensive literature review, J. Clean. Prod. 100 (2015) 4–16, https://doi.org/10.1016/j.jclepro.2015.03.031.
[20] P. Loganathan, G. Naidu, S. Vigneswaran, Mining valuable minerals from seawater: a critical review, Environ. Sci. (Camb) 3 (2017) 37–53, https://doi.org/10.1039/c6ew00268d.
[21] B. Daigle, S. Decarlo, Office of Industries Magnesium Price Spike: A Flash in the Pan?, 2021, pp. 1–18.
[22] J. Lu, Y.K. Kharaka, J.J. Thordsen, J. Horita, A. Karamalidis, C. Griffith, J. A. Hakala, G. Ambats, D.R. Cole, T.J. Phelps, M.A. Manning, P.J. Cook, S. D. Hovorka, CO2–rock–brine interactions in Lower Tuscaloosa Formation at Cranfield CO2 sequestration site, Mississippi, U.S.A. Chem. Geol. 291 (2012) 269–277, https://doi.org/10.1016/j.chemgeo.2011.10.020.
[23] J. Morillo, J. Usero, D. Rosado, H. El Bakouri, A. Riaza, F.J. Bernaola, Comparative study of brine management technologies for desalination plants, Desalination 336 (2014) 32–49, https://doi.org/10.1016/j.desal.2013.12.038.
[24] L. Cornejo-Ponce, C. Moraga-Contreras, P. Vilca-Salinas, Analysis of Chilean legal regime for brine obtained from desalination processes, Desalin. Water Treat. 203 (2020) 91–103, https://doi.org/10.5004/dwt.2020.26202.
[25] C. Morgante, F. Vassallo, D. Xevgenos, A. Cipollina, M. Micari, A. Tamburini, G. Micale, Valorisation of SWRO brines in a remote island through a circular approach: techno-economic analysis and perspectives, Desalination 542 (2022) 116005, https://doi.org/10.1016/j.desal.2022.116005.
[26] Z. Wang, A. Deshmukh, Y. Du, M. Elimelech, Minimal and zero liquid discharge with reverse osmosis using low-salt-rejection membranes, Water Res. 170 (2020) 115317, https://doi.org/10.1016/j.watres.2019.115317.
[27] Á. Rivero-Falcón, B.P. Suárez, N. Melián-Martel, SWRO brine characterisation and critical analysis of its industrial valorisation : a case study in the canary, Water (Switzerland) (2023), https://doi.org/10.3390/w15081600.
[28] M.O. Mavukkandy, C.M. Chabib, I. Mustafa, A. Al, Brine management in desalination industry : from waste to resources generation, Desalination 472 (2019) 114187, https://doi.org/10.1016/j.desal.2019.114187.
[29] I. Ihsanullah, J. Mustafa, A.M. Zafar, M. Obaid, M.A. Atieh, N. Ghaffour, Waste to wealth: a critical analysis of resource recovery from desalination brine, Desalination 543 (2022) 116093, https://doi.org/10.1016/j.desal.2022.116093.
[30] S. M.S., T. Elmakki, K. Schipper, S. Ihm, Y. Yoo, B. Park, H. Park, H.K. Shon, D. S. Han, Integrated seawater hub: a nexus of sustainable water, energy, and resource generation, Desalination 571 (2024) 117065, https://doi.org/10.1016/j.desal.2023.117065.
[31] P. Kumari, Y.S. Chang, G.J. Witkamp, J. Vrouwenvelder, L.F. Vega, L.F. Dumée, Brine valorization through resource mining and CO2 utilization in the Middle East – a perspective, Desalination 582 (2024), https://doi.org/10.1016/j.desal.2024.117598.
[32] G. Cipolletta, N. Lancioni, Ç. Akyol, A.L. Eusebi, F. Fatone, Brine treatment technologies towards minimum/zero liquid discharge and resource recovery: state of the art and techno-economic assessment, J. Environ. Manag. 300 (2021) 113681, https://doi.org/10.1016/j.jenvman.2021.113681.
[33] C.H. Lee, H.J. Ho, W.S. Chen, A. Iizuka, Total resource circulation of desalination brine: a review, Adv. Sustainable Syst. 8 (2024) 1–23, https://doi.org/10.1002/adsu.202300460.
[34] B.A. Sharkh, A.A. Al-Amoudi, M. Farooque, C.M. Fellows, S. Ihm, S. Lee, S. Li, N. Voutchkov, Seawater desalination concentrate—a new frontier for sustainable mining of valuable minerals, NPJ Clean Water 5 (2022) 1–16, https://doi.org/10.1038/s41545-022-00153-6.
[35] Global Water Intelligence, GWi DESALDATA, (n.d.). https://www.desaldata.com.
[36] S. Reigeluth, Lampedusa : The Forsaken Island, (n.d.). https://revolve.media/features/lampedusa-the-forsaken-island.
[37] R. Ktori, M.C.M. Van Loosdrecht, D. Xevgenos, Economic evaluation of water and resource recovery plants : a novel perspective on levelized cost, Desalination 599 (2025) 118475, https://doi.org/10.1016/j.desal.2024.118475.
[38] Sea4Value Project, (n.d.) 1–7. https://sea4value.eu/ (accessed January 10, 2023).
[39] A.W. Mohammad, Y.H. Teow, W.L. Ang, Y.T. Chung, D.L. Oatley-Radcliffe, N. Hilal, Nanofiltration membranes review : recent advances and future prospects, Desalination 356 (2015) 226–254, https://doi.org/10.1016/j.desal.2014.10.043.
[40] O.A. Hamed, A.M. Hassan, K. Al-Shail, M.A. Farooque, Performance analysis of a trihybrid NF/RO/MSF desalination plant, Desalin. Water Treat. 1 (2009) 215–222, https://doi.org/10.5004/dwt.2009.113.
[41] C. Kaya, G. Sert, N. Kabay, M. Arda, M. Yüksel, Ö. Egemen, Pre-treatment with nanofiltration (NF) in seawater desalination-preliminary integrated membrane tests in Urla, Turkey, Desalination 369 (2015) 10–17, https://doi.org/10.1016/j.desal.2015.04.029.
[42] M. Figueira, D. Rodríguez-Jiménez, J. López, M. Reig, J. Luis Cortina, C. Valderrama, Evaluation of the nanofiltration of brines from seawater desalination plants as pre-treatment in a multimineral brine extraction process,

Sep. Purif. Technol. 322 (2023) 124232, https://doi.org/10.1016/j.seppur.2023.124232.
[43] C. Morgante, T. Moghadamfar, J. Lopez, J.L. Cortina, A. Tamburini, Evaluation of enhanced nanofiltration membranes for improving magnesium recovery schemes from seawater/brine: integrating experimental performing data with a techno-economic assessment, J. Environ. Manag. 360 (2024) 121192, https://doi.org/10.1016/j.jenvman.2024.121192.
[44] M. Al-Shammiri, M. Ahmed, M. Al-Rageeb, Nanofiltration and calcium sulfate limitation for top brine temperature in Gulf desalination plants, Desalination 167 (2004) 335–346, https://doi.org/10.1016/j.desal.2004.06.143.
[45] P. Eriksson, M. Kyburz, W. Pergande, NF membrane characteristics and evaluation for sea water processing applications, Desalination 184 (2005) 281–294, https://doi.org/10.1016/j.desal.2005.04.030.
[46] M. Turek, M. Chorazewska, Nanofiltration process for seawater desalination-salt production integrated system, Desalin. Water Treat. 7 (2009) 178–181, https://doi.org/10.5004/dwt.2009.713.
[47] Y. Song, X. Gao, T. Li, C. Gao, J. Zhou, Improvement of overall water recovery by increasing RNF with recirculation in a NF-RO integrated membrane process for seawater desalination, Desalination 361 (2015) 95–104, https://doi.org/10.1016/j.desal.2015.01.023.
[48] A.S. Al-Amoudi, S. Ihm, A.M. Farooque, E.S.B. Al-Waznani, N. Voutchkov, Dual brine concentration for the beneficial use of two concentrate streams from desalination plant - concept proposal and pilot plant demonstration, Desalination 564 (2023) 116789, https://doi.org/10.1016/j.desal.2023.116789.
[49] C. Morgante, F. Vassallo, C. Cassaro, G. Virruso, D. Diamantidou, N. Van Linden, A. Trezzi, C. Xenogianni, R. Ktori, M. Rodriguez, G. Scelfo, S. Randazzo, A. Tamburini, A. Cipollina, G. Micale, D. Xevgenos, Pioneering minimum liquid discharge desalination: a pilot study in Lampedusa Island, Desalination 581 (2024) 117562, https://doi.org/10.1016/j.desal.2024.117562.
[50] M. Reig, S. Casas, O. Gibert, C. Valderrama, J.L. Cortina, Integration of nanofiltration and bipolar electrodialysis for valorization of seawater desalination brines: production of drinking and waste water treatment chemicals, Desalination 382 (2016) 13–20, https://doi.org/10.1016/j.desal.2015.12.013.
[51] J. Liu, J. Yuan, Z. Ji, B. Wang, Y. Hao, X. Guo, Concentrating brine from seawater desalination process by nanofiltration-electrodialysis integrated membrane technology, Desalination 390 (2016) 53–61, https://doi.org/10.1016/j.desal.2016.03.012.
[52] Y. Xu, Q.B. Chen, J. Wang, P.F. Li, J. Zhao, Fractionation of monovalent ions from seawater brine via softening nanofiltration and selective electrodialysis: which is better? Desalination 533 (2022) 115717 https://doi.org/10.1016/j.desal.2022.115717.
[53] G. Gilabert-Oriol, D. Arias, C. Niewersch, M.Á. Pérez Maciá, H. Alomar, Brine recovery: achieving high magnesium concentration using selective nanofiltration membranes, Desalin. Water Treat. 309 (2023) 154–157, https://doi.org/10.5004/dwt.2023.29920.
[54] P. Pasqualin, P.A. Davies, Multi-stage nanofiltration for brine concentration: experimental and modelling study, Desalination 566 (2023) 116928, https://doi.org/10.1016/j.desal.2023.116928.
[55] G. Al Bazedi, R.S. Ettouney, S.R. Tewfik, M.H. Sorour, M.A. El-Rifai, Salt recovery from brine generated by large-scale seawater desalination plants, Desalin. Water Treat. 52 (2014) 4689–4697, https://doi.org/10.1080/19443994.2013.810381.
[56] M. Figueira, D. Rodríguez-Jiménez, J. López, M. Reig, J.L. Cortina, C. Valderrama, Experimental and economic evaluation of nanofiltration as a pre-treatment for added-value elements recovery from seawater desalination brines, Desalination 549 (2023) 116321, https://doi.org/10.1016/j.desal.2022.116321.
[57] A. Altaee, N. Hilal, High recovery rate NF-FO-RO hybrid system for inland brackish water treatment, Desalination 363 (2015) 19–25, https://doi.org/10.1016/j.desal.2014.12.017.
[58] Y. Song, T. Li, J. Zhou, Z. Li, C. Gao, Analysis of nanofiltration membrane performance during softening process of simulated brackish groundwater, Desalination 399 (2016) 159–164, https://doi.org/10.1016/j.desal.2016.09.004.
[59] S. Mountadar, C. Carbonell-Alcaina, M.J. Luján-Facundo, E. Ferrer-Polonio, J. L. Soler-Cabezas, J.A. Mendoza-Roca, S. Tahiri, Desalination of brackish water and reverse osmotic retentate using nanofiltration membranes: effects of TMP and feed concentration on the treatment, Desalin. Water Treat. 87 (2017) 68–75, https://doi.org/10.5004/dwt.2017.21312.
[60] X. Su, Y. Song, T. Li, C. Gao, Effect of feed water characteristics on nanofiltration separating performance for brackish water treatment in the Huanghuai region of China, journal of water, Process. Eng. 19 (2017) 147–155, https://doi.org/10.1016/j.jwpe.2017.07.021.
[61] M.K. Wafi, N. Hussain, O. El-Sharief Abdalla, M.D. Al-Far, N.A. Al-Hajaj, K. F. Alzonnikah, Nanofiltration as a cost-saving desalination process, SN Appl. Sci. 1 (2019) 1–9, https://doi.org/10.1007/s42452-019-0775-y.
[62] F. Elazhar, M. Elazhar, S. El-Ghzizel, M. Tahaikt, M. Zait, D. Dhiba, A. Elmidaoui, M. Taky, Nanofiltration-reverse osmosis hybrid process for hardness removal in brackish water with higher recovery rate and minimization of brine discharges, Process Saf. Environ. Prot. 153 (2021) 376–383, https://doi.org/10.1016/j.psep.2021.06.025.
[63] Y. Liu, J. Ran, Q. Guo, L. Gao, S. Yin, S. Li, X. Jiang, N. Zhang, G. Zhou, Advancements in nanofiltration fouling phenomenon: from water treatment to salt lakes environments, Desalination 583 (2024) 117649, https://doi.org/10.1016/j.desal.2024.117649.
[64] M. Telzhensky, L. Birnhack, O. Lehmann, E. Windler, O. Lahav, Selective separation of seawater Mg 2+ ions for use in downstream water treatment processes, Chem. Eng. J. 175 (2011) 136–143, https://doi.org/10.1016/j.cej.2011.09.082.
[65] W. Song, L.Y. Lee, E. Liu, X. Shi, S.L. Ong, H.Y. Ng, Spatial variation of fouling behavior in high recovery nanofiltration for industrial reverse osmosis brine treatment towards zero liquid discharge, J. Membr. Sci. 609 (2020) 118185, https://doi.org/10.1016/j.memsci.2020.118185.
[66] T. Hubach, M. Pillath, C. Knaup, S. Schlüter, C. Held, Li+ separation from multi-ionic mixtures by Nanofiltration membranes: experiments and modeling, Modelling 4 (2023) 408–425, https://doi.org/10.3390/modelling4030024.
[67] P. Nativ, L. Birnhack, O. Lahav, DiaNanofiltration-based method for inexpensive and selective separation of Mg2+ and Ca2+ ions from seawater, for improving the quality of soft and desalinated waters, Sep. Purif. Technol. 166 (2016) 83–91, https://doi.org/10.1016/j.seppur.2016.04.026.
[68] P. Nativ, N. Fridman-Bishop, O. Nir, O. Lahav, Dia-nanofiltration-electrodialysis hybrid process for selective removal of monovalent ions from Mg2+ rich brines, Desalination 481 (2020) 114357, https://doi.org/10.1016/j.desal.2020.114357.
[69] V.H. Truong, T.H. Chong, A diafiltration-nanofiltration-reverse osmosis (DiaNF-RO) process for ion fractionation towards resource recovery in seawater desalination: comparison with a RO-DiaNF process and effect of NF membrane performance, Desalination 581 (2024) 117592, https://doi.org/10.1016/j.desal.2024.117592.
[70] V.H. Truong, T.H. Chong, Development of a diafiltration-nanofiltration-reverse osmosis (DiaNF-RO) process for ion fractionation towards resource recovery in seawater desalination, Desalination 583 (2024), https://doi.org/10.1016/j.desal.2024.117684.
[71] D.M. Davenport, A. Deshmukh, J.R. Werber, M. Elimelech, High-pressure reverse osmosis for energy-efficient hypersaline brine desalination: current status, Design Considerations, and Research Needs, Environ. Sci. Technol. Lett. 5 (2018) 467–475, https://doi.org/10.1021/acs.estlett.8b00274.
[72] A. Anvari, J. Wu, A. Edalat, N. Voutchkov, A. Al-Ahmoudi, S. Bhattacharjee, E.M. V. Hoek, What will it take to get to 250,000 ppm brine concentration via ultra-high pressure reverse osmosis? And is it worth it? Desalination 580 (2024) 117565 https://doi.org/10.1016/j.desal.2024.117565.
[73] K. Touati, C.N. Mulligan, Energy consumption and energy efficiency of high-pressure reverse osmosis: effect of water recovery, number of stages, and energy recovery, Appl. Energy 382 (2025) 125270, https://doi.org/10.1016/j.apenergy.2024.125270.
[74] J. Wu, B. Jung, A. Anvari, S.J. Im, M. Anderson, X. Zheng, D. Jassby, R.B. Kaner, D. Dlamini, A. Edalat, E.M.V. Hoek, Reverse osmosis membrane compaction and embossing at ultra-high pressure operation, Desalination 537 (2022) 115875, https://doi.org/10.1016/j.desal.2022.115875.
[75] G. Bargeman, Maximum allowable retention for low-salt-rejection reverse osmosis membranes and its effect on concentrating undersaturated NaCl solutions to saturation, Sep. Purif. Technol. 317 (2023) 123854, https://doi.org/10.1016/j.seppur.2023.123854.
[76] A.A. Atia, J. Allen, E. Young, B. Knueven, T.V. Bartholomew, Cost optimization of low-salt-rejection reverse osmosis, Desalination 551 (2023) 116407, https://doi.org/10.1016/j.desal.2023.116407.
[77] A. Naderi Beni, S.M. Alnajdi, J. Garcia-Bravo, D.M. Warsinger, Semi-batch and batch low-salt-rejection reverse osmosis for brine concentration, Desalination 583 (2024) 117670, https://doi.org/10.1016/j.desal.2024.117670.
[78] H. Zhao, Z. Wang, Y. Chen, A theoretical analysis on upgrading desalination plants with low-salt-rejection reverse osmosis, Desalination 565 (2023) 116827, https://doi.org/10.1016/j.desal.2023.116827.
[79] B.D. Van Houghton, J.S. Rosenblum, K. Lampi, E. Beaudry, J.J. Herron, M. del Cerro, C.T.K. De Finnda, M. Elimelech, J. Gilron, T.Y. Cath, Pilot scale demonstration of Low-salt-rejection reverse osmosis (LSRRO) desalination of high salinity brines, ACS ES T Water (2024), https://doi.org/10.1021/acsestwater.4c00673.
[80] Y.K. Chong, M. Li, D.E. Wiley, D.F. Fletcher, Y.Y. Liang, Review of modeling methodologies and state-of-the-art for osmotically assisted reverse osmosis membrane systems, Desalination 587 (2024), https://doi.org/10.1016/j.desal.2024.117893.
[81] K. Nakagawa, N. Togo, R. Takagi, T. Shintani, T. Yoshioka, E. Kamio, H. Matsuyama, Multistage osmotically assisted reverse osmosis process for concentrating solutions using hollow fiber membrane modules, Chem. Eng. Res. Des. 162 (2020) 117–124, https://doi.org/10.1016/j.cherd.2020.07.029.
[82] T. Nakao, S. Goda, Y. Miura, M. Yasukawa, M. Ishibashi, K. Nakagawa, T. Shintani, H. Matsuyama, T. Yoshioka, Development of cellulose triacetate asymmetric hollow fiber membranes with highly enhanced compaction resistance for osmotically assisted reverse osmosis operation applicable to brine concentration, J. Membr. Sci. 653 (2022) 120508, https://doi.org/10.1016/j.memsci.2022.120508.
[83] J. Ju, S. Lee, Y. Kim, H. Cho, S. Lee, Theoretical and experimental analysis of osmotically assisted reverse osmosis for minimum liquid discharge, Membranes (Basel) 13 (2023), https://doi.org/10.3390/membranes13100814.
[84] T.V. Bartholomew, L. Mey, J.T. Arena, N.S. Siefert, M.S. Mauter, Osmotically assisted reverse osmosis for high salinity brine treatment, Desalination 421 (2017) 3–11, https://doi.org/10.1016/j.desal.2017.04.012.
[85] E. Shamlou, R. Vidic, M.M. El-Halwagi, V. Khanna, Optimization-based modeling and analysis of brine reflux osmotically assisted reverse osmosis for application toward zero liquid discharge systems, Desalination 539 (2022) 115948, https://doi.org/10.1016/j.desal.2022.115948.
[86] A.A. Atia, N.Y. Yip, V. Fthenakis, Pathways for minimal and zero liquid discharge with enhanced reverse osmosis technologies: module-scale modeling and techno-economic assessment, Desalination 509 (2021) 115069, https://doi.org/10.1016/j.desal.2021.115069.

[87] Z. Wang, D. Feng, Y. Chen, D. He, M. Elimelech, Comparison of energy consumption of osmotically assisted reverse osmosis and Low-salt-rejection reverse osmosis for brine management, Environ. Sci. Technol. 55 (2021) 10714–10723, https://doi.org/10.1021/acs.est.1c01638.
[88] L. Chekli, S. Phuntsho, H.K. Shon, S. Vigneswaran, J. Kandasamy, A. Chanan, A review of draw solutes in forward osmosis process and their use in modern applications, Desalin. Water Treat. 43 (2012) 167–184, https://doi.org/10.1080/19443994.2012.672168.
[89] O.A. Bamaga, A. Yokochi, E.G. Beaudry, Application of forward osmosis in pretreatment of seawater for small reverse osmosis desalination units, Desalin. Water Treat. 5 (2009) 183–191, https://doi.org/10.5004/dwt.2009.574.
[90] M. Ahmad, M. Abdel-Jawad, Y. Al-Wazzan, A. Al-Odwani, J. Pallickal Thomas, Experimental study of a cellulose triacetate spiral wound forward osmosis membrane for desalination process integration, Desalin. Water Treat. 66 (2017) 50–59, https://doi.org/10.5004/dwt.2016.11142.
[91] M. Ahmed, B. Garudachari, K.A. Rajesha, J. Thomas, Evaluation of the separation performance of thin film composite forward osmosis membrane using sodium chloride draw solution for Arabian Gulf seawater desalination, Desalin. Water Treat. 107 (2018) 1–9, https://doi.org/10.5004/dwt.2018.22077.
[92] R.C. Eusebio, M.A. Promentilla, H.S. Kim, Optimization of forward osmosis system for the utilization of reverse osmosis brine, Desalin. Water Treat. 57 (2016) 27899–27904, https://doi.org/10.1080/19443994.2016.1168585.
[93] N. Akther, S. Daer, S.W. Hasan, Effect of flow rate, draw solution concentration and temperature on the performance of TFC FO membrane, and the potential use of ro reject brine as a draw solution in FO–RO hybrid systems, Desalin. Water Treat. 136 (2018) 65–71, https://doi.org/10.5004/dwt.2018.23195.
[94] S. Phuntsho, J.E. Kim, S. Hong, N. Ghaffour, T.O. Leiknes, J.Y. Choi, H.K. Shon, A closed-loop forward osmosis-nanofiltration hybrid system: understanding process implications through full-scale simulation, Desalination 421 (2017) 169–178, https://doi.org/10.1016/j.desal.2016.12.010.
[95] W. Tang, H.Y. Ng, Concentration of brine by forward osmosis: performance and influence of membrane structure, Desalination 224 (2008) 143–153, https://doi.org/10.1016/j.desal.2007.04.085.
[96] H. El Zayat, P. Nasr, H. Sewilam, Investigating sustainable management of desalination brine through concentration using forward osmosis, Environ. Sci. Pollut. Res. 28 (2021) 39938–39951, https://doi.org/10.1007/s11356-021-13311-z.
[97] S.J. Im, S. Jeong, A. Jang, Forward osmosis (FO)-reverse osmosis (RO) hybrid process incorporated with hollow fiber FO, NPJ Clean Water 4 (2021), https://doi.org/10.1038/s41545-021-00143-0.
[98] H.S. Son, S. Soukane, J. Lee, Y. Kim, Y.-D. Kim, N. Ghaffour, Towards sustainable circular brine reclamation using seawater reverse osmosis, membrane distillation and forward osmosis hybrids: An experimental investigation, J. Environ. Manag. 293 (2021) 112836, https://doi.org/10.1016/j.jenvman.2021.112836.
[99] G. Bhadrachari, M. Ahmed, R.K. Alambi, J.P. Thomas, Evaluation of pressure-assisted forward osmosis for concentrating desalination brine: a feasibility study, Desalin. Water Treat. 315 (2023) 40–48, https://doi.org/10.5004/dwt.2023.30092.
[100] A. Altaee, A. Mabrouk, K. Bourouni, A novel forward osmosis membrane pretreatment of seawater for thermal desalination processes, Desalination 326 (2013) 19–29, https://doi.org/10.1016/j.desal.2013.07.008.
[101] M.S. Thabit, A.H. Hawari, M.H. Ammar, S. Zaidi, G. Zaragoza, A. Altaee, Evaluation of forward osmosis as a pretreatment process for multi stage flash seawater desalination, Desalination 461 (2019) 22–29, https://doi.org/10.1016/j.desal.2019.03.015.
[102] Y. Yang, R. Tang, Y. Sun, X. Song, J. Yu, Degradation of forward osmosis (FO) membrane in multi-effect distillation (MED) brine: change of transport, physicochemical and anti-fouling properties, Desalination 496 (2020) 114734, https://doi.org/10.1016/j.desal.2020.114734.
[103] C.R. Martinetti, A.E. Childress, T.Y. Cath, High recovery of concentrated RO brines using forward osmosis and membrane distillation, J. Membr. Sci. 331 (2009) 31–39, https://doi.org/10.1016/j.memsci.2009.01.003.
[104] S. Lee, Y. Kim, A.S. Kim, S. Hong, Evaluation of membrane-based desalting processes for RO brine treatment, Desalin. Water Treat. 57 (2016) 7432–7439, https://doi.org/10.1080/19443994.2015.1030120.
[105] H. Sewilam, G. Al Bazedi, Hybrid BWRO/FO system for high recovery in-land brackish water desalination: techno-economic assessment, Sustain. Water Resour. Manag. 9 (2023) 1–11, https://doi.org/10.1007/s40899-023-00912-4.
[106] H. Kim, S. Park, Y. Choi, S. Lee, J. Choi, Fouling due to CaSo4 scale formation in forward osmosis (FO), reverse osmosis (RO), and pressure assisted forward osmosis (PAFO), Desalin. Water Treat. 104 (2018) 45–50, https://doi.org/10.5004/dwt.2018.21657.
[107] G. Chen, Z. Wang, X.M. Li, J. Song, B. Zhao, S. Phuntsho, H.K. Shon, T. He, Concentrating underground brine by FO process: influence of membrane types and spacer on membrane scaling, Chem. Eng. J. 285 (2016) 92–100, https://doi.org/10.1016/j.cej.2015.09.096.
[108] C. Boo, M. Elimelech, S. Hong, Fouling control in a forward osmosis process integrating seawater desalination and wastewater reclamation, J. Membr. Sci. 444 (2013) 148–156, https://doi.org/10.1016/j.memsci.2013.05.004.
[109] V. Yangali-Quintanilla, L. Olesen, J. Lorenzen, C. Rasmussen, H. Laursen, E. Vestergaard, K. Keiding, Lowering desalination costs by alternative desalination and water reuse scenarios, Desalin. Water Treat. 55 (2015) 2437–2445, https://doi.org/10.1080/19443994.2014.940660.
[110] M. Darwish, A. Hassan, A.N. Mabrouk, H. Abdulrahim, A. Sharif, Viability of integrating forward osmosis (FO) as pretreatment for existing MSF desalting unit, Desalin. Water Treat. 57 (2016) 14336–14346, https://doi.org/10.1080/19443994.2015.1066270.
[111] C.F. Wan, T.S. Chung, Techno-economic evaluation of various RO+PRO and RO+FO integrated processes, Appl. Energy 212 (2018) 1038–1050, https://doi.org/10.1016/j.apenergy.2017.12.124.
[112] M. Guizani, T. Maeda, R. Ito, N. Funamizu, Combined FO and RO system for the recovery of energy from wastewater and the desalination of seawater, Desalin. Water Treat. 154 (2019) 14–20, https://doi.org/10.5004/dwt.2019.24083.
[113] A. Naderi Beni, I. Ghofrani, A. Nouri-Borujerdi, A. Moosavi, D.M. Warsinger, Membrane properties overview in integrated forward osmosis/osmotically assisted reverse osmosis systems, Desalination 569 (2024) 117008, https://doi.org/10.1016/j.desal.2023.117008.
[114] Y. Li, E.R. Thomas, M.H. Molina, S. Mann, W.S. Walker, M.L. Lind, F. Perreault, Desalination by membrane pervaporation: a review, Desalination 547 (2023) 116223, https://doi.org/10.1016/j.desal.2022.116223.
[115] R. Ge, T. Huo, Z. Gao, J. Li, X. Zhan, GO-based membranes for desalination, Membranes (Basel) 13 (2023) 220, https://doi.org/10.3390/membranes13020220.
[116] H. Zhao, Y. Kong, M. Xu, C. Wang, Y. Liu, Y. Li, Tannic acid crosslinked chitosan membranes for pervaporation desalination, Sep. Purif. Technol. 364 (2025) 132405, https://doi.org/10.1016/j.seppur.2025.132405.
[117] M. Mukherjee, S. Roy, K. Bhowmick, S. Majumdar, I. Prihatiningtyas, B. Van der Bruggen, P. Mondal, Development of high performance pervaporation desalination membranes: a brief review, Process. Saf. Environ. Prot. 159 (2022) 1092–1104, https://doi.org/10.1016/j.psep.2022.01.076.
[118] M.M. Elewa, Emerging and conventional water desalination technologies powered by renewable energy and energy storage systems toward zero liquid discharge, Separations 11 (2024) 291, https://doi.org/10.3390/separations11100291.
[119] C. Du, J. Runhong Du, X. Feng, F. Du, F. Cheng, M.E.A. Ali, Pervaporation-assisted desalination of seawater reverse osmosis brine, Sep. Purif. Technol. 290 (2022) 120820, https://doi.org/10.1016/j.seppur.2022.120820.
[120] C.-M. Bell, Comparison of polyelectrolyte coated PVDF membranes in thermopervaporation with porous hydrophobic membranes in membrane distillation using plate-and-frame modules, Chem. Eng. Process. Process Intensif. 104 (2016) 58–65, https://doi.org/10.1016/j.cep.2016.02.013.
[121] Q. Wang, N. Li, B. Bolto, M. Hoang, Z. Xie, Desalination by pervaporation: a review, Desalination 387 (2016) 46–60, https://doi.org/10.1016/j.desal.2016.02.036.
[122] L. Wang, Y. Wang, L. Wu, G. Wei, Fabrication, properties, performances, and separation application of polymeric pervaporation membranes: a review, Polymers (Basel) 12 (2020) 1466, https://doi.org/10.3390/polym12071466.
[123] R. Castro-Muñoz, Breakthroughs on tailoring pervaporation membranes for water desalination: a review, Water Res. 187 (2020) 116428, https://doi.org/10.1016/j.watres.2020.116428.
[124] E.R. Thomas, A. Jain, S.C. Mann, Y. Yang, M.D. Green, W.S. Walker, F. Perreault, M.L. Lind, R. Verduzco, Freestanding self-assembled sulfonated pentablock terpolymer membranes for high flux pervaporation desalination, J. Membr. Sci. 613 (2020) 118460, https://doi.org/10.1016/j.memsci.2020.118460.
[125] Z. Xie, M. Hoang, T. Duong, D. Ng, B. Dao, S. Gray, Sol–gel derived poly(vinyl alcohol)/maleic acid/silica hybrid membrane for desalination by pervaporation, J. Membr. Sci. 383 (2011) 96–103, https://doi.org/10.1016/j.memsci.2011.08.036.
[126] B. Liang, K. Pan, L. Li, E.P. Giannelis, B. Cao, High performance hydrophilic pervaporation composite membranes for water desalination, Desalination 347 (2014) 199–206, https://doi.org/10.1016/j.desal.2014.05.021.
[127] G. Yang, Z. Xie, M. Cran, D. Ng, S. Gray, Enhanced desalination performance of poly (vinyl alcohol)/carbon nanotube composite pervaporation membranes via interfacial engineering, J. Membr. Sci. 579 (2019) 40–51, https://doi.org/10.1016/j.memsci.2019.02.034.
[128] Q. Wang, Y. Lu, N. Li, Preparation, characterization and performance of sulfonated poly(styrene-ethylene/butylene-styrene) block copolymer membranes for water desalination by pervaporation, Desalination 390 (2016) 33–46, https://doi.org/10.1016/j.desal.2016.04.005.
[129] B. Liang, Q. Li, B. Cao, P. Li, Water permeance, permeability and desalination properties of the sulfonic acid functionalized composite pervaporation membranes, Desalination 433 (2018) 132–140, https://doi.org/10.1016/j.desal.2018.01.028.
[130] W. Kaminski, J. Marszalek, E. Tomczak, Water desalination by pervaporation – comparison of energy consumption, Desalination 433 (2018) 89–93, https://doi.org/10.1016/j.desal.2018.01.014.
[131] Z. Xie, D. Ng, M. Hoang, J. Zhang, S. Gray, Study of hybrid PVA/MA/TEOS pervaporation membrane and evaluation of energy requirement for desalination by pervaporation, Int. J. Environ. Res. Public Health 15 (2018) 1913, https://doi.org/10.3390/ijerph15091913.
[132] J. Wang, D. Tanuwidjaja, S. Bhattacharjee, A. Edalat, D. Jassby, E.M.V. Hoek, Produced water desalination via Pervaporative distillation, Water (Basel) 12 (2020) 3560, https://doi.org/10.3390/w12123560.
[133] I. Prihatiningtyas, A.-H.A.H. Al-Kebsi, Y. Hartanto, T.M. Zewdie, B. Van der Bruggen, Techno-economic assessment of pervaporation desalination of hypersaline water, Desalination 527 (2022) 115538, https://doi.org/10.1016/j.desal.2021.115538.
[134] M. Kazemimoghadam, T. Mohammadi, The pilot-scale pervaporation plant using tubular-type module with nano pore zeolite membrane, Desalination 255 (2010) 196–200, https://doi.org/10.1016/j.desal.2009.12.027.

[135] J. Liu, J. Chen, X. Zhan, M. Fang, T. Wang, J. Li, Preparation and characterization of ZSM-5/PDMS hybrid pervaporation membranes: laboratory results and pilot-scale performance, Sep. Purif. Technol. 150 (2015) 257–267, https://doi.org/10.1016/j.seppur.2015.06.036.
[136] Desal+ Living Lab, Desal+ Living Lab, (n.d.). https://www.desalinationlab.com/ (accessed April 3, 2025).
[137] A. Subramani, J.G. Jacangelo, Emerging desalination technologies for water treatment: a critical review, Water Res. 75 (2015) 164–187, https://doi.org/10.1016/j.watres.2015.02.032.
[138] J.W. Post, H.V.M. Hamelers, C.J.N. Buisman, Energy recovery from controlled mixing salt and fresh water with a reverse electrodialysis system, Environ. Sci. Technol. 42 (2008) 5785–5790, https://doi.org/10.1021/es8004317.
[139] T. Sampedro, E. Mazo, L. Gómez-Coma, A. Arruti, M. Fallanza, J. Pinedo, J. Rioyo, M. Sainz, R. Ibañez, I. Ortiz, Harnessing salinity gradient energy: pushing forward in water reclamation via on-site reverse electrodialysis technology, J. Environ. Manag. 371 (2024) 123251, https://doi.org/10.1016/j.jenvman.2024.123251.
[140] I.O. Carolina Tristán, Marta Rumayor, Antonio Dominguez-Ramos, Marcos Fallanza, Raquel Ibáñez, Life Cycle Assessment of Salinity Gradient Energy Recovery by Reverse Electrodialysis in a Seawater Reverse Osmosis Desalination Plant, Green Energy and Technology, 2020, pp. 17–33, https://doi.org/10.1039/D0SE00372G.
[141] X. Zhu, W. He, B.E. Logan, Reducing pumping energy by using different flow rates of high and low concentration solutions in reverse electrodialysis cells, J. Membr. Sci. 486 (2015) 215–221, https://doi.org/10.1016/j.memsci.2015.03.035.
[142] A.M. Benneker, T. Rijnaarts, R.G.H. Lammertink, J.A. Wood, Effect of temperature gradients in (reverse) electrodialysis in the Ohmic regime, J. Membr. Sci. (2018), https://doi.org/10.1016/j.memsci.2017.11.029.
[143] R. Ortiz-Imedio, L. Gomez-Coma, M. Fallanza, A. Ortiz, R. Ibañez, I. Ortiz, Comparative performance of salinity gradient power-reverse Electrodialysis under different operating conditions, Desalination 457 (2019) 8–21, https://doi.org/10.1016/j.desal.2019.01.005.
[144] V.M. Ortiz-Martínez, L. Gómez-Coma, C. Tristán, G. Pérez, M. Fallanza, A. Ortiz, R. Ibañez, I. Ortiz, A comprehensive study on the effects of operation variables on reverse electrodialysis performance, Desalination 482 (2020) 114389, https://doi.org/10.1016/j.desal.2020.114389.
[145] L. Gómez-Coma, J.A. Abarca, M. Fallanza, A. Ortiz, R. Ibáñez, I. Ortiz, Optimum recovery of saline gradient power using reversal electrodialysis: influence of the stack components, J. Water Process Eng. 48 (2022) 102816, https://doi.org/10.1016/j.jwpe.2022.102816.
[146] H. Kim, S. Yang, J. Choi, J.-O. Kim, N. Jeong, Optimization of the number of cell pairs to design efficient reverse electrodialysis stack, Desalination 497 (2021) 114676, https://doi.org/10.1016/j.desal.2020.114676.
[147] S. Mehdizadeh, M. Yasukawa, T. Abo, Y. Kakihana, M. Higa, Effect of spacer geometry on membrane and solution compartment resistances in reverse electrodialysis, J. Membr. Sci. 572 (2019) 271–280, https://doi.org/10.1016/j.memsci.2018.09.051.
[148] R. Long, B. Li, Z. Liu, W. Liu, Performance analysis of reverse electrodialysis stacks: channel geometry and flow rate optimization, Energy 158 (2018) 427–436, https://doi.org/10.1016/j.energy.2018.06.067.
[149] T. Sampedro, L. Gómez-Coma, I. Ortiz, R. Ibañez, Unlocking energy potential: decarbonizing water reclamation plants with salinity gradient energy recovery, Sci. Total Environ. 906 (2024) 167154, https://doi.org/10.1016/j.scitotenv.2023.167154.
[150] C. Tristán, M. Fallanza, R. Ibáñez, I. Ortiz, Recovery of salinity gradient energy in desalination plants by reverse electrodialysis, Desalination 496 (2020) 114699, https://doi.org/10.1016/j.desal.2020.114699.
[151] L. Gómez-Coma, V.M. Ortiz-Martínez, M. Fallanza, A. Ortiz, R. Ibañez, I. Ortiz, Blue energy for sustainable water reclamation in WWTPs, J. Water Process Eng. 33 (2020) 101020, https://doi.org/10.1016/j.jwpe.2019.101020.
[152] M. Vanoppen, T. van Vooren, L. Gutierrez, M. Roman, L.J.P. Croué, K. Verbeken, J. Philips, A.R.D. Verliefde, Secondary treated domestic wastewater in reverse electrodialysis: what is the best pre-treatment? Sep. Purif. Technol. 218 (2019) 25–42, https://doi.org/10.1016/j.seppur.2018.12.057.
[153] J. Luque Di Salvo, A. Cosenza, A. Tamburini, G. Micale, A. Cipollina, Long-run operation of a reverse electrodialysis system fed with wastewaters, J. Environ. Manag. 217 (2018) 871–887, https://doi.org/10.1016/j.jenvman.2018.03.110.
[154] J. Veerman, Concepts and misconceptions concerning the influence of divalent ions on the performance of reverse Electrodialysis using natural waters, Membranes (Basel) 13 (2023), https://doi.org/10.3390/membranes13010069.
[155] S. Mikhaylin, L. Bazinet, Fouling on ion-exchange membranes: classification, characterization and strategies of prevention and control, Adv. Colloid Interf. Sci. 229 (2016) 34–56, https://doi.org/10.1016/j.cis.2015.12.006.
[156] Y.D. Raka, R. Bock, H. Karoliussen, Ø. Wilhelmsen, O. Stokke Burheim, The influence of concentration and temperature on the membrane resistance of ion exchange membranes and the levelised cost of hydrogen from reverse electrodialysis with ammonium bicarbonate, Membranes (Basel) 11 (2021) 1–22, https://doi.org/10.3390/membranes11020135.
[157] L. Gómez-Coma, V.M. Ortiz-Martínez, J. Carmona, L. Palacio, P. Prádanos, M. Fallanza, A. Ortiz, R. Ibañez, I. Ortiz, Modeling the influence of divalent ions on membrane resistance and electric power in reverse electrodialysis, J. Membr. Sci. 592 (2019) 117385, https://doi.org/10.1016/j.memsci.2019.117385.
[158] J. Veerman, L. Gómez-Coma, A. Ortiz, I. Ortiz, Resistance of ion exchange membranes in aqueous mixtures of monovalent and divalent ions and the effect on reverse Electrodialysis, Membranes (Basel) 13 (2023) 322, https://doi.org/10.3390/membranes13030322.
[159] T. Rijnaarts, E. Huerta, W. van Baak, K. Nijmeijer, Effect of Divalent Cations on RED Performance and Cation Exchange Membrane Selection to Enhance Power Densities, 2017, https://doi.org/10.1021/acs.est.7b03858.
[160] J. Heo, H. Kim, N. Her, S. Lee, Y.G. Park, Y. Yoon, Natural organic matter removal in single-walled carbon nanotubes-ultrafiltration membrane systems, Desalination 298 (2012) 75–84, https://doi.org/10.1016/j.desal.2012.05.003.
[161] C. Hu, M. Li, J. Sun, R. Liu, H. Liu, J. Qu, NOM fouling resistance in response to electric field during electro-ultrafiltration: significance of molecular polarity and weight, J. Colloid Interface Sci. 539 (2019) 11–18, https://doi.org/10.1016/j.jcis.2018.12.048.
[162] A. Zoungrana, M. Çakmakci, From non-renewable energy to renewable by harvesting salinity gradient power by reverse electrodialysis: a review, Int. J. Energy Res. 45 (2021) 3495–3522, https://doi.org/10.1002/er.6062.
[163] W. Cui, J. Liu, Z. Ji, X. Guo, F. Li, Y. Zhao, S. Wang, J. Yuan, Typical organic fouling in the electrodialysis concentration/desalination process of shale gas fracturing flowback water, Environ. Sci. (Camb) 8 (2022) 2254–2264, https://doi.org/10.1039/D2EW00337F.
[164] A. Nazif, H. Karkhanechi, E. Saljoughi, S.M. Mousavi, H. Matsuyama, Recent progress in membrane development, affecting parameters, and applications of reverse electrodialysis: a review, J. Water Process Eng. 47 (2022) 102706, https://doi.org/10.1016/j.jwpe.2022.102706.
[165] A. Cosenza, G. Campisi, F. Giacalone, S. Randazzo, A. Cipollina, A. Tamburini, G. Micale, Power production from produced waters via reverse Electrodialysis: a preliminary assessment, Energies (Basel) 15 (2022) 4177, https://doi.org/10.3390/en15114177.
[166] S. Chae, H. Kim, J. Gi Hong, J. Jang, M. Higa, M. Pishnamazi, J.-Y. Choi, R. Chandula Walgama, C. Bae, I.S. Kim, J.-S. Park, Clean power generation from salinity gradient using reverse electrodialysis technologies: recent advances, bottlenecks, and future direction, Chem. Eng. J. 452 (2023) 139482, https://doi.org/10.1016/j.cej.2022.139482.
[167] J. Veerman, M. Saakes, S.J. Metz, G.J. Harmsen, Electrical power from sea and river water by reverse Electrodialysis: a first step from the laboratory to a real power plant, Environ. Sci. Technol. 44 (2010) 9207–9212, https://doi.org/10.1021/es1009345.
[168] M. Tedesco, C. Scalici, D. Vaccari, A. Cipollina, A. Tamburini, G. Micale, Performance of the first reverse electrodialysis pilot plant for power production from saline waters and concentrated brines, J. Membr. Sci. 500 (2016) 33–45, https://doi.org/10.1016/j.memsci.2015.10.057.
[169] M. Tedesco, A. Cipollina, A. Tamburini, G. Micale, Towards 1 kW power production in a reverse electrodialysis pilot plant with saline waters and concentrated brines, J. Membr. Sci. 522 (2017) 226–236, https://doi.org/10.1016/j.memsci.2016.09.015.
[170] A. D'Angelo, M. Tedesco, A. Cipollina, A. Galia, G. Micale, O. Scialdone, Reverse electrodialysis performed at pilot plant scale: evaluation of redox processes and simultaneous generation of electric energy and treatment of wastewater, Water Res. 125 (2017) 123–131, https://doi.org/10.1016/j.watres.2017.08.008.
[171] J.-Y. Nam, K.-S. Hwang, H.-C. Kim, H. Jeong, H. Kim, E. Jwa, S. Yang, J. Choi, C.-S. Kim, J.-H. Han, N. Jeong, Assessing the behavior of the feed-water constituents of a pilot-scale 1000-cell-pair reverse electrodialysis with seawater and municipal wastewater effluent, Water Res. 148 (2019) 261–271, https://doi.org/10.1016/j.watres.2018.10.054.
[172] S. Mehdizadeh, M. Yasukawa, T. Abo, M. Kuno, Y. Noguchi, M. Higa, The effect of feed solution temperature on the power output performance of a pilot-scale reverse Electrodialysis (RED) system with different intermediate distance, Membranes (Basel) 9 (2019) 73, https://doi.org/10.3390/membranes9060073.
[173] REAPower, REAPower, (n.d.). https://www.reapower.eu/ (accessed December 30, 2024).
[174] LIFE-3E, LIFE-3E, (n.d.). https://life3e.eu/home (accessed April 3, 2023).
[175] C. Tristán, M. Fallanza, R. Ibáñez, I. Ortiz, Reverse electrodialysis: potential reduction in energy and emissions of desalination, Appl. Sci. (Switz.) 10 (2020) 1–21, https://doi.org/10.3390/app10207317.
[176] J.N. Weinstein, F.B. Leitz, Electric power from differences in salinity: the dialytic battery, Science 191 (1976) (1979) 557–559, https://doi.org/10.1126/science.191.4227.557.
[177] E. Güler, W. van Baak, M. Saakes, K. Nijmeijer, Monovalent-ion-selective membranes for reverse electrodialysis, J. Membr. Sci. (2014), https://doi.org/10.1016/j.memsci.2013.12.054.
[178] D.A. Vermaas, M. Saakes, K. Nijmeijer, Power generation using profiled membranes in reverse electrodialysis, J. Membr. Sci. 385–386 (2011) 234–242, https://doi.org/10.1016/j.memsci.2011.09.043.
[179] J.G. Hong, Y. Chen, Nanocomposite reverse electrodialysis (RED) ion-exchange membranes for salinity gradient power generation, J. Membr. Sci. 460 (2014) 139–147, https://doi.org/10.1016/j.memsci.2014.02.027.
[180] A. Zlotorowicz, R.V. Strand, O.S. Burheim, S. Kjelstrup Wilhelmsen, The permselectivity and water transference number of ion exchange membranes in reverse electrodialysis, J. Membr. Sci. (2017), https://doi.org/10.1016/j.memsci.2016.10.003.
[181] A.T. Besha, M.T. Tsehaye, D. Aili, W. Zhang, R.A. Tufa, Design of monovalent ion selective membranes for reducing the impacts of multivalent ions in reverse electrodialysis, Membranes (Basel) 10 (2020), https://doi.org/10.3390/membranes10010007.
[182] M.N.Z. Abidin, M.M. Nasef, J. Veerman, Towards the development of new generation of ion exchange membranes for reverse electrodialysis: a review, Desalination 537 (2022) 115854, https://doi.org/10.1016/j.desal.2022.115854.
[183] Y. Shi, M. Zhang, H. Zhang, F. Yang, C.Y. Tang, Y. Dong, Recent development of pressure retarded osmosis membranes for water and energy sustainability: a

critical review, Water Res. 189 (2021) 116666, https://doi.org/10.1016/j.watres.2020.116666.
[184] A. Achilli, K.L. Hickenbottom, Pressure retarded osmosis, in: Sustainable Energy from Salinity Gradients, Elsevier, 2016, pp. 55–75, https://doi.org/10.1016/B978-0-08-100312-1.00003-1.
[185] G. O'Toole, L. Jones, C. Coutinho, C. Hayes, M. Napoles, A. Achilli, River-to-sea pressure retarded osmosis: resource utilization in a full-scale facility, Desalination 389 (2016) 39–51, https://doi.org/10.1016/j.desal.2016.01.012.
[186] K. Saito, M. Irie, S. Zaitsu, H. Sakai, H. Hayashi, A. Tanioka, Power generation with salinity gradient by pressure retarded osmosis using concentrated brine from SWRO system and treated sewage as pure water, Desalin. Water Treat. 41 (2012) 114–121, https://doi.org/10.1080/19443994.2012.664696.
[187] A. Achilli, J.L. Prante, N.T. Hancock, E.B. Maxwell, A.E. Childress, Experimental results from RO-PRO: a next generation system for Low-energy desalination, Environ. Sci. Technol. 48 (2014) 6437–6443, https://doi.org/10.1021/es405556s.
[188] J.L. Prante, J.A. Ruskowitz, A.E. Childress, A. Achilli, RO-PRO desalination: An integrated low-energy approach to seawater desalination, Appl. Energy 120 (2014) 104–114, https://doi.org/10.1016/j.apenergy.2014.01.013.
[189] T.Y. Cath, M. Elimelech, J.R. McCutcheon, R.L. McGinnis, A. Achilli, D. Anastasio, A.R. Brady, A.E. Childress, I.V. Farr, N.T. Hancock, J. Lampi, L.D. Nghiem, M. Xie, N.Y. Yip, Standard methodology for evaluating membrane performance in osmotically driven membrane processes, Desalination 312 (2013) 31–38, https://doi.org/10.1016/j.desal.2012.07.005.
[190] M. Rastgar, K. Moradi, C. Burroughs, A. Hemmati, E. Hoek, M. Sadrzadeh, Harvesting blue energy based on salinity and temperature gradient: challenges, solutions, and opportunities, Chem. Rev. 123 (2023) 10156–10205, https://doi.org/10.1021/acs.chemrev.3c00168.
[191] H. Kim, J.-S. Choi, S. Lee, Pressure retarded osmosis for energy production: membrane materials and operating conditions, Water Sci. Technol. 65 (2012) 1789–1794, https://doi.org/10.2166/wst.2012.025.
[192] G. Han, S. Zhang, X. Li, T.-S. Chung, Progress in pressure retarded osmosis (PRO) membranes for osmotic power generation, Prog. Polym. Sci. 51 (2015) 1–27, https://doi.org/10.1016/j.progpolymsci.2015.04.005.
[193] S. Patel, Norway inaugurates osmotic power plant, Power 154 (2010). https://www.powermag.com/norway-inaugurates-osmotic-power-plant/. (Accessed 13 February 2025).
[194] K. Gerstandt, K.-V. Peinemann, S.E. Skilhagen, T. Thorsen, T. Holt, Membrane processes in energy supply for an osmotic power plant, Desalination 224 (2008) 64–70, https://doi.org/10.1016/j.desal.2007.02.080.
[195] ForwardOsmosisTech, Is PRO economically feasible? Not according to Statkraft. https://web.archive.org/web/20170118220928/http:/www.forwardosmosistech.com/statkraft-discontinues-investments-in-pressure-retarded-osmosis/, 2014. (Accessed 13 February 2025).
[196] J.H. Kim, Key Issue and Innovation in Desalination Focusing on Korean Projects, 2015.
[197] H.S.K. Kurihara, A. Tanioka, Role of PRO in the Mega-Ton Water Project, San Diego, CA, 2015.
[198] H.T. Madsen, T. Bruun Hansen, T. Nakao, S. Goda, E.G. Søgaard, Combined geothermal heat and pressure retarded osmosis as a new green power system, Energy Convers. Manag. 226 (2020) 113504, https://doi.org/10.1016/j.enconman.2020.113504.
[199] I. Caldwell, Japan has opened its first osmotic power plant – so what is it and how does it work? The Guardian (2025). https://www.theguardian.com/world/2025/aug/25/japan-osmotic-power-plant-fukuoka?CMP=share_btn_url (accessed September 21, 2025).
[200] A.P. Straub, A. Deshmukh, M. Elimelech, Pressure-retarded osmosis for power generation from salinity gradients: is it viable?, energy, Environ. Sci. 9 (2016) 31–48, https://doi.org/10.1039/C5EE02985F.
[201] A.P. Straub, N.Y. Yip, M. Elimelech, Raising the Bar: increased hydraulic pressure allows unprecedented high power densities in pressure-retarded osmosis, Environ. Sci. Technol. Lett. 1 (2014) 55–59, https://doi.org/10.1021/ez400117d.
[202] K. Touati, G. Nouri, C.N. Mulligan, Assessing process feasibility of salinity gradient systems through maximum extractable and net energy outputs, J. Environ. Chem. Eng. 13 (2025) 118490, https://doi.org/10.1016/j.jece.2025.118490.
[203] G. Hopsort, Q. Cacciuttolo, D. Pasquier, Electrodialysis as a key operating unit in chemical processes: from lab to pilot scale of latest breakthroughs, Chem. Eng. J. 494 (2024) 153111, https://doi.org/10.1016/j.cej.2024.153111.
[204] H. Strathmann, Electrodialysis, a mature technology with a multitude of new applications, Desalination 264 (2010) 268–288, https://doi.org/10.1016/j.desal.2010.04.069.
[205] P. P., D. Thampan, S. Karthika, M.K. Ravichandran, A. Subramanian, A. M. Nagarajan, R. Hussain, K. Sivagami, Emerging investigator series: a state-of-the-art review on large-scale desalination technologies and their brine management, Environ. Sci. (Camb) 11 (2025) 167–195, https://doi.org/10.1039/D4EW00662C.
[206] S. Al-Amshawee, M.Y.B.M. Yunus, A.A.M. Azoddein, D.G. Hassell, I.H. Dakhil, H. A. Hasan, Electrodialysis desalination for water and wastewater: a review, Chem. Eng. J. 380 (2020) 122231, https://doi.org/10.1016/j.cej.2019.122231.
[207] L. Bazinet, T.R. Geoffroy, Electrodialytic processes: market overview, membrane phenomena, recent developments and sustainable strategies, Membranes (Basel) 10 (2020) 221, https://doi.org/10.3390/membranes10090221.
[208] G. Cao, M.M. Alam, A.Z. Juthi, Z. Zhang, Y. Wang, C. Jiang, T. Xu, Electro-desalination: state-of-the-art and prospective, Adv. Membr. 3 (2023) 100058, https://doi.org/10.1016/j.advmem.2022.100058.
[209] D. Zhao, L.Y. Lee, S.L. Ong, P. Chowdhury, K.B. Siah, H.Y. Ng, Electrodialysis reversal for industrial reverse osmosis brine treatment, Sep. Purif. Technol. 213 (2019) 339–347, https://doi.org/10.1016/j.seppur.2018.12.056.
[210] S.K. Patel, B. Lee, P. Westerhoff, M. Elimelech, The potential of electrodialysis as a cost-effective alternative to reverse osmosis for brackish water desalination, Water Res. 250 (2024) 121009, https://doi.org/10.1016/j.watres.2023.121009.
[211] Y. Tanaka, Ion-exchange membrane Electrodialysis for saline water desalination and its application to seawater concentration, Ind. Eng. Chem. Res. 50 (2011) 7494–7503, https://doi.org/10.1021/ie102386d.
[212] Y. Tanaka, R. Ehara, S. Itoi, T. Goto, Ion-exchange membrane electrodialytic salt production using brine discharged from a reverse osmosis seawater desalination plant, J. Membr. Sci. 222 (2003) 71–86, https://doi.org/10.1016/S0376-7388(03)00217-5.
[213] Y. Tanaka, M. Reig, S. Casas, C. Aladjem, J.L. Cortina, Computer simulation of ion-exchange membrane electrodialysis for salt concentration and reduction of RO discharged brine for salt production and marine environment conservation, Desalination 367 (2015) 76–89, https://doi.org/10.1016/j.desal.2015.03.022.
[214] Y. Tanaka, Development of a computer simulation program of batch ion-exchange membrane electrodialysis for saline water desalination, Desalination 320 (2013) 118–133, https://doi.org/10.1016/j.desal.2013.04.022.
[215] Y. Tanaka, Ion-exchange membrane electrodialysis program and its application to multi-stage continuous saline water desalination, Desalination 301 (2012) 10–25, https://doi.org/10.1016/j.desal.2012.06.007.
[216] Y. Tanaka, Simulation of an ion exchange membrane electrodialysis process for continuous saline water desalination, Desalin. Water Treat. 22 (2010) 271–285, https://doi.org/10.5004/dwt.2010.1858.
[217] Y. Tanaka, A computer simulation of continuous ion exchange membrane electrodialysis for desalination of saline water, Desalination 249 (2009) 809–821, https://doi.org/10.1016/j.desal.2009.04.011.
[218] M. Reig, S. Casas, C. Aladjem, C. Valderrama, O. Gibert, F. Valero, C.M. Centeno, E. Larrotcha, J.L. Cortina, Concentration of NaCl from seawater reverse osmosis brines for the chlor-alkali industry by electrodialysis, Desalination 342 (2014) 107–117, https://doi.org/10.1016/j.desal.2013.12.021.
[219] I. Ihsanullah, M.A. Atieh, M. Sajid, M.K. Nazal, Desalination and environment: a critical analysis of impacts, mitigation strategies, and greener desalination technologies, Sci. Total Environ. 780 (2021) 146585, https://doi.org/10.1016/j.scitotenv.2021.146585.
[220] N. Mir, Y. Bicer, Integration of electrodialysis with renewable energy sources for sustainable freshwater production: a review, J. Environ. Manag. 289 (2021) 112496, https://doi.org/10.1016/j.jenvman.2021.112496.
[221] C. Fernandez-Gonzalez, A. Dominguez-Ramos, R. Ibañez, A. Irabien, Sustainability assessment of electrodialysis powered by photovoltaic solar energy for freshwater production, Renew. Sust. Energ. Rev. 47 (2015) 604–615, https://doi.org/10.1016/j.rser.2015.03.018.
[222] A. Campione, A. Cipollina, F. Calise, A. Tamburini, M. Galluzzo, G. Micale, Coupling electrodialysis desalination with photovoltaic and wind energy systems for energy storage: dynamic simulations and control strategy, Energy Convers. Manag. 216 (2020) 112940, https://doi.org/10.1016/j.enconman.2020.112940.
[223] J.M. Ortiz, E. Expósito, F. Gallud, V. García-García, V. Montiel, A. Aldaz, Desalination of underground brackish waters using an electrodialysis system powered directly by photovoltaic energy, Sol. Energy Mater. Sol. Cells 92 (2008) 1677–1688, https://doi.org/10.1016/J.SOLMAT.2008.07.020.
[224] J.M.M. Ortiz, E. Expósito, F. Gallud, V. García-García, V. Montiel, A. Aldaz, Photovoltaic electrodialysis system for brackish water desalination: modeling of global process, J. Membr. Sci. 274 (2006) 138–149, https://doi.org/10.1016/j.memsci.2005.08.006.
[225] M. Alrbai, H.S. Hayajneh, A. Omar, M.A. Alkader, H. Al-Riaty, Experimental investigation of lab scale solar powered Electrodialysis system with corrugated membrane configuration, Sol. Energy 224 (2021) 390–400, https://doi.org/10.1016/j.solener.2021.06.028.
[226] D.W. Bian, S.M. Watson, N.C. Wright, S.R. Shah, T. Buonassisi, D. Ramanujan, I. M. Peters, A.G. Winter, Optimization and design of a low-cost, village-scale, photovoltaic-powered, electrodialysis reversal desalination system for rural India, Desalination 452 (2019) 265–278, https://doi.org/10.1016/j.desal.2018.09.004.
[227] P. Malek, J.M. Ortiz, H.M.A. Schulte-Herbrüggen, Decentralized desalination of brackish water using an electrodialysis system directly powered by wind energy, Desalination 377 (2016) 54–64, https://doi.org/10.1016/j.desal.2015.08.023.
[228] C. Jiang, Y. Wang, Z. Zhang, T. Xu, Electrodialysis of concentrated brine from RO plant to produce coarse salt and freshwater, J. Membr. Sci. 450 (2014) 323–330, https://doi.org/10.1016/j.memsci.2013.09.020.
[229] H. Yan, Y. Wang, L. Wu, M.A. Shehzad, C. Jiang, R. Fu, Z. Liu, T. Xu, Multistage-batch electrodialysis to concentrate high-salinity solutions: process optimisation, water transport, and energy consumption, J. Membr. Sci. 570–571 (2019) 245–257, https://doi.org/10.1016/j.memsci.2018.10.008.
[230] S. Gmar, A. Chagnes, Recent advances on electrodialysis for the recovery of lithium from primary and secondary resources, Hydrometallurgy 189 (2019) 105124, https://doi.org/10.1016/j.hydromet.2019.105124.
[231] Z.-Y. Guo, Z.-Y. Ji, Q.-B. Chen, J. Liu, Y.-Y. Zhao, F. Li, Z.-Y. Liu, J.-S. Yuan, Prefractionation of LiCl from concentrated seawater/salt lake brines by electrodialysis with monovalent selective ion exchange membranes, J. Clean. Prod. 193 (2018) 338–350, https://doi.org/10.1016/j.jclepro.2018.05.077.
[232] X.-Y. Nie, S.-Y. Sun, Z. Sun, X. Song, J.-G. Yu, Ion-fractionation of lithium ions from magnesium ions by electrodialysis using monovalent selective ion-exchange membranes, Desalination 403 (2017) 128–135, https://doi.org/10.1016/j.desal.2016.05.010.

[233] X.-Y. Nie, S.-Y. Sun, X. Song, J.-G. Yu, Further investigation into lithium recovery from salt lake brines with different feed characteristics by electrodialysis, J. Membr. Sci. 530 (2017) 185–191, https://doi.org/10.1016/j.memsci.2017.02.020.
[234] P.-Y. Ji, Z.-Y. Ji, Q.-B. Chen, J. Liu, Y.-Y. Zhao, S.-Z. Wang, F. Li, J.-S. Yuan, Effect of coexisting ions on recovering lithium from high Mg2+/Li+ ratio brines by selective-electrodialysis, Sep. Purif. Technol. 207 (2018) 1–11, https://doi.org/10.1016/j.seppur.2018.06.012.
[235] J. Ying, M. Luo, Y. Jin, J. Yu, Selective separation of lithium from high Mg/Li ratio brine using single-stage and multi-stage selective electrodialysis processes, Desalination 492 (2020) 114621, https://doi.org/10.1016/j.desal.2020.114621.
[236] C. Li, D.L. Ramasamy, M. Sillanpää, E. Repo, Separation and concentration of rare earth elements from wastewater using electrodialysis technology, Sep. Purif. Technol. 254 (2021) 117442, https://doi.org/10.1016/j.seppur.2020.117442.
[237] S. Mosadeghsedghi, M.E. Sauber, M. Baghbanzadeh, S.L.D. Kenari, K. Volchek, S. Issa, S. Mortazavi, Separation of rare earth elements using chelation-assisted electrodialysis, J. Environ. Chem. Eng. 11 (2023) 111313, https://doi.org/10.1016/j.jece.2023.111313.
[238] L. Ding, G. Azimi, Mathematical modeling of rare earth element separation in electrodialysis with adjacent anion exchange membranes and ethylenediaminetetraacetic acid as chelating agent, Sci. Rep. 14 (2024) 12240, https://doi.org/10.1038/s41598-024-62885-4.
[239] REvivED water, REvivED water, (n.d.). https://www.revivedwater.eu/ (accessed March 15, 2025).
[240] T. Chen, J. Bi, Z. Ji, J. Yuan, Y. Zhao, Application of bipolar membrane electrodialysis for simultaneous recovery of high-value acid/alkali from saline wastewater: An in-depth review, Water Res. 226 (2022) 119274, https://doi.org/10.1016/j.watres.2022.119274.
[241] Y. Luo, Y. Liu, J. Shen, B. Van der Bruggen, Application of bipolar membrane Electrodialysis in environmental protection and resource recovery: a review, Membranes (Basel) 12 (2022), https://doi.org/10.3390/membranes12090829.
[242] R. Ibáñez, A. Pérez-González, P. Gómez, A.M. Urtiaga, I. Ortiz, Acid and base recovery from softened reverse osmosis (RO) brines. Experimental assessment using model concentrates, Desalination 309 (2013) 165–170, https://doi.org/10.1016/j.desal.2012.10.006.
[243] Y. Yang, X. Gao, A. Fan, L. Fu, C. Gao, An innovative beneficial reuse of seawater concentrate using bipolar membrane electrodialysis, J. Membr. Sci. 449 (2014) 119–126, https://doi.org/10.1016/j.memsci.2013.07.066.
[244] M. Reig, S. Casas, C. Valderrama, O. Gibert, J.L. Cortina, Integration of monopolar and bipolar electrodialysis for valorization of seawater reverse osmosis desalination brines: production of strong acid and base, Desalination 398 (2016) 87–97, https://doi.org/10.1016/j.desal.2016.07.024.
[245] T. León, S. Abdullah Shah, J. López, A. Culcasi, L. Jofre, A. Cipollina, J.L. Cortina, A. Tamburini, G. Micale, Electrodialysis with bipolar membranes for the generation of NaOH and HCl solutions from brines: An inter-laboratory evaluation of thin and ultrathin non-woven cloth-based ion-exchange membranes, Membranes (Basel) 12 (2022) 1204, https://doi.org/10.3390/membranes12121204.
[246] C. Cassaro, G. Virruso, A. Culcasi, A. Cipollina, A. Tamburini, G. Micale, Electrodialysis with bipolar membranes for the sustainable production of chemicals from seawater brines at pilot plant scale, ACS Sustain. Chem. Eng. (2023), https://doi.org/10.1021/acssuschemeng.2c06636.
[247] M. Herrero-Gonzalez, J. López, G. Virruso, C. Cassaro, A. Tamburini, A. Cipollina, J.L. Cortina, R. Ibañez, G. Micale, Analysis of operational parameters in acid and base production using an Electrodialysis with bipolar membranes pilot plant, Membranes (Basel) 13 (2023) 200, https://doi.org/10.3390/membranes13020200.
[248] C. Fernandez-Gonzalez, A. Dominguez-Ramos, R. Ibañez, A. Irabien, Electrodialysis with bipolar membranes for valorization of brines, Sep. Purif. Rev. 45 (2016) 275–287, https://doi.org/10.1080/15422119.2015.1128951.
[249] M. Herrero-Gonzalez, P. Diaz-Guridi, A. Dominguez-Ramos, A. Irabien, R. Ibañez, Highly concentrated HCl and NaOH from brines using electrodialysis with bipolar membranes, Sep. Purif. Technol. 242 (2020) 116785, https://doi.org/10.1016/j.seppur.2020.116785.
[250] M. Herrero-Gonzalez, R. Ibañez, Technical and environmental feasibilities of the commercial production of NaOH from brine by means of an integrated EDBM and evaporation process, Membranes (Basel) 12 (2022) 885, https://doi.org/10.3390/membranes12090885.
[251] R. Fu, H. Wang, J. Yan, R. Li, B. Wang, C. Jiang, Y. Wang, T. Xu, A cost-effective and high-efficiency online ED-BMED integrated system enables the conversion of 3.5 wt% NaCl aqueous solution into 6.20 Mol/L NaOH, Chem. Eng. Sci. 270 (2023) 118523, https://doi.org/10.1016/j.ces.2023.118523.
[252] S. Wu, R. Fu, J. Yan, H. Wang, B. Wang, Y. Wang, T. Xu, Online neutralization promotes water dissociation equilibrium forward in bipolar membranes to achieve 9.2 Mol/L NaOH production, Chem. Eng. J. 490 (2024) 151610, https://doi.org/10.1016/j.cej.2024.151610.
[253] T. León, D. Rodríguez, J. López, L. Jofre, J.L. Cortina, Optimizing Operational Parameters for Highly-Concentrated Sodium Hydroxide Production Via Electrodialysis with Bipolar Membranes from Concentrated Brines, Sep Purif Technol, 2024, p. 127637, https://doi.org/10.1016/j.seppur.2024.127637.
[254] A. Filingeri, M. Herrero-Gonzalez, J. O'Sullivan, J.L. Rodriguez, A. Culcasi, A. Tamburini, A. Cipollina, R. Ibañez, M.C. Ferrari, J.L. Cortina, G. Micale, Acid/base production via bipolar membrane Electrodialysis: brine feed streams to reduce fresh water consumption, Ind. Eng. Chem. Res. 63 (2024) 3198–3210, https://doi.org/10.1021/acs.iecr.3c03553.
[255] M. Herrero-Gonzalez, P. Diaz-Guridi, A. Dominguez-Ramos, R. Ibañez, A. Irabien, Photovoltaic solar electrodialysis with bipolar membranes, Desalination 433 (2018) 155–163, https://doi.org/10.1016/j.desal.2018.01.015.
[256] M. Herrero-Gonzalez, A. Wolfson, A. Dominguez-Ramos, R. Ibañez, A. Irabien, Monetizing environmental footprints: index development and application to a solar-powered chemicals self-supplied desalination plant, ACS Sustain. Chem. Eng. 6 (2018) 14533–14541, https://doi.org/10.1021/acssuschemeng.8b03161.
[257] M. Herrero-Gonzalez, N. Admon, A. Dominguez-Ramos, R. Ibañez, A. Wolfson, A. Irabien, Environmental sustainability assessment of seawater reverse osmosis brine valorization by means of electrodialysis with bipolar membranes, Environ. Sci. Pollut. Res. 27 (2020) 1256–1266, https://doi.org/10.1007/s11356-019-04788-w.
[258] M. Herrero-Gonzalez, A. Culcasi, A. Tamburini, R. Ibañez, A. Cipollina, G. Micale, Techno-economic feasibility of photovoltaic solar electrodialysis with bipolar membranes, Desalination 582 (2024) 117624, https://doi.org/10.1016/j.desal.2024.117624.
[259] L. Wu, C. Zhang, S. Kim, T.A. Hatton, H. Mo, T.D. Waite, Lithium recovery using electrochemical technologies: advances and challenges, Water Res. 221 (2022) 118822, https://doi.org/10.1016/j.watres.2022.118822.
[260] Y.A. Jarma, E. Çermikli, D. İpekçi, E. Altıok, N. Kabay, Comparison of two electrodialysis stacks having different ion exchange and bipolar membranes for simultaneous separation of boron and lithium from aqueous solution, Desalination 500 (2021) 114850, https://doi.org/10.1016/j.desal.2020.114850.
[261] C. Jiang, Y. Wang, Q. Wang, H. Feng, T. Xu, Production of Lithium Hydroxide from Lake Brines through Electro–Electrodialysis with Bipolar Membranes (EEDBM), Ind. Eng. Chem. Res. 53 (2014) 6103–6112, https://doi.org/10.1021/ie404334s.
[262] J. Lopez, A. Filingeri, A. Culcasi, M. Fernández de Labastida, A. Tamburini, J. L. Cortina, G. Micale, A. Cipollina, Electrodialysis with bipolar membranes to valorise saline waste streams: Analysing the fate of valuable minor elements, Sci. Total Environ. 958 (2025) 177934, https://doi.org/10.1016/j.scitotenv.2024.177934.
[263] WATER-MINING, WATER-MINING. https://watermining.eu/, 2023. (Accessed 27 April 2023).
[264] SEArcular Mine, (n.d.). https://searcularmine.eu/ (accessed July 18, 2021).
[265] Sea4value - Mining value from brines - Sea4value, (n.d.). https://sea4value.eu/ (accessed July 21, 2021).
[266] A. Filingeri, J. Lopez, A. Culcasi, T. Leon, A. Tamburini, J. Luis Cortina, G. Micale, A. Cipollina, In-depth insights on multi-ionic transport in Electrodialysis with bipolar membrane systems, Chem. Eng. J. 468 (2023) 143673, https://doi.org/10.1016/j.cej.2023.143673.
[267] T. León, J. López, R. Torres, J. Grau, L. Jofre, J.-L. Cortina, Describing ion transport and water splitting in an electrodialysis stack with bipolar membranes by a 2-D model: experimental validation, J. Membr. Sci. 660 (2022) 120835, https://doi.org/10.1016/j.memsci.2022.120835.
[268] A. Filingeri, A. Culcasi, M. Nanfara, C. Cassaro, A. Tamburini, G. Micale, A. Cipollina, Exploring differential pressure-induced hydraulic flows in pilot-scale Electrodialysis with bipolar membranes, J. Environ. Manag. 373 (2025) 123538, https://doi.org/10.1016/j.jenvman.2024.123538.
[269] M. Figueira, M. Reig, J. Luis Cortina, M. Reza Moradi, A. Pihlajamäki, C. Valderrama, Production of boric acid by bipolar membrane electrodialysis: evaluation of commercial and polyelectrolyte multilayers-coated ion exchange membranes, Sep. Purif. Technol. 354 (2025) 129467, https://doi.org/10.1016/j.seppur.2024.129467.
[270] Indesal, Life INDESAL, (n.d.). https://indesal.revolve.media/.
[271] M. Herrero-Gonzalez, I. Ortiz, R. Ibañez, A. Urtiaga, Electromembrane processes for waste valorization: energy recovery and storage, Curr. Opin. Electrochem. 45 (2024) 101477, https://doi.org/10.1016/j.coelec.2024.101477.
[272] M. Herrero-Gonzalez, R. Ibañez, Chemical and energy recovery alternatives in SWRO desalination through electro-membrane technologies, Appl. Sci. 11 (2021) 8100, https://doi.org/10.3390/app11178100.
[273] Y. Ding, P. Cai, Z. Wen, Electrochemical neutralization energy: from concept to devices, Chem. Soc. Rev. 50 (2021) 1495–1511, https://doi.org/10.1039/D0CS01239D.
[274] J. Muñoz-Cruzado-Alba, R. Musca, J. Ballestín-Fuertes, J.F. Sanz-Osorio, D. M. Rivas-Ascaso, M.P. Jones, A. Catania, E. Goosen, Power grid integration and use-case study of Acid-Base flow battery technology, Sustainability 13 (2021) 6089, https://doi.org/10.3390/su13116089.
[275] M.C. Díaz-Ramírez, M. Blecua-de-Pedro, A.J. Arnal, J. Post, Acid/base flow battery environmental and economic performance based on its potential service to renewables support, J. Clean. Prod. 330 (2022) 129529, https://doi.org/10.1016/j.jclepro.2021.129529.
[276] R. Pärnamäe, L. Gurreri, J. Post, W.J. van Egmond, A. Culcasi, M. Saakes, J. Cen, E. Goosen, A. Tamburini, D.A. Vermaas, M. Tedesco, The acid–base flow battery: sustainable energy storage via reversible water dissociation with bipolar membranes, Membranes (Basel) 10 (2020) 1–20, https://doi.org/10.3390/membranes10120409.
[277] J. Wu, E.M. Hoek, Current opportunities and challenges in membrane-based brine management, Curr. Opin. Chem. Eng. 47 (2025) 101079, https://doi.org/10.1016/j.coche.2024.101079.
[278] X. Ma, L. Flanjak, X.X. Chen, C. Morgante, B.S. Kirkebæk, V. Boffa, C.A. Quist-Jensen, A. Ali, V. Maurino, P. Roslev, Efficient treatment of high-salinity aquaculture effluents through synergistic membrane distillation and VUV/UVC photolysis, J. Water Process Eng. 66 (2024) 106042, https://doi.org/10.1016/j.jwpe.2024.106042.

[279] A. Ali, M.M.A. Shirazi, L.N. Nthunya, R. Castro-Muñoz, N. Ismail, N. Tavajohi, G. Zaragoza, C.A. Quist-jensen, Progress in module design for membrane distillation, Desalination 581 (2024), https://doi.org/10.1016/j.desal.2024.117584.
[280] H. Kaur, G. Chauhan, S.S. Siwal, P. Hart, V.K. Thakur, Underpinning the role of Nanofiltration and other desalination Technologies for Water Remediation and Brine Valorization: mechanism and challenges for waste-to-wealth approach, Adv. Energy Sustainability Res. 2400070 (2024), https://doi.org/10.1002/aesr.202400070.
[281] Z. Triki, M.N. Bouaziz, M. Boumaza, Techno-economic and environmental analysis of an integrated solar vacuum membrane distillation system for the treatment of reverse osmosis desalination brine, Desalin. Water Treat. 83 (2017) 193–203, https://doi.org/10.5004/dwt.2017.20983.
[282] Y. Chen, R. Zheng, J. Wang, Y. Liu, Y. Wang, X.M. Li, T. He, Laminated PTFE membranes to enhance the performance in direct contact membrane distillation for high salinity solution, Desalination 424 (2017) 140–148, https://doi.org/10.1016/j.desal.2017.10.007.
[283] M. Rezaei, A. Alsaati, D.M. Warsinger, F. Hell, W.M. Samhaber, Long-running comparison of feed-water scaling in membrane distillation, Membranes (Basel) 10 (2020) 1–21, https://doi.org/10.3390/membranes10080173.
[284] Y. Chen, S. Yang, Z. Wang, M. Elimelech, Transforming membrane distillation to a membraneless fabric distillation for desalination, nature, Water 2 (2024) 52–61, https://doi.org/10.1038/s44221-023-00174-6.
[285] Z. Li, Y. Liu, J. Yan, K. Wang, B. Xie, Y. Hu, W. Kang, B. Cheng, Electrospun polyvinylidene fluoride/fluorinated acrylate copolymer tree-like nanofiber membrane with high flux and salt rejection ratio for direct contact membrane distillation, Desalination 466 (2019) 68–76, https://doi.org/10.1016/j.desal.2019.05.005.
[286] T. Tong, A.F. Wallace, S. Zhao, Z. Wang, Mineral scaling in membrane desalination: mechanisms, mitigation strategies, and feasibility of scaling-resistant membranes, J. Membr. Sci. 579 (2019) 52–69, https://doi.org/10.1016/j.memsci.2019.02.049.
[287] Applications - Aquastill, (n.d.). https://www.aquastill.nl/applications-of-aquastill-membrane-distillation/.
[288] H. Elcik, L. Fortunato, A. Alpatova, S. Soukane, J. Orfi, E. Ali, H. AlAnsary, T. O. Leiknes, N. Ghaffour, Multi-effect distillation brine treatment by membrane distillation: effect of antiscalant and antifoaming agents on membrane performance and scaling control, Desalination 493 (2020), https://doi.org/10.1016/j.desal.2020.114653.
[289] R. Schwantes, A. Cipollina, F. Gross, J. Koschikowski, D. Pfeifle, M. Rolletschek, V. Subiela, Membrane distillation: solar and waste heat driven demonstration plants for desalination, Desalination 323 (2013) 93–106, https://doi.org/10.1016/j.desal.2013.04.011.
[290] F. Banat, N. Jwaied, M. Rommel, J. Koschikowski, M. Wieghaus, Desalination by a "compact SMADES" autonomous solarpowered membrane distillation unit, Desalination 217 (2007) 29–37, https://doi.org/10.1016/j.desal.2006.11.028.
[291] A. Kullab, A. Martin, Membrane distillation and applications for water purification in thermal cogeneration plants, Sep. Purif. Technol. 76 (2011) 231–237, https://doi.org/10.1016/j.seppur.2010.09.028.
[292] E. Guillén-Burrieza, G. Zaragoza, S. Miralles-Cuevas, J. Blanco, Experimental evaluation of two pilot-scale membrane distillation modules used for solar desalination, J. Membr. Sci. 409–410 (2012) 264–275, https://doi.org/10.1016/j.memsci.2012.03.063.
[293] J. Ju, K. Fejjari, Y. Cheng, M. Liu, Z. Li, W. Kang, Y. Liao, Engineering hierarchically structured superhydrophobic PTFE/POSS nanofibrous membranes for membrane distillation, Desalination 486 (2020) 114481, https://doi.org/10.1016/j.desal.2020.114481.
[294] Z. Yan, Y. Jiang, L. Liu, Z. Li, X. Chen, M. Xia, G. Fan, A. Ding, Membrane distillation for wastewater treatment: a mini review, Water (Switzerland) 13 (2021), https://doi.org/10.3390/w13243480.
[295] S. Adham, A. Hussain, J.M. Matar, R. Dores, A. Janson, Application of membrane distillation for desalting brines from thermal desalination plants, DES 314 (2013) 101–108, https://doi.org/10.1016/j.desal.2013.01.003.
[296] J. Minier-Matar, A. Hussain, A. Janson, F. Benyahia, S. Adham, Field evaluation of membrane distillation technologies for desalination of highly saline brines, Desalination 351 (2014) 101–108, https://doi.org/10.1016/j.desal.2014.07.027.
[297] R. Schwantes, L. Bauer, K. Chavan, D. Dücker, C. Felsmann, J. Pfafferott, Air gap membrane distillation for hypersaline brine concentration: operational analysis of a full-scale module–new strategies for wetting mitigation, Desalination 444 (2018) 13–25, https://doi.org/10.1016/j.desal.2018.06.012.
[298] K. Rajwade, A.C. Barrios, S. Garcia-Segura, F. Perreault, Pore wetting in membrane distillation treatment of municipal wastewater desalination brine and its mitigation by foam fractionation, Chemosphere 257 (2020) 127214, https://doi.org/10.1016/j.chemosphere.2020.127214.
[299] H.W. Chung, J. Swaminathan, D.M. Warsinger, J.H. Lienhard V, Multistage vacuum membrane distillation (MSVMD) systems for high salinity applications, J. Membr. Sci. 497 (2016) 128–141, https://doi.org/10.1016/j.memsci.2015.09.009.
[300] A. Deshmukh, C. Boo, V. Karanikola, S. Lin, A.P. Straub, T. Tong, D.M. Warsinger, M. Elimelech, Membrane distillation at the water-energy nexus: limits, opportunities, and challenges, Energy Environ. Sci. 11 (2018) 1177–1196, https://doi.org/10.1039/c8ee00291f.
[301] Z. Yan, F. Qu, H. Liang, H. Yu, H. Pang, H. Rong, G. Fan, B. Van der Bruggen, Effect of biopolymers and humic substances on gypsum scaling and membrane wetting during membrane distillation, J. Membr. Sci. 617 (2021) 118638, https://doi.org/10.1016/j.memsci.2020.118638.
[302] Y. Choi, G. Naidu, S. Jeong, S. Vigneswaran, S. Lee, R. Wang, A.G. Fane, Experimental comparison of submerged membrane distillation configurations for concentrated brine treatment, Desalination 420 (2017) 54–62, https://doi.org/10.1016/j.desal.2017.06.024.
[303] A. Politano, P. Argurio, G. Di Profio, V. Sanna, A. Cupolillo, S. Chakraborty, H. A. Arafat, E. Curcio, Photothermal Membrane Distillation for Seawater Desalination, 2017, pp. 1–6, https://doi.org/10.1002/adma.201603504.
[304] M.O. Mavukkandy, C.M. Chabib, I. Mustafa, A. Al Ghaferi, F. AlMarzooqi, Brine management in desalination industry: from waste to resources generation, Desalination 472 (2019) 114187, https://doi.org/10.1016/j.desal.2019.114187.
[305] E. Ali, J. Orfi, A. Najib, J. Saleh, Enhancement of brackish water desalination using hybrid membrane distillation and reverse osmosis systems, PLoS One 13 (2018) 1–18, https://doi.org/10.1371/journal.pone.0205012.
[306] G. Naidu, S. Jeong, M.A.H. Johir, A.G. Fane, J. Kandasamy, S. Vigneswaran, Rubidium extraction from seawater brine by an integrated membrane distillation-selective sorption system, Water Res. 123 (2017) 321–331, https://doi.org/10.1016/j.watres.2017.06.078.
[307] J. Mericq, S. Laborie, C. Cabassud, Vacuum Membrane Distillation for an Integrated Seawater Desalination Process 9, 2009, p. 2009, https://doi.org/10.5004/dwt.2009.859.
[308] C.A. Quist-Jensen, F. Macedonio, E. Drioli, Integrated membrane desalination systems with membrane crystallization units for resource recovery: a new approach for mining from the sea, Crystals (Basel) 6 (2016), https://doi.org/10.3390/cryst6040036.
[309] X. Zhang, R. Koirala, B. Pramanik, L. Fan, Y. Zhang, A. Date, V. Jegatheesan, Performance of membrane distillation assisted crystallization and crystal characteristics for resource recovery from desalination brine, Desalination 574 (2024) 117244, https://doi.org/10.1016/j.desal.2023.117244.
[310] F. Macedonio, A. Criscuoli, L. Gzara, M. Albeirutty, E. Drioli, Water and salts recovery from desalination brines: An exergy evaluation, J. Environ. Chem. Eng. 9 (2021) 105884, https://doi.org/10.1016/j.jece.2021.105884.
[311] A. Cipollina, G.D.M. Micale, L. Rizzuti, Seawater Desalin. Convent. Renew. Energy Process. (2006), https://doi.org/10.2174/9781608052851106010l.
[312] T. Altmann, J. Robert, A. Bouma, J. Swaminathan, J.H. Lienhard, Primary energy and exergy of desalination technologies in a power-water cogeneration scheme, Appl. Energy 252 (2019) 113319, https://doi.org/10.1016/j.apenergy.2019.113319.
[313] H. El-Dessouky, I. Alatiqi, S. Bingulac, H. Ettouney, Steady-state analysis of the multiple effect evaporation desalination process, Chem. Eng. Technol. 21 (1998) 437–451, https://doi.org/10.1002/(SICI)1521-4125(199805)21:5<437::AID-CEAT437>3.0.CO;2-D.
[314] A.S. Stillwell, M.E. Webber, Predicting the specific energy consumption of reverse osmosis desalination, Water (Switzerland) 8 (2016) 1–18, https://doi.org/10.3390/w8120601.
[315] A.M. Mahmoud, K. Bamardouf, A. Al Ghamdi, S. Ahmed, Pilot plant evaluation of 95°C TBT MED-TVC desalination technology, Desalin. Water Treat. 259 (2022) 244–251, https://doi.org/10.5004/dwt.2022.28076.
[316] H.W. Chung, K.G. Nayar, J. Swaminathan, K.M. Chehayeb, J.H. Lienhard V, Thermodynamic analysis of brine management methods: zero-discharge desalination and salinity-gradient power production, Desalination 404 (2017) 291–303, https://doi.org/10.1016/j.desal.2016.11.022.
[317] G.P. Thiel, E.W. Tow, L.D. Banchik, H.W. Chung, J.H. Lienhard V, Energy consumption in desalinating produced water from shale oil and gas extraction, Desalination 366 (2015) 94–112, https://doi.org/10.1016/j.desal.2014.12.038.
[318] D. Xevgenos, A. Vidalis, K. Moustakas, D. Malamis, M. Loizidou, Sustainable management of brine effluent from desalination plants: the SOL-BRINE system, Desalin. Water Treat. 53 (2015) 3151–3160, https://doi.org/10.1080/19443994.2014.933621.
[319] Q. Chen, M. Burhan, M.W. Shahzad, D. Ybyraiymkul, F.H. Akhtar, Y. Li, K.C. Ng, A zero liquid discharge system integrating multi-effect distillation and evaporative crystallization for desalination brine treatment, Desalination 502 (2021) 114928, https://doi.org/10.1016/j.desal.2020.114928.
[320] G. Scelfo, A. Trezzi, F. Vassallo, A. Cipollina, V. Landi, C. Xenogianni, A. Tamburini, D. Xevgenos, G. Micale, Demonstration of ultra-high-water recovery and brine concentration in a prototype evaporation unit: towards zero liquid discharge desalination, Sep. Purif. Technol. 354 (2025) 129427, https://doi.org/10.1016/j.seppur.2024.129427.
[321] T. Tong, M. Elimelech, The global rise of zero liquid discharge for wastewater management: drivers, technologies, and future directions, Environ. Sci. Technol. 50 (2016) 6846–6855, https://doi.org/10.1021/acs.est.6b01000.
[322] J.H. Imholze, H. Glade, Corrosion-resistant polymer composite tubes with enhanced thermal conductivity for heat exchangers, Inventions 9 (2024), https://doi.org/10.3390/inventions9050111.
[323] M. Mickley, Survey of High-Recovery and Zero Liquid Discharge Technologies for Water Utilities, 2008.
[324] D.L. Shaffer, L.H. Arias Chavez, M. Ben-Sasson, S. Romero-Vargas Castrillón, N. Y. Yip, M. Elimelech, Desalination and reuse of high-salinity shale gas produced water: drivers, technologies, and future directions, Environ. Sci. Technol. 47 (2013) 9569–9583, https://doi.org/10.1021/es401966e.
[325] I.S. Al-Mutaz, Msf challenges and survivals, Desalin. Water Treat. 177 (2020) 14–22, https://doi.org/10.5004/dwt.2020.24908.
[326] J. Sikandar, S. Ismail, U. Aswalekar, K. Vishwanath, Theoretical and experimental investigation of a pilot-scale solar air-heated humidification dehumidification desalination system, Sol. Energy 285 (2025) 113122, https://doi.org/10.1016/j.solener.2024.113122.

[327] M.A. Younis, M.A. Darwish, F. Juwayhel, Experimental and theoretical study of a humidification-dehumidification desalting system 94, 1993, pp. 11–24.
[328] I. Nabil, A.M. Abdalla, T.M. Mansour, A.I. Shehata, M.M.K. Dawood, Salinity impacts on humidification dehumidification (HDH) desalination systems: review, Environ. Sci. Pollut. Res. Int. 31 (2024) 1907–1925, https://doi.org/10.1007/s11356-023-31327-5.
[329] K. Quoc, C. Hiep, A. Quoc, Optimization of mass flow rate ratio of water and air in humidification – dehumidification desalination systems, Desalin. Water Treat. 246 (2022) 82–91, https://doi.org/10.5004/dwt.2022.28034.
[330] J.S. Shaikh, S. Ismail, Performance evaluation of a solar humidification dehumidification desalination system employing a multistage bubble column dehumidifier, Sol. Energy 263 (2023) 111933, https://doi.org/10.1016/j.solener.2023.111933.
[331] M.T. Ghazal, U. Atikol, F. Egelioglu, An experimental study of a solar humidifier for HDD systems, Energy Convers. Manag. 82 (2014) 250–258, https://doi.org/10.1016/j.enconman.2014.03.019.
[332] A.S. Nafey, Solar Desalination Using Humidification – Dehumidification Part II. An Experimental Investigation 45, 2004, pp. 1263–1277, https://doi.org/10.1016/S0196-8904(03)00152-3.
[333] A. Eslamimanesh, M.S. Hatamipour, Economical study of a small-scale direct contact humidification – dehumidification desalination plant 250, 2010, pp. 203–207, https://doi.org/10.1016/j.desal.2008.11.015.
[334] Y. Elhenawy, M. Bassyouni, K. Fouad, A. Marni, M.A.E. Abu-zeid, T. Majozi, Experimental and numerical simulation of solar membrane distillation and humidification – dehumidification water desalination system direct contact membrane distillation sweep gas membrane distillation, Renew. Energy 215 (2023) 118915, https://doi.org/10.1016/j.renene.2023.118915.
[335] Q. Chen, F.H. Akhtar, M. Burhan, K. M, K.C. Ng, A novel zero-liquid discharge desalination system based on the humidification-dehumidification process: a preliminary study, Water Res. 207 (2021) 117794, https://doi.org/10.1016/j.watres.2021.117794.
[336] O. Shamet, D.U. Lawal, S.M. Alawad, M. Antar, M. Zubair, I.B. Mansir, I. H. Aljundi, Multi-stage humidification – dehumidification system integrated with a crystallizer for zero liquid discharge of desalination brine, Energy Convers. Manag. 307 (2024) 118340, https://doi.org/10.1016/j.enconman.2024.118340.
[337] A. Panagopoulos, K.J. Haralambous, M. Loizidou, Desalination brine disposal methods and treatment technologies - a review, Sci. Total Environ. 693 (2019) 133545, https://doi.org/10.1016/j.scitotenv.2019.07.351.
[338] X. Zhang, W. Zhao, Y. Zhang, V. Jegatheesan, A review of resource recovery from seawater desalination brine, Rev. Environ. Sci. Biotechnol. 20 (2021) 333–361, https://doi.org/10.1007/s11157-021-09570-4.
[339] S. Marinova, L. Roche, A. Link, M. Finkbeiner, Water footprint of battery-grade lithium production in the Salar de Atacama, Chile, J. Clean Prod. 487 (2025) 144635, https://doi.org/10.1016/j.jclepro.2024.144635.
[340] A. Ravizky, N. Nadav, Salt production by the evaporation of SWRO brine in Eilat: a success story, Desalination 205 (2007) 374–379, https://doi.org/10.1016/j.desal.2006.03.559.
[341] A. Campione, M. Salem, S. Chamam, F. Vicari, R. Cucchiara, A. Hannachi, D. Pastorelli, A. Cipollina, Boosting sustainable water production by upstream integration of desalination with saltworks in the Mediterranean region, Desalin. Water Treat. 317 (2024) 100134, https://doi.org/10.1016/j.dwt.2024.100134.
[342] D.S. Ayou, H.M. Ega, A. Coronas, A feasibility study of a small-scale photovoltaic-powered reverse osmosis desalination plant for potable water and salt production in Madura Island : a techno-economic evaluation, Thermal Sci. Eng. Progr. 35 (2022) 101450, https://doi.org/10.1016/j.tsep.2022.101450.
[343] L. Katzir, Y. Volkmann, N. Daltrophe, E. Korngold, R. Mesalem, Y. Oren, J. Gilron, WAIV - wind aided intensified evaporation for brine volume reduction and generating mineral byproducts, Desalin. Water Treat. 13 (2010) 63–73, https://doi.org/10.5004/dwt.2010.772.
[344] A. Kumar, V.V.N. Kishore, Construction and operational experience of a 6000 M2 solar pond at kutch, India, Sol. Energy 65 (1999) 237–249, https://doi.org/10.1016/S0038-092X(98)00134-0.
[345] A. Akbarzadeh, P. Johnson, R. Singh, Examining potential benefits of combining a chimney with a salinity gradient solar pond for production of power in salt affected areas, Sol. Energy 83 (2009) 1345–1359, https://doi.org/10.1016/j.solener.2009.02.010.
[346] C. Chen, Y. Jiang, Z. Ye, Y. Yang, L. Hou, Sustainably integrating desalination with solar power to overcome future freshwater scarcity in China, Global Energy Interconnect. 2 (2019) 98–113, https://doi.org/10.1016/j.gloei.2019.07.009.
[347] M. Farrokhi, M.R. Jaefarzadeh, M. Bawahab, H. Faqeha, A. Akbarzadeh, Integration of a solar pond in a salt work in Sabzevar in Northeast Iran, Sol. Energy 244 (2022) 115–125, https://doi.org/10.1016/j.solener.2022.08.032.
[348] A. Alcaraz, M. Montalà, J.L. Cortina, A. Akbarzadeh, C. Aladjem, A. Farran, Design, construction, and operation of the first industrial salinity-gradient solar pond in Europe: An efficiency analysis perspective, Sol. Energy 164 (2018) 316–326, https://doi.org/10.1016/j.solener.2018.02.053.
[349] A. Alcaraz, M. Montalà, C. Valderrama, J.L. Cortina, A. Akbarzadeh, A. Farran, Increasing the storage capacity of a solar pond by using solar thermal collectors : heat extraction and heat supply processes using in-pond heat exchangers, Sol. Energy 171 (2018) 112–121, https://doi.org/10.1016/j.solener.2018.06.061.
[350] O.V. Mbelu, A.M. Adeyinka, D.I. Yahya, Y.B. Adediji, H. Njoku, Advances in solar pond technology and prospects of efficiency improvement methods, Sustain. Energy Res. 11 (2024), https://doi.org/10.1186/s40807-024-00111-5.
[351] A. Abbassi, H.B. Mahood, A.N. Campbell, Regeneration of dimethyl ether as a draw solute in forward osmosis by utilising thermal energy from a solar pond, Desalination 415 (2017) 104–114, https://doi.org/10.1016/j.desal.2017.03.034.
[352] A. Al-othman, M. Tawalbeh, M. El, H. Assad, T. Alkayyali, A. Eisa, Novel multi-stage flash (MSF) desalination plant driven by parabolic trough collectors and a solar pond : a simulation study in UAE, Desalination 443 (2018) 237–244, https://doi.org/10.1016/j.desal.2018.06.005.
[353] K. Manzoor, S.J. Khan, Y. Jamal, M.A. Shahzad, Heat extraction and brine management from salinity gradient solar pond and membrane distillation, Chem. Eng. Res. Des. 118 (2017) 226–237, https://doi.org/10.1016/j.cherd.2016.12.017.
[354] A.H. Sayer, H. Al-hussaini, A.N. Campbell, New comprehensive investigation on the feasibility of the gel solar pond and a comparison with the salinity gradient solar pond, Appl. Therm. Eng. 130 (2018) 672–683, https://doi.org/10.1016/j.applthermaleng.2017.11.056.
[355] A. Abdulsalam, A. Idris, T.A. Mohamed, A. Ahsan, An integrated technique using solar and evaporation ponds for effective brine disposal management, Int. J. Sustain. Energy 36 (2017) 914–925, https://doi.org/10.1080/14786451.2015.1135923.
[356] M. Khan, M.A. Al-ghouti, DPSIR framework and sustainable approaches of brine management from seawater desalination plants in Qatar, J. Clean. Prod. 319 (2021) 128485, https://doi.org/10.1016/j.jclepro.2021.128485.
[357] N. Afrasiabi, E. Shahbazali, Ro brine treatment and disposal methods, Desalin. Water Treat. 35 (2011) 39–53, https://doi.org/10.5004/dwt.2011.3128.
[358] X. Luo, X. Li, C. Wei, Z. Deng, Y. Liu, M. Li, S. Zheng, X. Huang, Recovery of NaCl and Na2SO4 from high salinity brine by purification and evaporation, Desalination 530 (2022) 115631, https://doi.org/10.1016/j.desal.2022.115631.
[359] K. Poirier, N. Al Mhanna, K. Patchigolla, Techno-economic analysis of brine treatment by multi-crystallization separation process for zero liquid discharge, Separations 9 (2022), https://doi.org/10.3390/separations9100295.
[360] D.G. Randall, J. Nathoo, A succinct review of the treatment of reverse osmosis brines using freeze crystallization, journal of water, Process. Eng. 8 (2015) 186–194, https://doi.org/10.1016/j.jwpe.2015.10.005.
[361] A.E. Lewis, J. Chivavava, L.A. Motsepe, B. Nxiwa, K. Netshiomvani, N. Zimu, Novel materials and crystallizer design for freeze concentration 20, 2023, https://doi.org/10.1016/j.sciaf.2023.e01675.
[362] D.G. Randall, J. Nathoo, C. Town, C. Town, S. Africa, Resource recovery by freezing: A thermodynamic comparison between a reverse osmosis brine, seawater and stored urine, J. Water Process. Eng. 26 (2018) 242–249, https://doi.org/10.1016/j.jwpe.2018.10.020.
[363] F. van der Ham, M.M. Seckler, G.J. Witkamp, Eutectic freeze crystallization in a new apparatus: the cooled disk column crystallizer, Chem. Eng. Process. Process Intensif. 43 (2004) 161–167, https://doi.org/10.1016/S0255-2701(03)00018-7.
[364] R.J.C. Vaessen, B.J.H. Janse, M.M. Seckler, G.J. Witkamp, EVALUATION OF THE PERFORMANCE OF A NEWLY DEVELOPED EUTECTIC FREEZE CRYSTALLIZER Scraped Cooled Wall Crystallizer 81, 2003.
[365] L. Wang, Z. Liu, J. Xu, K. Wang, Q. Wang, G. Liu, Conical solar-thermo-radiative evaporator for sustainable desalination and salt recovery, Desalination 567 (2023) 116993, https://doi.org/10.1016/j.desal.2023.116993.
[366] A. Bouazza, S. Ait, A. Faddouli, K. Khaless, R. Benhida, Kainite crystallization from RO bittern : a novel approach using discontinuous evaporation, Desalination 582 (2024) 117652, https://doi.org/10.1016/j.desal.2024.117652.
[367] S. Santoro, M. Aquino, D. Han Seo, T. Van Der Laan, M. Lee, J. Sung Yun, M. Jun Park, A. Bendavid, H. Kyong Shon, A. Halil Avci, E. Curcio, Dimensionally controlled graphene-based surfaces for photothermal membrane crystallization, J. Colloid Interface Sci. 623 (2022) 607–616, https://doi.org/10.1016/j.jcis.2022.05.062.
[368] M.A. Caraballo, T.S. Rötting, F. Macías, J.M. Nieto, C. Ayora, Field multi-step limestone and MgO passive system to treat acid mine drainage with high metal concentrations, Appl. Geochem. 24 (2009) 2301–2311, https://doi.org/10.1016/j.apgeochem.2009.09.007.
[369] F. Vassallo, C. Morgante, G. Battaglia, D. La Corte, M. Micari, A. Cipollina, A. Tamburini, G. Micale, A simulation tool for ion exchange membrane crystallization of magnesium hydroxide from waste brine, Chem. Eng. Res. Des. 173 (2021) 193–205, https://doi.org/10.1016/j.cherd.2021.07.008.
[370] C. Morgante, F. Vassallo, G. Battaglia, A. Cipollina, F. Vicari, A. Tamburini, G. Micale, Influence of operational strategies for the recovery of magnesium hydroxide from brines at a pilot scale, Ind. Eng. Chem. Res. (2022), https://doi.org/10.1021/acs.iecr.2c02935.
[371] European Commission, Innovative Marine Magnesium Minerals for a Circular, Safe and Sustainable Chemicals Production, https://ec.europa.eu/info/funding-tenders/opportunities/portal/screen/opportunities/projects-details/43252405/101147407, 2025.
[372] M.H. Nielsen, C. Quist-Jensen, A. Ali, Development of ceramic membranes for resource recovery from brine through percrystallization, Resour. Conserv. Recycl. 189 (2023) 106768, https://doi.org/10.1016/j.resconrec.2022.106768.
[373] Z.H. Foo, C. Stetson, E. Dach, A. Deshmukh, H. Lee, A.K. Menon, R. Prasher, N. Y. Yip, J.H. Lienhard, A.D. Wilson, Solvent-driven aqueous separations for hypersaline brine concentration and resource recovery, Trends Chem. 4 (2022) 1078–1093, https://doi.org/10.1016/j.trechm.2022.09.004.
[374] D. Hasson, M. Shmulevsky-Lisitsin, R. Semiat, H. Shemer, High recovery MSF desalination process, Desalin. Water Treat. 106 (2018) 1–10, https://doi.org/10.5004/dwt.2018.22127.
[375] I. Mohammed, S.W. Svenningsen, F.S. Kamounah, T. Chen, M. Pittelkow, T. I. Sølling, M. Mahmoud, Calcium sulfate scale: a review of state-of-the-art, Geoenergy Sci. Eng. 242 (2024), https://doi.org/10.1016/j.geoen.2024.213228.
[376] A. Antony, J.H. Low, S. Gray, A.E. Childress, P. Le-Clech, G. Leslie, Scale formation and control in high pressure membrane water treatment systems: a

review, J. Membr. Sci. 383 (2011) 1–16, https://doi.org/10.1016/j.memsci.2011.08.054.
[377] E. Drioli, E. Curcio, A. Criscuoli, G. Di Di Profio, Integrated system for recovery of CaCO3, NaCl and MgSO 4·7H2O from nanofiltration retentate, J. Membr. Sci. 239 (2004) 27–38, https://doi.org/10.1016/j.memsci.2003.09.028.
[378] S. Casas, C. Aladjem, E. Larrotcha, O. Gibert, C. Valderrama, J.L. Cortina, Valorisation of ca and Mg by-products from mining and seawater desalination brines for water treatment applications, J. Chem. Technol. Biotechnol. 89 (2014) 872–883, https://doi.org/10.1002/jctb.4326.
[379] G.M. Ayoub, R.M. Zayyat, M. Al-Hindi, Precipitation softening: a pretreatment process for seawater desalination, Environ. Sci. Pollut. Res. 21 (2014) 2876–2887, https://doi.org/10.1007/s11356-013-2237-1.
[380] R. Molinari, A.H. Avci, P. Argurio, E. Curcio, S. Meca, M. Plà-Castellana, J. L. Cortina, Selective precipitation of calcium ion from seawater desalination reverse osmosis brine, J. Clean. Prod. 328 (2021), https://doi.org/10.1016/j.jclepro.2021.129645.
[381] W. Wang, M. Hu, Y. Zheng, P. Wang, C. Ma, CO2 fixation in Ca2+-/Mg2+-rich aqueous solutions through enhanced carbonate precipitation, Ind. Eng. Chem. Res. 50 (2011) 8333–8339, https://doi.org/10.1021/ie1025419.
[382] Y. Choi, G. Naidu, S. Jeong, S. Lee, S. Vigneswaran, Effect of chemical and physical factors on the crystallization of calcium sulfate in seawater reverse osmosis brine, Desalination 426 (2018) 78–87, https://doi.org/10.1016/j.desal.2017.10.037.
[383] Y. Zhang, R.A. Dawe, Influence of Mg2+ on the kinetics of calcite precipitation and calcite crystal morphology, Chem. Geol. 163 (2000) 129–138, https://doi.org/10.1016/S0009-2541(99)00097-2.
[384] M.H. Sorour, H.A. Hani, H.F. Shaalan, G.A. Al-Bazedi, Schemes for salt recovery from seawater and RO brines using chemical precipitation, desalination, Desalin. Water Treat. 55 (2015) 2398–2407, https://doi.org/10.1080/19443994.2014.946720.
[385] M.H. Sorour, H.A. Hani, H.F. Shaalan, Separation of calcium and magnesium using dual precipitation/chelation scheme from saline solutions, desalination, Desalin. Water Treat. 57 (2016) 22818–22823, https://doi.org/10.1080/19443994.2015.1114170.
[386] R. Molinari, A.H. Avci, E. Curcio, D.S. Domene, C. Villa González, J.J.E. Gallart, P. Argurio, Selective calcium removal at near-ambient temperature in a multimineral recovery process from seawater reverse osmosis synthetic brine and ex ante life cycle assessment, Water (Switzerland) 16 (2024), https://doi.org/10.3390/w16050667.
[387] K.Y. Chang, N.N.N. Mahasti, Y.H. Huang, Brine treatment using fluidized bed homogeneous crystallization technology for the simultaneous recovery of calcium and magnesium as dolomite-like granules, J. Environ. Chem. Eng. 12 (2024) 113792, https://doi.org/10.1016/j.jece.2024.113792.
[388] I. Rom, S. Klas, Kinetics of CaCO3 precipitation in seeded aeration softening of brackish water desalination concentrate, Chemosphere 260 (2020) 127527, https://doi.org/10.1016/j.chemosphere.2020.127527.
[389] H. Cherif, A. Labbaoui, H. Risse, H. Boughanmi, H. Elfil, Magnesium recovery from brackish water desalination brine and valorization in fertilizer production, J. Environ. Chem. Eng. 12 (2024) 113799, https://doi.org/10.1016/j.jece.2024.113799.
[390] N. Mahmud, M.H. Ibrahim, D.V. Fraga Alvarez, D.V. Esposito, M.H. El-Naas, Evaluation of parameters controlling calcium recovery and CO2 uptake from desalination reject brine: An optimization approach, J. Clean. Prod. 369 (2022) 133405, https://doi.org/10.1016/j.jclepro.2022.133405.
[391] D. Almasri, K.A. Mahmoud, A. Abdel-Wahab, Two-stage sulfate removal from reject brine in inland desalination with zero-liquid discharge, Desalination 362 (2015) 52–58, https://doi.org/10.1016/j.desal.2015.02.008.
[392] K.J. Howe, D.W. Hand, J.C. Crittenden, R.R. Trussell, G. Tchobanoglous, Chapter 10 - Adsorption and Ion Exchange, in: Principles of Water Treatment, John Wiley & Sons, Inc., Hoboken, 2012, pp. 369–436.
[393] A.A. Zagorodni, I.I. Appendix, Definitions, in: Ion Exchange Materials: Properties and Applications, Elsevier, Oxford, 2007, pp. 421–436, https://doi.org/10.1016/B978-008044552-6/50022-8.
[394] Ecolab, Industrial Water Softeners and Ion Exchange, (n.d.). https://www.ecolab.com/nalco-water/offerings/industrial-water-softeners-and-ion-exchange.
[395] Lanxess, Brine purification with finely dispersed ion exchange resins, (n.d.). https://lanxess.com/en/products-and-brands/brands/lewatit/case-studies-and-stories/brine-purification-with-finely-dispersed-ixr.
[396] N. Najid, S. Kouzbour, A. Ruiz-Garcia, S. Fellaou, B. Gourich, Y. Stiriba, Comparison analysis of different technologies for the removal of boron from seawater: a review, J. Environ. Chem. Eng. 9 (2021) 105133, https://doi.org/10.1016/j.jece.2021.105133.
[397] S. Jung, M.J. Kim, Optimal conditions for recovering boron from seawater using boron selective resins, Korean J. Chem. Eng. 33 (2016) 2411–2417, https://doi.org/10.1007/s11814-016-0096-4.
[398] S. Hameed, H.A. Awad, R.A.H. Al-Uqaily, Boron removal from seawater using adsorption and ion exchange techniques, Ecol. Environ. Conserv. 26 (2020) 480–487.
[399] M. Figueira, M. Reig, M. Fernández de Labastida, J.L. Cortina, C. Valderrama, Boron recovery from desalination seawater brines by selective ion exchange resins, J. Environ. Manag. 314 (2022), https://doi.org/10.1016/j.jenvman.2022.114984.
[400] V. Vallès, M.F. de Labastida, J. López, J.L. Cortina, Selective recovery of boron, cobalt, gallium and germanium from seawater solar saltworks brines using N-methylglucamine sorbents: column operation performance, Sci. Total Environ. 923 (2024), https://doi.org/10.1016/j.scitotenv.2024.171438.
[401] L. Bonin, D. Deduytsche, M. Wolthers, V. Flexer, K. Rabaey, Boron extraction using selective ion exchange resins enables effective magnesium recovery from lithium rich brines with minimal lithium loss, Sep. Purif. Technol. 275 (2021), https://doi.org/10.1016/j.seppur.2021.119177.
[402] J. López, G. Battaglia, D. Lupo, M. Fernández de Labastida, V. Vallès, J. Luis Cortina, A. Cipollina, G. Micale, Integration of ion-exchange and crystallisation processes to recover boric acid and magnesium hydroxide from saltworks bitterns, Sep. Purif. Technol. 354 (2025) 129532, https://doi.org/10.1016/j.seppur.2024.129532.
[403] H. Barbosa, A.M.V.M. Soares, E. Pereira, R. Freitas, Lithium: a review on concentrations and impacts in marine and coastal systems, Sci. Total Environ. 857 (2023) 159374, https://doi.org/10.1016/j.scitotenv.2022.159374.
[404] Q.H. Zhang, S.P. Li, S.Y. Sun, X.S. Yin, J.G. Yu, LiMn2O4 spinel direct synthesis and lithium ion selective adsorption, Chem. Eng. Sci. 65 (2010) 169–173, https://doi.org/10.1016/j.ces.2009.06.045.
[405] L. Liu, H. Zhang, Y. Zhang, D. Cao, X. Zhao, Lithium extraction from seawater by manganese oxide ion sieve MnO2·0.5H2O, Colloids Surf. A Physicochem. Eng. Asp. 468 (2015) 280–284, https://doi.org/10.1016/j.colsurfa.2014.12.025.
[406] G. Xiao, K. Tong, L. Zhou, J. Xiao, S. Sun, P. Li, J. Yu, Adsorption and desorption behavior of lithium ion in spherical PVC-MnO 2 ion sieve, Ind. Eng. Chem. Res. 51 (2012) 10921–10929, https://doi.org/10.1021/ie300087s.
[407] H.J. Park, N. Singhal, E.H. Jho, Lithium sorption properties of HMnO in seawater and wastewater, Water Res. 87 (2015) 320–327, https://doi.org/10.1016/j.watres.2015.09.032.
[408] L. Chen, X. Xu, J. Song, X. Zhu, Z. Qi, Microwave assisted hydrothermal synthesis of MnO2·0.5H2O ion-sieve for lithium ion selective adsorption, Separ. Sci. Technol. (Philadelphia) 51 (2016) 874–882, https://doi.org/10.1080/01496395.2015.1117100.
[409] K. Yoshizuka, S. Nishihama, M. Takano, S. Asano, Lithium recovery from brines with novel λ-MnO2 adsorbent synthesized by hydrometallurgical method, Solvent Extract. Ion Exc. 39 (2021) 604–621, https://doi.org/10.1080/07366299.2021.1876443.
[410] G. Naidu, P. Loganathan, S. Jeong, M.A.H. Johir, V.H.P. To, J. Kandasamy, S. Vigneswaran, Rubidium extraction using an organic polymer encapsulated potassium copper hexacyanoferrate sorbent, Chem. Eng. J. 306 (2016) 31–42, https://doi.org/10.1016/j.cej.2016.07.038.
[411] G. Naidu, S. Jeong, Y. Choi, M.H. Song, U. Oyunchuluun, S. Vigneswaran, Valuable rubidium extraction from potassium reduced seawater brine, J. Clean. Prod. 174 (2018) 1079–1088, https://doi.org/10.1016/j.jclepro.2017.11.042.
[412] D. Quyet Truong, Y. Choo, N. Akther, S. Roobavannan, A. Norouzi, V. Gupta, M. Blumenstein, T. Vinh Nguyen, G. Naidu, Selective rubidium recovery from seawater with metal-organic framework incorporated potassium cobalt hexacyanoferrate nanomaterial, Chem. Eng. J. 454 (2023) 140107, https://doi.org/10.1016/j.cej.2022.140107.
[413] J. Bok-Badura, A. Kazek-Kesik, K. Karon, A. Jakóbik-Kolon, Highly efficient copper hexacyanoferrate-embedded pectin sorbent for radioactive cesium ions removal, Water Resour. Ind. 28 (2022), https://doi.org/10.1016/j.wri.2022.100190.
[414] S.R.H. Vanderheyden, J. Yperman, R. Carleer, S. Schreurs, Enhanced cesium removal from real matrices by nickel-hexacyanoferrate modified activated carbons, Chemosphere 202 (2018) 569–575, https://doi.org/10.1016/j.chemosphere.2018.03.096.
[415] S. Khandaker, M. Fujibayashi, T. Kuba, Innovative potassium hexacyanoferrate intercalated into layered double hydroxide adsorbent for efficient cesium removal from seawater, Sep. Purif. Technol. 354 (2025) 128984, https://doi.org/10.1016/j.seppur.2024.128984.
[416] O. Gibert, C. Valderrama, M. Peterkóva, J.L. Cortina, Evaluation of selective sorbents for the extraction of valuable metal ions (Cs, Rb, Li, U) from reverse osmosis rejected brine, Solvent Extr. Ion Exch. 28 (2010) 543–562, https://doi.org/10.1080/07366299.2010.480931.
[417] K. Suresh, M.S. Surendra Babu, P. Jagasia, Zirconium based metal-organic framework as highly efficient and acid-stable adsorbent for the rapid removal of Sr2+ and Cs+ from solution, Sep. Purif. Technol. 335 (2024) 126052, https://doi.org/10.1016/j.seppur.2023.126052.
[418] Y. Kakutani, P. Weerachawanasak, Y. Hirata, M. Sano, T. Suzuki, T. Miyake, Highly effective K-Merlinoite adsorbent for removal of Cs+ and Sr2+ in aqueous solution, RSC Adv. 7 (2017) 30919–30928, https://doi.org/10.1039/c7ra03867d.
[419] J. Ryu, S. Kim, H.J. Hong, J. Hong, M. Kim, T. Ryu, I.S. Park, K.S. Chung, J. S. Jang, B.G. Kim, Strontium ion (Sr2+) separation from seawater by hydrothermally structured titanate nanotubes: removal vs. recovery, Chem. Eng. J. 304 (2016) 503–510, https://doi.org/10.1016/j.cej.2016.06.131.
[420] E.E. Angino, G.K. Billings, N. Andersen, Observed variations in the strontium concentration of sea water, Chem. Geol. 1 (1966) 145–153, https://doi.org/10.1016/0009-2541(66)90013-1.
[421] H.J. Hong, J. Ryu, I.S. Park, T. Ryu, K.S. Chung, B.G. Kim, Investigation of the strontium (Sr(II)) adsorption of an alginate microsphere as a low-cost adsorbent for removal and recovery from seawater, J. Environ. Manag. 165 (2016) 263–270, https://doi.org/10.1016/j.jenvman.2015.09.040.
[422] W. Chouyyok, J.W. Pittman, M.G. Warner, K.M. Nell, D.C. Clubb, G.A. Gill, R. S. Addleman, Surface functionalized nanostructured ceramic sorbents for the effective collection and recovery of uranium from seawater, Dalton Trans. 45 (2016) 11312–11325, https://doi.org/10.1039/c6dt01318j.
[423] X. Zhu, L. Liu, Y. Wang, F. Ma, Y. Tian, H. Dong, C. Zhang, Phosphorylated hyper-crosslinked calix[4]arene for selective uranyl extraction from seawater, J. Water Process Eng. 50 (2022) 103321, https://doi.org/10.1016/j.jwpe.2022.103321.

[424] H. Wang, H. Yao, L. Chen, Z. Yu, L. Yang, C. Li, K. Shi, C. Li, S. Ma, Highly efficient capture of uranium from seawater by layered double hydroxide composite with benzamidoxime, Sci. Total Environ. 759 (2021) 143483, https://doi.org/10.1016/j.scitotenv.2020.143483.
[425] J. Zhu, Y. Luo, J. Liu, Q. Liu, J. Yu, J. Liu, R. Chen, R. Li, J. Wang, Effect of fiber surface functionalization on adsorption behavior of uranium from seawater desalination brine, Desalination 564 (2023) 116774, https://doi.org/10.1016/j.desal.2023.116774.
[426] T. Kanagasundaram, O. Murphy, M.N. Haji, J.J. Wilson, The recovery and separation of lithium by using solvent extraction methods, Coord. Chem. Rev. 509 (2024) 215727, https://doi.org/10.1016/j.ccr.2024.215727.
[427] K.C. Kim, N. Il Kim, T. Jiang, J.C. Kim, C.I. Kang, Boron recovery from salt lake brine, seawater, and wastewater – a review, Hydrometallurgy 218 (2023) 106062, https://doi.org/10.1016/j.hydromet.2023.106062.
[428] R. Zhu, S. Wang, C. Srinivasakannan, S. Li, S. Yin, L. Zhang, X. Jiang, G. Zhou, N. Zhang, Lithium extraction from salt lake brines with high magnesium/lithium ratio: a review, Environ. Chem. Lett. 21 (2023) 1611–1626, https://doi.org/10.1007/s10311-023-01571-9.
[429] S.K. Sharma, D.Q. Truong, J. Guo, A.K. An, G. Naidu, B.J. Deka, Recovery of rubidium from brine sources utilizing diverse separation technologies, Desalination 556 (2023) 116578, https://doi.org/10.1016/j.desal.2023.116578.
[430] J. Farahbakhsh, F. Arshadi, Z. Mofidi, M. Mohseni-Dargah, C. Kök, M. Assefi, A. Soozanipour, M. Zargar, M. Asadnia, Y. Boroumand, V. Presser, A. Razmjou, Direct lithium extraction: a new paradigm for lithium production and resource utilization, Desalination 575 (2024), https://doi.org/10.1016/j.desal.2023.117249.
[431] Q. Sun, H. Chen, J. Yu, Investigation on the Lithium extraction process with the TBP-FeCl3Solvent system using experimental and DFT methods, Ind. Eng. Chem. Res. 61 (2022) 4672–4682, https://doi.org/10.1021/acs.iecr.1c05072.
[432] Z. Li, K. Binnemans, Mechanism of ferric chloride facilitating efficient Lithium extraction from magnesium-rich brine with tri-n-butyl phosphate, Ind. Eng. Chem. Res. 60 (2021) 8538–8547, https://doi.org/10.1021/acs.iecr.1c01003.
[433] X. Yu, X. Fan, Y. Guo, T. Deng, Recovery of lithium from underground brine by multistage centrifugal extraction using tri-isobutyl phosphate, Sep. Purif. Technol. 211 (2019) 790–798, https://doi.org/10.1016/j.seppur.2018.10.054.
[434] Z. Zhou, J. Fan, X. Liu, Y. Hu, X. Wei, Y. Hu, W. Wang, Z. Ren, Recovery of lithium from salt-lake brines using solvent extraction with TBP as extractant and FeCl3 as co-extraction agent, Hydrometallurgy 191 (2020) 105244, https://doi.org/10.1016/j.hydromet.2019.105244.
[435] J. Hua, X. Ma, W. Ji, Q. Li, B. He, Z. Cui, X. Liang, F. Yan, J. Li, Unveiling the mechanism of liquid-liquid extraction separation of Li+/Mg2+ using tributyl phosphate/ionic liquid mixed solvents, J. Mol. Liq. 365 (2022) 120080, https://doi.org/10.1016/j.molliq.2022.120080.
[436] R. Bai, J. Wang, D. Wang, J. Cui, Y. Zhang, Recovery of lithium from high Mg/Li ratio salt-lake brines using ion-exchange with NaNTf2 and TBP, Hydrometallurgy 213 (2022) 105914, https://doi.org/10.1016/j.hydromet.2022.105914.
[437] H. Li, Y. Yue, X. Wang, D. Liu, An environmentally friendly lithium extraction system utilizing Cyanex 272 as iron-fixed reagent, Desalination 602 (2025) 118574, https://doi.org/10.1016/j.desal.2025.118574.
[438] Z. Li, K. Binnemans, Opposite selectivities of tri-n-butyl phosphate and Cyanex 923 in solvent extraction of lithium and magnesium, AICHE J. 67 (2021) 1–11, https://doi.org/10.1002/aic.17219.
[439] G.R. Harvianto, S.H. Kim, C.S. Ju, Solvent extraction and stripping of lithium ion from aqueous solution and its application to seawater, Rare Metals 35 (2016) 948–953, https://doi.org/10.1007/s12598-015-0453-1.
[440] L.Y. Yu, K.J. Wu, C.H. He, A two-step green liquid-liquid extraction strategy for selective lithium recovery and application to seawater, Hydrometallurgy 220 (2023) 106102, https://doi.org/10.1016/j.hydromet.2023.106102.
[441] E. Fernández-Escalante, R. Ibañez, M.F. San-Román, Selective lithium separation from desalination concentrates via the synergy of extractant mixtures, Desalination 556 (2023), https://doi.org/10.1016/j.desal.2023.116525.
[442] S. Raiguel, V.T. Nguyen, I. Reis Rodrigues, C. Deferm, S. Riaño, K. Binnemans, Recovery of Lithium from simulated Nanofiltration-treated seawater desalination brine using solvent extraction and selective precipitation, Solvent Extract. Ion Exc. 41 (2023) 425–448, https://doi.org/10.1080/07366299.2023.2206440.
[443] J. Guo, Y. Yang, X. Gao, J. Yu, Boron extraction from lithium-rich brine using mixed alcohols, Hydrometallurgy 197 (2020) 105477, https://doi.org/10.1016/j.hydromet.2020.105477.
[444] Y. Huang, H. Lu, S. Xie, C. Zhao, J. Dong, L. Xu, Y. Qin, C. Shi, X. Peng, Solvent extraction of boron from mildly alkaline salt lake brine in Tibet, China, RSC Adv. 15 (2025) 6342–6356, https://doi.org/10.1039/d4ra08859j.
[445] X. Peng, D. Shi, Y. Zhang, L. Zhang, L. Ji, L. Li, Recovery of boron from unacidified salt lake brine by solvent extraction with 2,2,4-trimethyl-1,3-pentanediol, J. Mol. Liq. 326 (2021) 115301, https://doi.org/10.1016/j.molliq.2021.115301.
[446] C.H. Lee, W.S. Chen, W.C. Chen, Circulation of boron resources from desalination brine through solvent extraction (TMPD/2-ethylhexanol with kerosene) and ionic-liquid extraction (ALiCy/kerosene) methods, Korean J. Chem. Eng. 40 (2023) 2480–2488, https://doi.org/10.1007/s11814-023-1533-9.
[447] X. Peng, L. Li, D. Shi, L. Zhang, H. Li, F. Nie, F. Song, Recovery of boric acid from salt lake brines by solvent extraction with 2-butyl-1-n-octanol, Hydrometallurgy 177 (2018) 161–167, https://doi.org/10.1016/j.hydromet.2018.03.013.
[448] Z. Xu, H. Su, J. Zhang, W. Liu, Z. Zhu, J. Wang, J. Chen, T. Qi, Recovery of boron from brines with high magnesium content by solvent extraction using aliphatic alcohol, RSC Adv. 11 (2021) 16096–16105, https://doi.org/10.1039/d1ra01906f.
[449] R. Zhang, Y. Xie, J. Song, L. Xing, D. Kong, X.M. Li, T. He, Extraction of boron from salt lake brine using 2-ethylhexanol, Hydrometallurgy 160 (2016) 129–136, https://doi.org/10.1016/j.hydromet.2016.01.001.
[450] R. Zhao, M. Huo, Q. Wei, X. Ren, Y. Zhu, A study on the coupling of Li+ and H3BO3 extraction and their mutual promotion mechanism, Desalination 593 (2025), https://doi.org/10.1016/j.desal.2024.118221.
[451] A. Bao, Q. Zhiqiang, Study on solvent extraction behavior of rubidium by T-baMBP-sulphonated kerosene system from salt Lake brine, J. Chem. Soc. Pak. 41 (2019) 1004–1013, https://doi.org/10.52568/000808/jcsp/41.06.2019.
[452] Z. Li, Y. Pranolo, Z. Zhu, C.Y. Cheng, Solvent extraction of cesium and rubidium from brine solutions using 4-tert-butyl-2-(α-methylbenzyl)-phenol, Hydrometallurgy 171 (2017) 1–7, https://doi.org/10.1016/j.hydromet.2017.03.007.
[453] S.M. Liu, H.H. Liu, Y.J. Huang, W.J. Yang, Solvent extraction of rubidium and cesium from salt lake brine with t-BAMBP-kerosene solution, Transact. Nonferrous Metals Soc. China (English Edition) 25 (2015) 329–334, https://doi.org/10.1016/S1003-6326(15)63608-1.
[454] J. Wang, D. Che, W. Qin, Extraction of rubidium by t-BAMBP in cyclohexane, Chin. J. Chem. Eng. 23 (2015) 1110–1113, https://doi.org/10.1016/j.cjche.2015.04.005.
[455] D. Pang, Z. Zhang, Y. Zhou, Z. Fu, Q. Li, Y. Zhang, G. Wang, Z. Jing, The process and mechanism for cesium and rubidium extraction with saponified 4-tert-butyl-2-(α-methylbenzyl) phenol, Chin. J. Chem. Eng. 46 (2022) 31–39, https://doi.org/10.1016/j.cjche.2021.07.001.
[456] W.S. Chen, C.H. Lee, Y.F. Chung, K.W. Tien, Y.J. Chen, Y.A. Chen, Recovery of rubidium and cesium resources from brine of desalination through t-BAMBP extraction, Metals (Basel) 10 (2020), https://doi.org/10.3390/met10050607.
[457] D. Huang, G. Ma, P. Lv, Q. Zhou, Extraction of rubidium ion from brine solutions by dicyclohexano-18-crown-6 / ionic liquid system, polish journal of, Chem. Technol. 25 (2023) 61–68, https://doi.org/10.2478/pjct-2023-0009.
[458] M. Simonnet, T. Sittel, P. Weßling, A. Geist, Cs extraction from chloride media by Calixarene crown-ethers, Energies (Basel) 15 (2022), https://doi.org/10.3390/en15207724.
[459] V. Vallès, M.F. de Labastida, O. Gibert, A. Leskinen, R.T. Koivula, J. López, J. L. Cortina, Sorption strategies for recovering critical raw materials: Extracting trace elements from saltworks brines, J. Environ. Chem. Eng. 12 (5) (2024) 114070, https://doi.org/10.1016/j.jece.2024.114070.